AD_____

Award Number: DAMD17-99-1-9096

TITLE: BARC: A Novel Apoptosis Regulator

PRINCIPAL INVESTIGATOR: Can Jin, Ph.D.
John C. Reed
Hong Zhang
Han Jun Chae

CONTRACTING ORGANIZATION: The Burnham Institute
La Jolla, CA 92037

REPORT DATE: June 2005

TYPE OF REPORT: Annual Summary

PREPARED FOR: U.S. Army Medical Research and Materiel Command
Fort Detrick, Maryland 21702-5012

REPORT DOCUMENTATION PAGE

Form Approved
OMB No. 0704-0188

1. REPORT DATE *(DD-MM-YYYY)*	2. REPORT TYPE	3. DATES COVERED *(From - To)*
01-06-2005	Annual Summary	1 Jun 99 – 31 May 05

4. TITLE AND SUBTITLE
BARC: A Novel Apoptosis Regulator

5a. CONTRACT NUMBER

5b. GRANT NUMBER
DAMD17-99-1-9096

5c. PROGRAM ELEMENT NUMBER

6. AUTHOR(S)
Can Jin, Ph.D., John C. Reed, Hong Zhang, Han Jun Chae

E-Mail: jreed@burnham.org

5d. PROJECT NUMBER

5e. TASK NUMBER

5f. WORK UNIT NUMBER

7. PERFORMING ORGANIZATION NAME(S) AND ADDRESS(ES)

The Burnham Institute
La Jolla, CA 92037

8. PERFORMING ORGANIZATION REPORT NUMBER

9. SPONSORING / MONITORING AGENCY NAME(S) AND ADDRESS(ES)
U.S. Army Medical Research and Materiel Command
Fort Detrick, Maryland 21702-5012

10. SPONSOR/MONITOR'S ACRONYM(S)

11. SPONSOR/MONITOR'S REPORT NUMBER(S)

12. DISTRIBUTION / AVAILABILITY STATEMENT
Approved for Public Release; Distribution Unlimited

13. SUPPLEMENTARY NOTES

14. ABSTRACT

Breast cancers arise due to an imbalance in cell production relative to cell turnover, resulting in a net accumulation of abnormal cells. Cell turnover is normally achieved in the body by a process known as apoptosis. Defects in apoptosis mechanisms commonly occur in breast cancers and other types of malignancies, making tumor cells difficult to kill by chemotherapy, hormonal therapy, and radiation. Restoring function of cell death pathways is a strategy for improving treatment of breast cancer.

This project focused on two anti-apoptotic proteins discovered by our laboratory, BI-1 and BI-2 (also known as BAR). The findings provided insights into the mechanism by which these proteins protect cancer cells from specific types of death stimuli. We demonstrated that interfering with expression or function of BI-2 (BAR) restores sensitivity of tumor cells to the killing mechanisms employed by immune cells, such as activators of the TNF-family receptor member Fas (CD95). We found that BI-1 protects cells from endoplasmic reticulum (ER) stress induced apoptosis. BI-1 and anti-apoptotic Bcl-2-family protein, regulate ER calcium. Our work revealed structural elements in Bcl-2 and other ER proteins that interact with Bcl-2 to regulate ER calcium. Green tea compounds that inhibit Bcl-2 restore ER calcium. These findings provide new insights into cell death regulation in breast cancer.

15. SUBJECT TERMS
Apoptosis; Bax; Bcl-2; BI-1; BAR

16. SECURITY CLASSIFICATION OF:			17. LIMITATION OF ABSTRACT	18. NUMBER OF PAGES	19a. NAME OF RESPONSIBLE PERSON
a. REPORT	b. ABSTRACT	c. THIS PAGE			USAMRMC
U	U	U	UU	65	19b. TELEPHONE NUMBER *(include area code)*

Table of Contents

Ref. 4 BAR: An apoptosis regulator at the intersection of caspase and Bcl-2 family proteins.

Ref. 5 Bifunctional apoptosis inhibitor (BAR) protects neurons from diverse cell death pathways.

Ref. 8 BI-1 regulates an apoptosis pathway linked to endoplasmic reticulum stress.

Ref. 9 Evolutionarily conserved cytoprotection provided by Bax Inhibitor-1 (BI-1) homologs from animals, plants, and yeast.

Ref. 15 Bcl-2-mediated alterations in endoplasmic reticulum Ca2+ analyzed with an improved genetically encoded fluorescent sensor.

DAMD17-99-1-9096
ANNUAL REPORT

Trainees: Hong Zhang; Han Jun Chae; Can Jin
(Mentor: John C. Reed)

INTRODUCTION

An important reason for breast cancer is the lack of programmed cell death, also known as apoptosis (1). A group of structurally conserved proteins, including Bcl-2 and Bax (2), are key players in apoptosis. To better understand this process, our lab screened human cancer cDNA libraries for inhibitors of Bax-induced cell death in yeast. Two proteins were identified: BI-1 and BI-2 (also known as BAR or BARC) (3,4). The purpose of this fellowship was to "investigate the role of BI-2 in regulating apoptosis and the effects of its interactions with Bcl-2 and Caspase-8 on programmed cell death in breast cancer." Another purpose for this fellowship is to compare the anti-apoptotic mechanism of BI-1 and BI-2 with Bcl-2-family proteins.

BODY

BI-2 (BAR) is an integral membrane protein mainly localized to endoplasmic reticulum (ER) (4, 5). The BAR protein contains a DED-like and a SAM-like domain. Previously, we showed that the BI-2 (BAR) is predominantly expressed in neurons (brain cells) in vivo (5). We showed that the BI-2 (BAR) interacts with several other DED-containing proteins, including pro-Caspase-8 (4,6), Hip, Hippi, and Bap31 (5). The interactions with the Huntingtin-interacting protein, Hip, and its partner Hippi, have suggested a potential role for BAR in suppressing a cell death pathway of relevance to Huntington's disease (7).

BI-2 (BAR) is also over-expressed in several types of cancers and cancer cell lines, including breast cancer lines such as MCF7 (4, 6), suggesting a link to cancer. In these cancer cell lines, reduced BI-2 (BAR) expression by antisense-RNA sensitizes the cells to Fas involved cell death pathway. Consistently, over-expression of BI-2 (BAR) by transfection rendered cells more resistant to this cell death pathway. In addition, when co-expressed with anti-apoptotic proteins Bcl-2 or Bcl-xL, the BAR protein provides protection from Fas-induced apoptosis under circumstances where neither BAR nor Bcl-2/Bcl-xL alone is adequate (6).

We also studied another Bax inhibitor, BI-1. BI-1 is an integral ER membrane protein (3). Over-expression of BI-1 protects cells against ER-stress induced apoptosis, as well as Bax-induced apoptosis (8). Homologous BI-1 proteins from other species can also prevent cell death induced by Bax and some other types of

stimuli (9). This pathway involves activation of the Bax protein, where Bax undergoes a conformational change and translocates to mitochondria, inducing downstream steps in this apoptosis pathway. Using BI-1 knockout mice characterized by our lab, we have found that ablation of BI-1 expression sensitize cells to apoptosis induced by ER-stress agents such as Thapsigargin (ER calcium ATPase inhibitor) and Tunicamycin (ER/Golgi glycosyl transferase inhibitor). Consequently, in adult *bi-1*$^{-/-}$ mice, the neurons, fibrablasts, and hepatocytes are more sensitive to ER stress-induced apoptosis. These mice also display increased sensitivity to tunicamycin-induced renal tubule, kidney and hippocampal neuron injury, and ischemia-reperfusion injury in brain, liver and kidney (8, manuscript submitted).

An important pathway for ER to regulate apoptosis is through calcium. If less calcium from ER is dumped into cytosol, the chance to overcome some apoptotic stimuli is better. Using Fura-2 as an indicator for cellular calcium concentrations, we demonstrated that over-expressing BI-1 reduces ER calcium levels in HT1080 and HeLa cells (8), and ablation of BI-1 expression in mouse embryo fibroblast (MEF) cells increases resting ER calcium levels (8).

To extend these observations regarding Ca^{2+} regulation, we studied Bcl-2 effect on ER calcium regulation. An engineered ER targeted protein cameleon is used to directly measure ER calcium levels (10). Bcl-2 is over-expressed in most Estrogen Receptor-positive breast cancers. Bcl-2 overexpression reduces the basal ER calcium concentration, and causes faster ER calcium leakage into cytosol upon blocking ER calcium pump (15). We conclude therefore that BI-1 shares in common with Bcl-2 the ability to decrease ER stores of Ca^{2+} thus causing less accumulation of Ca^{2+} in the cytosol when cells are stressed.

To explore the therapeutic potential of targeting this ER calcium mechanism, we treated MCF7 breast cancer cells with (-) epigallecatechin gallate (EGCG) from green tea, a compound that our laboratory previously showed binds to and suppresses the anti-apoptotic mechanisms of Bcl-2 and Bcl-xL. EGCG (but not an inactive compound from the same structural class) restored ER Ca^{2+} concentrations to normal levels in breast cancer cells over-expressing Bcl-2 (15). We concluded therefore that chemical inhibitors of anti-apoptotic proteins of the Bcl-2 family have the potential to restore normal Ca^{2+} homeostasis, correlating with restoration of tumor sensitivity to apoptosis.

To elucidate the structural motifs of Bcl-2-family proteins in reducing ER calcium, a systematic mutagenesis study of Bcl-2 was undertaken. First, we discovered that compared to mitochondrial localized Bcl-2, only Bcl-2 localized on ER can lower ER calcium (Fig. 1). Deletion of the predicted pore-forming domain (i.e.: the α5-α6 helices) also leads to the loss of ER calcium regulatory

activity of Bcl-2 (Fig. 2). Further study with point mutations in the predicted pore-forming domain indicated that conversion of some of the polar residues to alanine disrupted Bcl-2 function in lowering ER calcium levels, especially for Bcl-2 targeted to ER membranes (Fig 2). The results suggest that the pore-forming domain is required for Bcl-2 to regulate ER calcium. To study whether the ability of Bcl-2 to lower ER calcium levels is related to its anti-apoptotic function, apoptotic protection analyses were performed with the Bcl-2 mutants. Fig. 3 revealed no correlation between resting ER calcium levels and the anti-apoptotic abilities of the mutants, suggest that calcium is not the single most important factor in the ER stress pathway (Fig 3).

In addition, other members of the human anti-apoptotic Bcl-2 family were also analyzed for their effects on ER calcium regulation, in hope of revealing the common structural determinants that are important for calcium regulation. We observed that over-expression of Bcl-2, Bcl-xL, Bcl-B, Bfl-1 reduces basal concentrations of Ca^{2+} in the ER, and thus causes less Ca^{2+} release into the cytosol when cells are stressed with agents such as Thapsigargin (Fig. 4 and unpublished data from our laboratory).

ER calcium homeostasis is balanced by the activities of ER calcium pump (mainly SERCA) and ER calcium release channel (mainly IP3R for most cell types). Therefore, the interaction between BI-1 and Bcl-2 with Serca and IP3R was also studied. Over-expression of Serca2b restored ER calcium levels originally reduced by overexpression of BI-1 and Bcl-2, suggesting SERCA functions at the downstream of or in parallel to BI-1 and Bcl-2 (Fig 5A). In 293T cells, overexpressed Bcl-2, Bcl-xL and Mcl-1 co-immunoprecipitated with Serca2p (Fig.5B), suggesting Bcl-2 can directly interact with Serca2 to regulate SERCA activity. Because Bcl-B, Bfl-1 and Bcl-w were not detected in the immunoprecipitated fractions, it is unclear at this stage whether they also physically interact with Serca2p.

To explore the interaction between Bcl-2 and IP3R-1, recombinant GST Bcl-2-family proteins with deletion of their transmembrane domains were used to pull-down IP3R1 enriched in mouse brain microsomes. Preliminary experiments revealed only weak interactions of IP3R1 with Bcl-2 and Bfl-1, (data not shown). More thorough screening of GST pull-down conditions and in vivo co-immunoprecipitation experiments in cells overexpressing full length myc-Bcl-2 family proteins are in progress. If verified, the data suggest Bcl-2 can interact with multiple proteins to regulate ER calcium homeostasis. Similar GST pull-down experiments will be carried out with BI-1 knockout mouse brain microsomes to address whether BI-1 is needed as a bridge for IP3R1 to interact with Bcl-2/Bfl-1. Using HA-BI-1 transformed mouse brain, and cells

overexpressing IP3R/Serca and HA-BI-1 for immunoprecipitation, the physical interaction between BI-1 and IP3R/Serca will also be studied.

KEY RESEARCH ACCOMPLISHMENTS

BI-2 (BAR)

- BI-2 (BAR) is an ER membrane protein interacting with other DED-containing proteins and Bcl-2.
- BI-2 (BAR) is over-expressed in several cancers and cancer cell lines, including some breast cancers.
- BI-2 (BAR) protects cells against FAS/TNF-induced apoptosis in tumor cells, including breast cancers.

BI-1

- BI-1 is a structurally and functionally highly conserved cytoprotective protein among fungi, plants, and animals.
- Endogenous BI-1 is required to protect cells against ER stress-induced apoptosis.
- BI-1-deficient mice display increased sensitivity to ER-dependent tissue injury.
- BI-1 over-expression interrupts cell death signaling between ER and mitochondria.
- BI-1 regulates resting ER calcium levels and facilitates calcium leakage from ER.
- The effects of BI-1 on ER calcium mimic the effects of anti-apoptotic proteins such as Bcl-2 and Bcl-xL, which are over-expressed in most breast cancers, and Bcl-B and Bfl-1.
- Chemicals from green tea that bind and inhibit Bcl-2 and Bcl-xL restore normal homeostasis of ER calcium regulation.
- Bcl-2 pore-forming domain is required for its ER calcium regulation activity.
- Basal ER calcium levels appear to cooperate with other cellular factors to affect apoptosis.
- Calcium pump Serca2 can reverse the effects of BI-1 and Bcl-2 on basal ER calcium levels, and Serca2 can physically interact with Bcl-2.

REPORTABLE OUTCOMES

1. Publications: Trainees working on this grant published 4 papers directly germane to the goals of the grant (4, 8, 9, 15), and published two additional papers indirectly relevant to the goals of this grant (12, 13). Also, trainees associated with this grant wrote two review articles (11, 14).

2. Reagents: Multiple reagents were generated as a result of this grant, including many plasmids encoding BI-2 (BAR) and BI-1, and fragments of these proteins containing or missing some of the functionally important domains; antibodies that recognize BAR; antisense oligonucleotides with optimized sequences for suppressing expression of BAR; and cell lines stably expressing transfected BAR and BI-1 or fragments of BAR. BI-1 knockout mice and BI-1 knock-out cells were also generated.

3. Employment. Drs. Hong Zhang and Han Jun Chae who trained on this grant obtained employment. Dr. Zhang worked as a senior research scientist in the division of Oncology Research at Dupont, Inc (Glen Olden, PA) and is now a Project Leader at Conforma Pharmaceuticals, Inc. (San Diego, CA). Dr. Zhang is dedicated to discovery and development of new drugs for cancer, including breast cancer. Her current work focuses on small-molecule inhibitors of Hsp90, a protein over-expressed in many chemorefractory breast cancers. Dr Han Jun Chae is now an Assistant Professor in the College of Medicine, Chonbk National University, in Seoul, Korea. Dr. Chae's work focuses on apoptosis dysregulation in cancer, including breast cancers. She devotes 80% of her effort to cancer research, and also teaches medical students. Dr. Can Jin continues her training in the laboratory.

CONCLUSION

BI-1 and BI-2 (BAR) were identified in our laboratory as inhibitors of Bax lethality. Bax is a pro-apoptotic protein who expression becomes lost in approximately one-third of breast cancers, correlating with poor responses to combination chemotherapy and shorter patient survival. The research supported under this fellowship proved that both of these proteins can protect tumor cells from cell death induced by specific types of stimuli, with BI-1 working predominantly on an ER calcium pathway and BAR working mostly on the TNF/Fas death receptor pathway for apoptosis. These results help to elucidate through which mechanisms tumor cells achieve resistance to stress, allowing them to gain a selective survival advantage relative to normal cells. Bcl-2 and Bcl-xL are anti-apoptotic proteins over-expressed in most breast cancers, they interact with BI-1 and BI-2 (BAR) and they also regulate ER calcium levels. Using Bcl-2 as a model to study the ER calcium regulation mechanism, we showed that the pore-forming domain of Bcl-2 is required for its ER calcium regulation function. Bcl-2 can interact with ER calcium pump Serca2 and calcium release channel protein IP3R1. Other anti-apoptotic Bcl-2 family proteins Bfl-1 and Bcl-B may also lower ER calcium through similar mechanisms. In addition, we demonstrated that chemical compounds from green tea that inhibit Bcl-2 and Bcl-

xL restore normal ER calcium regulation, providing insights into the mechanisms of these medicinal products and suggesting paths forward for new therapies.

REFERENCES

1. Reed, J. Dysregulation of apoptosis in cancer. J Clin Oncol, 17: 2941, 1999.
2. Oltvai, Z., Milliman, C., and Korsmeyer, S. Bcl-2 heterodimerizes in vivo with a conserved homolog, Bax, that accelerates programmed cell death. CELL, 74: 609-619, 1993.
3. Xu, Q. and Reed, J. C. BAX inhibitor-1, a mammalian apoptosis suppressor identified by functional screening in yeast. Mol Cell, 1: 337-346, 1998.
4. Zhang, H., Xu, Q., Krajewski, S., Krajewska, M., Xie, Z., Fuess, S., Kitada, S., Pawloski, K., Godzik, A., and Reed, J. C. BAR: An apoptosis regulator at the intersection of caspase and bcl-2 family proteins. Proc Natl Acad Sci USA, 97: 2597-2602, 2000.
5. Roth, W., Kermer, P., Krajewska, M., Welsh, K., Davis, S., Krajewski, S., and Reed, J. C. Bifunctional apoptosis inhibitor (BAR) protects neurons from diverse cell death pathways. Cell Death & Differ, 10: 1178-1187, 2003.
6. Stegh, A. H., Barnhart, B. C., Volkland, J., Ke, N., Reed, J., and Peter, M. E. Inactivation of caspase-8 on mitochondria of Bcl-xL expressing MCF7-Fas cells. J Biol Chem, 277: 4351-4360, 2002.
7. Gervais, F. G., Singaraja, R., Xanthoudakis, S., Gutekunst, C. A., Leavitt, B. R., Metzler, M., Hackam, A. S., Tam, J., Vaillancourt, J. P., Houtzager, V., Rasper, D. M., Roy, S., Hayden, M. R., and Nicholson, D. W. Recruitment and activation of caspase-8 by the Huntingtin-interacting protein Hip-1 and a novel partner Hippi. Nat Cell Biol, 4: 95-105, 2002.
8. Chae, H.-J., Kim, H.R., Xu, C., Bailly-Maitre, B., Krajewska, M., Krajewski, S., Banares, S., Cui, J., Digicaylioglu, M., Ke, N., Kidata, S., Monosov, E., Thomas, M., Kress, C. L., Babendure, J., Tsien, R. Y., Lipton, S. A., and Reed, J. C. BI-1 regulates an apoptosis pathway linked to endoplasmic reticulum stress. Mol Cell, 15: 355-366, 2004.
9. Chae, H.-J., Ke, N., Kim, H.-R., Chen,S., Godzik, A., Dickman, M., and Reed, J. C. Evolutionarily conserved cytoprotection provided by Bax Inhibitor-1 (BI-1) homologs from animals, plants, and yeast. Gene, 323:101-113, 2003.
10. Miyawaki A, Llopis J, Heim R, McCaffery JM, Adams JA, Ikura M, Tsien RY. Fluorescent indicators for Ca2+ based on green fluorescent proteins and calmodulin. Nature, 388:882-887, 2003.
11. Zhang, H. and Reed, J. C. Studies of apoptosis proteins in yeast. *In:* L. Schwartz and Ashwell (eds.), Methods in Cell Biology, 2nd edition, Vol. 66, pp. 453-468: Academic Press, 2001.
12. Zhang, H., Huang, Q., Ke, N., Matsuyama, S., Hammock, B., Godzik, A., and Reed, J. C. Drosophila pro-apoptotic bcl-2/bax homologue reveals evolutionary conservation of cell death mechanisms. J Biol Chem, *275:* 27303-27306, 2000.
13. Zhai, D., Ke, N., Zhang, H., Ladror, U., Joseph, M., Eichinger, A., Godzik, A., Ng, S. C., and Reed, J. C. Characterization of anti-apoptotic mechanism of Bcl-B. Biochem J, 376: 229-236, 2003.
14. Jin, C., and Reed, J.C. Yeast and apoptosis. Nat Rev Mol Cell Biol., 3: 453-459, 2002.
15. Palmer, A. E., Jin, C., Reed, J. C., and Tsien, R. Y. Bcl-2-mediated alterations in endoplasmic reticulum Ca2+ analyzed with an improved genetically encoded fluorescent sensor. Proc Natl Acad Sci USA, 101: 17404-17409, 2004.

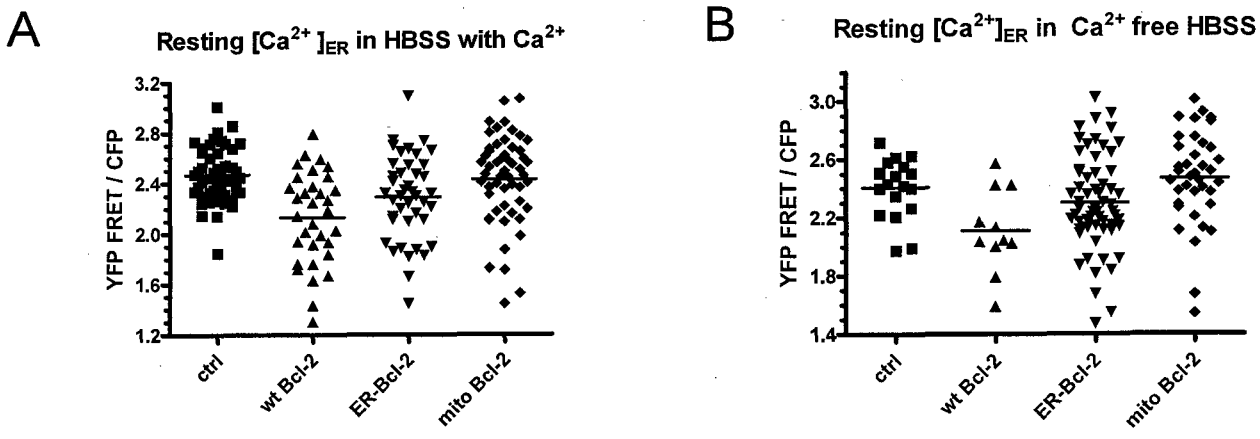

Fig. 1 Over-expression of Bcl-2 lowers resting $[Ca^{2+}]_{ER}$ in HeLa cells. HeLa cells were transiently transfected with ER-targeted cameleon and plasmids carrying wild-type, ER-targeted or mitochondria-targeted Bcl-2 at 1:10 ratio. After 2 to 3 days, YFP FRET/CFP fluorescence ratios of cameleon were analyzed in live cells in HBSS media **(A)** with 1.2 mM calcium or **(B)** without calcium. The emission ratios reflect resting $[Ca^{2+}]_{ER}$. Each dot represents the emission ratio of a single cell.

Fig. 2

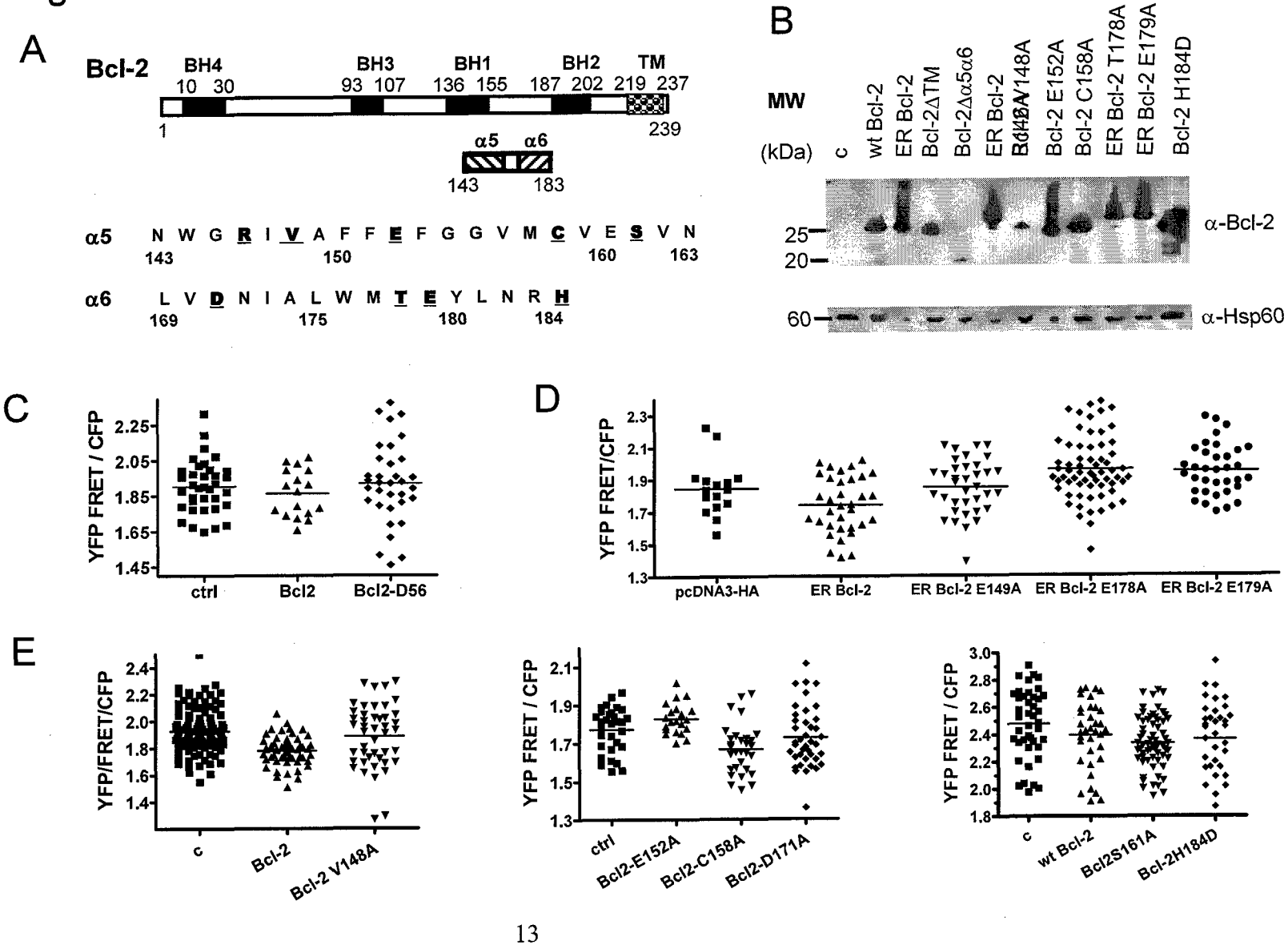
A
Bcl-2
BH4
BH3
BH1
BH2
TM
10 30
93 107
136 155
187 202
219 237
1
239
α5 α6
143 183
α5 N W G R I V A F F E F G G V M C V E S V N
143 150 160 163
α6 L V D N I A L W M T E Y L N R H
169 175 180 184
B
MW
(kDa)
c
wt Bcl-2
ER Bcl-2
Bcl-2ΔTM
Bcl-2Δα5α6
ER Bcl-2
Bcl-2 E152A
Bcl-2 C158A
ER Bcl-2 T178A
ER Bcl-2 E179A
Bcl-2 H184D
25
20
α-Bcl-2
60
α-Hsp60
C
YFP FRET / CFP
2.25
2.05
1.85
1.65
1.45
ctrl
Bcl2
Bcl2-D56
D
YFP FRET/CFP
2.3
2.1
1.9
1.7
1.5
1.3
pcDNA3-HA
ER Bcl-2
ER Bcl-2 E149A
ER Bcl-2 E178A
ER Bcl-2 E179A
E
YFP/FRET/CFP
2.4
2.2
2.0
1.8
1.6
1.4
c
Bcl-2
Bcl-2 V148A
YFP FRET / CFP
2.1
1.9
1.7
1.5
1.3
ctrl
Bcl2-E152A
Bcl2-C158A
Bcl2-D171A
YFP FRET / CFP
3.0
2.8
2.6
2.4
2.2
2.0
1.8
c
wt Bcl-2
Bcl2S161A
Bcl-2H184D

Fig. 2. The potential pore-forming domain of Bcl-2 is required for ER calcium regulation. A. The structure of Bcl-2 protein is shown, and the design of point mutations in the potential pore-forming α5-α6 helices are indicated. The bold underlined amino acids were mutated to alanine. **B.** The mutant Bcl-2 proteins expressional levels are similar to wild-type Bcl-2. 30 ug cell lysates from 293T cells transfected with Bcl-2 and mutants were analyze by Western blotting. Hsp60p levels are shown as an internal control. **C.** Deletion of the potential pore-forming domain of Bcl-2 abolishes ability to lower resting $[Ca^{2+}]_{ER}$. HeLa cells transfected with cameleon and Bcl-2 or Bcl-2 mutants were analyzed for the emission ratio in HBSS with calcium. **D.** Point mutations in ER-targeted Bcl-2 pore-forming domain abolished Bcl-2's function to lower resting $[Ca^{2+}]_{ER}$ in HeLa cells. **E.** Some point mutations in Bcl-2 pore-forming domain abolished Bcl-2's function to lower resting $[Ca^{2+}]_{ER}$ in HeLa cells.

Fig. 3. Resting $[Ca^{2+}]_{ER}$ is insufficient to account for apoptosis regulation by Bcl-2. HeLa cells were transiently transfected with 10:1 plamids carrying Bcl-2 or mutants and EGFP. After 6 hrs, cells were split and incubated at 37°C overnight. Then the cells were exposed to different apoptosis-inducing agents. Both floating and attached cells were collected and stained with Annexin V-APC. The percentage of Annexin V-APC positive cells among GFP-positive cells was counted. Each experiment was repeated 3 to 4 times. **A.** The abilities of Bcl-2 mutants to regulate resting $[Ca^{2+}]_{ER}$ did not correlate with their abilities to protect cells from apoptosis induced by UV irradiation (24 hrs after irradiation) and staurosporin treatment (0.1 μM, 6 hrs). **B.** The abilities of Bcl-2 mutants to regulate resting $[Ca^{2+}]_{ER}$ did not correlate with their abilities to protect cells from apoptosis induced by ER stress reagents. H2O2 : cells were treated with 0.6 mM H2O2 for 6 hrs; TG: 10 μM thapsigargin treated for 48 hrs; TU: 10 µg/ml tunicamycin treated for 48 hrs.

Fig. 3A

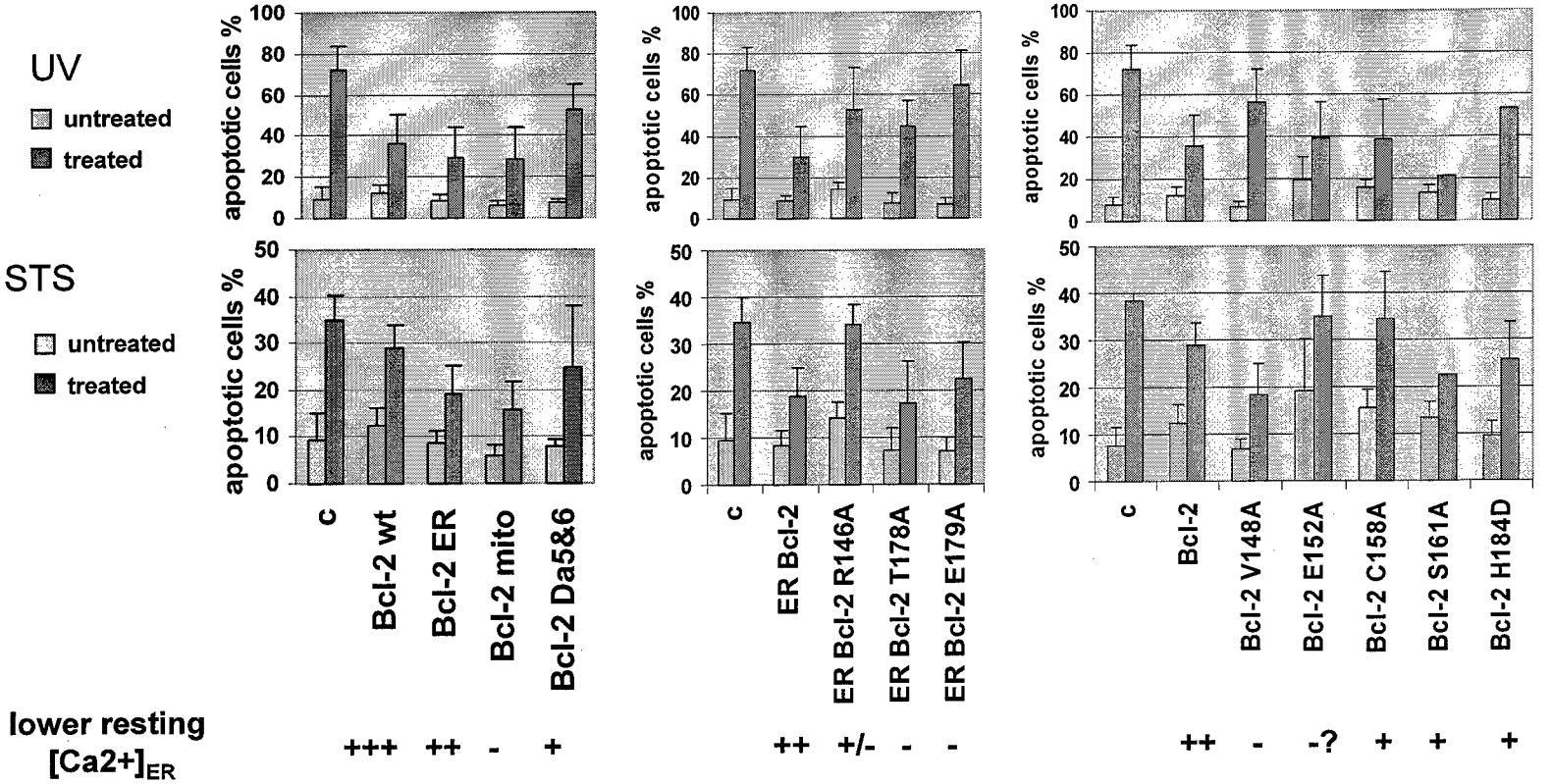
UV
untreated
treated
STS
untreated
treated
apoptotic cells %
100
80
60
40
20
0
50
40
30
20
10
0
c
Bcl-2 wt
Bcl-2 ER
Bcl-2 mito
Bcl-2 Da5&6
ER Bcl-2
ER Bcl-2 R146A
ER Bcl-2 T178A
ER Bcl-2 E179A
Bcl-2
Bcl-2 V148A
Bcl-2 E152A
Bcl-2 C158A
Bcl-2 S161A
Bcl-2 H184D
lower resting
[Ca2+]ER
+++ ++ - +
++ +/- - -
++ - -? + + +

Fig. 3B

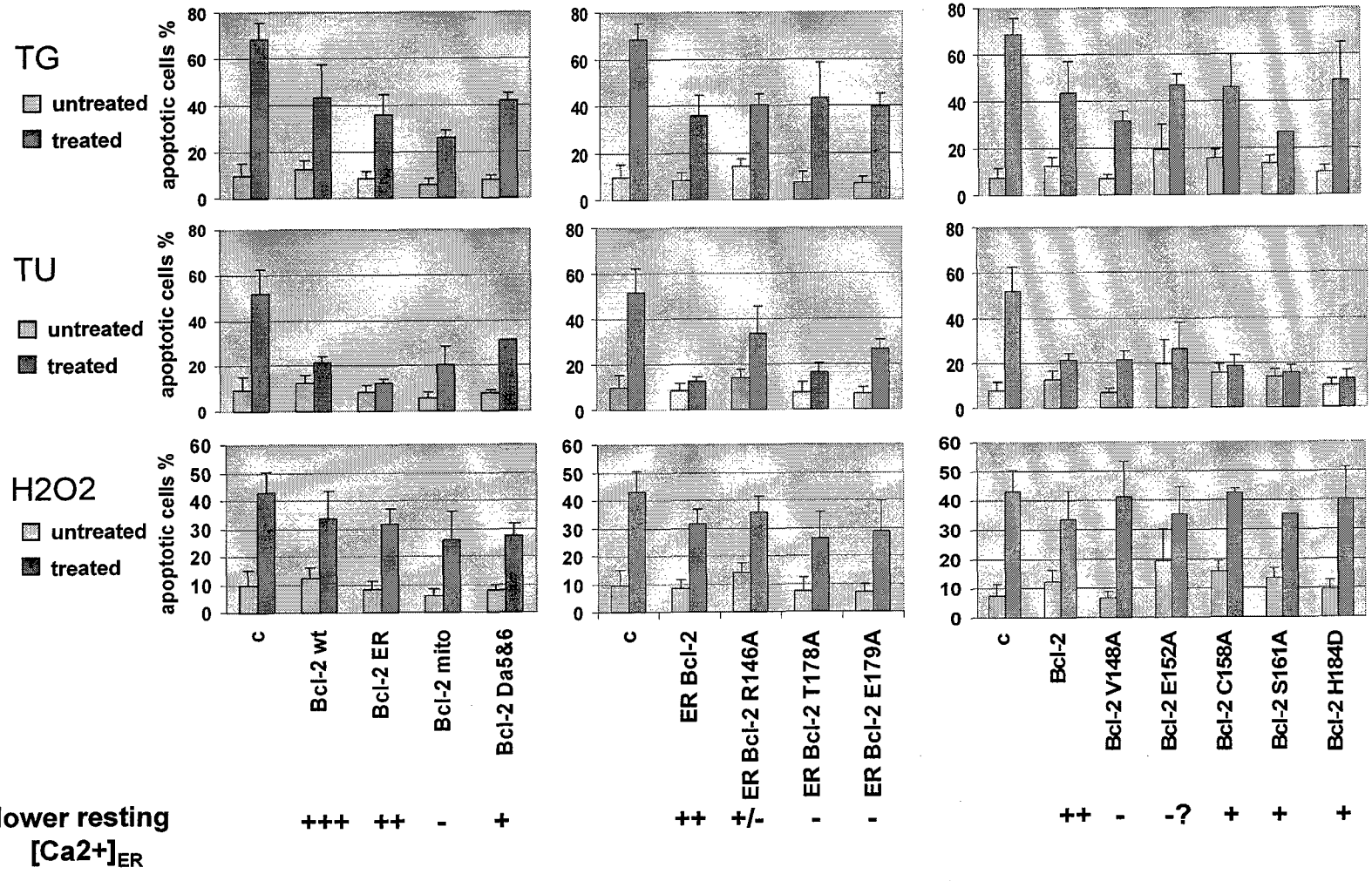
TG
untreated
treated
apoptotic cells %
TU
untreated
treated
apoptotic cells %
H2O2
untreated
treated
apoptotic cells %
c
Bcl-2 wt
Bcl-2 ER
Bcl-2 mito
Bcl-2 Da5&6
c
ER Bcl-2
ER Bcl-2 R146A
ER Bcl-2 T178A
ER Bcl-2 E179A
c
Bcl-2
Bcl-2 V148A
Bcl-2 E152A
Bcl-2 C158A
Bcl-2 S161A
Bcl-2 H184D
lower resting [Ca2+]ER
+++
++
-
+
++
+/-
-
-
++
-
-?
+
+
+

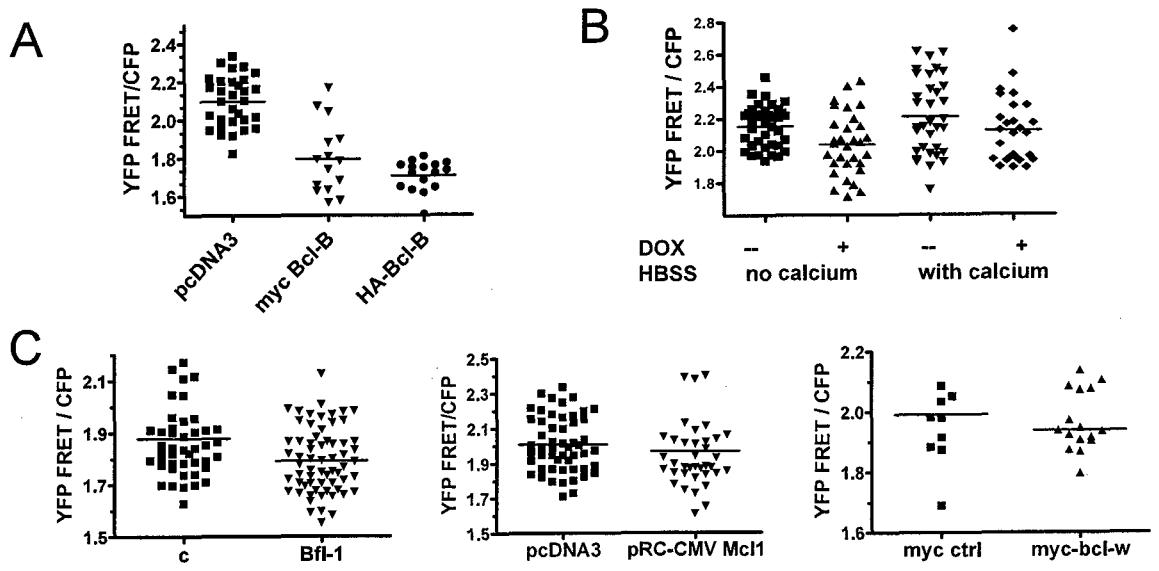

Fig. 4 Effects of other anti-apoptotic Bcl-2 family proteins on resting $[Ca^{2+}]_{ER}$ in HeLa cells. A. Transiently overexpressed Bcl-B lowers ER calcium in HeLa cells. HeLa cells were transiently transfected with 1/10 cameleon and pcDNA3, or pcDNA3-myc-Bcl-B, or pcDNA3-HA-Bcl-B. 3 days later, the cameleon emission ratio from individual cells was recorded as described in Fig. 1A. **B.** Stably overexpressed Bcl-B lowers resting $[Ca^{2+}]_{ER}$ in HeLa cells. HeLa cells stably expressing Bcl-B under the Tet-ON promoter were transfected with ER-targeted cameleon and split the next day. At 48 hrs after transfection, doxycyclin (Dox) was added to some of the cultures to induce Bcl-B expression for 24 hrs. The cells were analyzed in HBSS with or without calcium to determine cameleon emission ratios. **C.** Transient overexpression of Bfl-1 lowers resting $[Ca^{2+}]_{ER}$ in HeLa cells. **D.** Transient overexpression of Mcl-1 has marginal effect on resting $[Ca^{2+}]_{ER}$ in HeLa cells. **E.** Transient overexpression of Bcl-W has marginal effect on resting $[Ca^{2+}]_{ER}$ in HeLa cells.

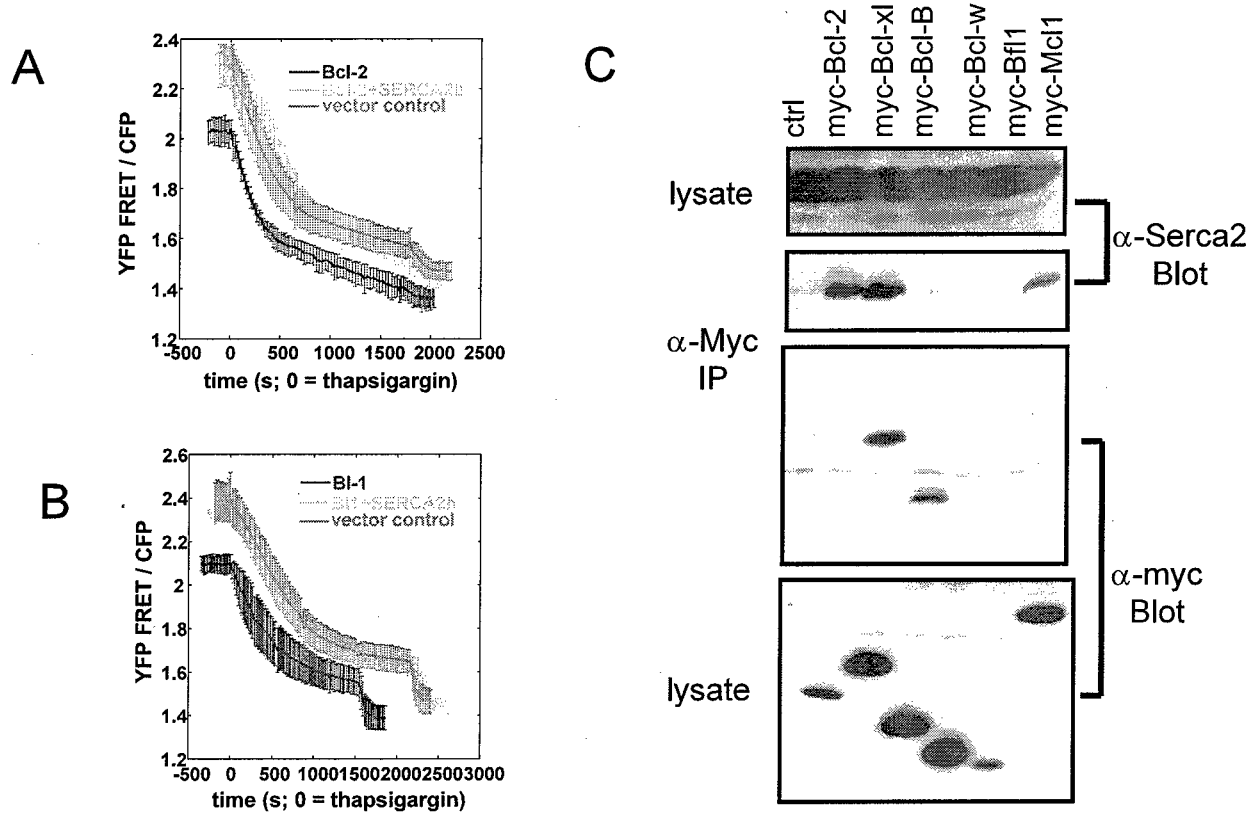

Fig. 5 Overexpression of Serca2b reverses abilities of Bcl-2 or Bl-1 to lower resting $[Ca^{2+}]_{ER}$. **A.** Serca2b (S2b) overexpression restored resting $[Ca^{2+}]_{ER}$ in HeLa cells overexpressing Bcl-2. HeLa cells were transiently transfected with 1/20 cameleon with pcDNA3 or pcDNA3-Bcl-2, or pcDNA3-Bcl-2 and pcDNA3-SERCA2B. After three days, YFP FRET/CFP fluorescence ratio of cameleon was analyzed in live cells in HBSS media with calcium. The emission ratios were then converted to calcium concentration as described (10). Each trace represents the average of > 20 cells. **B.** Serca2b (S2b) overexpression restored resting $[Ca^{2+}]_{ER}$ in HeLa cells overexpressing Bl-1. Each trace represents the average of > 20 cells. **C.** Bcl-2 and Bcl-xL physically interact with Serca2b. 293T cells were transiently transfected with plasmids encoding myc-Bcl-2 family anti-apoptotic proteins. The cells were collected 24 hrs later, and lysates were prepared in 2% CHAPS lysis buffer with proteinase inhibitors. Myc-protein G beads were added to the 1 mg/ml lysates and incubated at 4 °C overnight. Both lysates and washed beads were analyzed by Western blotting using antibodies specific to Serca (top panels) and myc epitope (lower panels).

BAR: An apoptosis regulator at the intersection of caspases and Bcl-2 family proteins

Hong Zhang*, Qunli Xu*, Stanislaw Krajewski, Maryla Krajewska, Zhihua Xie, Sally Fuess, Shinichi Kitada, Krzysztof Pawłowski, Adam Godzik, and John C. Reed†

Program on Apoptosis and Cell Death Regulation, The Burnham Institute, La Jolla, CA 92037

Communicated by Erkki Ruoslahti, The Burnham Institute, La Jolla, CA, December 27, 1999 (received for review October 26, 1999)

Two major pathways for induction of apoptosis have been identified—intrinsic and extrinsic. The extrinsic pathway is represented by tumor necrosis factor family receptors, which utilize protein interaction modules known as death domains and death effector domains (DEDs) to assemble receptor signaling complexes that recruit and activate certain caspase-family cell death proteases, namely procaspases-8 and -10. The intrinsic pathway for apoptosis involves the participation of mitochondria, which release caspase-activating proteins. Bcl-2 family proteins govern this mitochondria-dependent apoptosis pathway, with proteins such as Bax functioning as inducers and proteins such as Bcl-2 and Bcl-X_L serving as suppressors of cell death. An apoptosis regulator, BAR, was identified by using a yeast-based screen for inhibitors of Bax-induced cell death. The BAR protein contains a SAM domain, which is required for its interactions with Bcl-2 and Bcl-X_L and for suppression of Bax-induced cell death in both mammalian cells and yeast. In addition, BAR contains a DED-like domain responsible for its interaction with DED-containing procaspases and suppression of Fas-induced apoptosis. Furthermore, BAR can bridge procaspase-8 and Bcl-2 into a protein complex. The BAR protein is anchored in intracellular membranes where Bcl-2 resides. BAR therefore may represent a scaffold protein capable of bridging two major apoptosis pathways.

Two major pathways for induction of apoptosis have been identified in recent years. One of these apoptosis pathways is represented by tumor necrosis factor (TNF)-family receptors that contain protein interaction modules known as death domains (DD) in their cytosolic regions (reviewed in refs. 1–3). On binding ligand or when overexpressed in cells, DD-containing TNF receptor family members such as Fas (CD95) aggregate, resulting in recruitment of an adaptor protein Fadd, which contains both a DD and a similar protein interaction module known as the death effector domain (DED) (4, 5). The zymogen pro-forms of certain caspase-family cell death proteases, namely procaspases-8 and -10, also contain DEDs in their N-terminal prodomains, allowing binding to Fadd/Fas complexes. This is followed by proteolytic processing and activation of the receptor-associated proteases, thereby initiating a subsequent cascade of additional processing and activation of downstream effector caspases (reviewed in refs. 1–3).

DED-containing proteins that function as antagonists of death receptor signaling have been identified in humans, mammals, and viruses (6–8). These antiapoptotic DED-containing proteins function as transdominant inhibitors, which compete for binding to the DED domains of Fadd or procaspases-8 or -10, thereby preventing assembly of a functional death-inducing complex (9).

A second major pathway for apoptosis involves the participation of mitochondria, which release cytochrome *c* (cyt-*c*), resulting in caspase activation through the effects of Apaf-1 (10, 11). Members of the Bcl-2 family play a major role in governing this mitochondria-dependent apoptosis pathway, with proteins such as Bax functioning as inducers of apoptosis and proteins such as Bcl-2 and Bcl-X_L serving as suppressors of cell death (12, 13).

The Bax protein shares predicted structural similarity with the pore-forming domains of certain bacterial toxins (14) and induces release of cyt-*c* and triggers dissipation of the electrochemical gradient in mitochondria, even in the absence of caspases (15–17). When ectopically expressed in yeast, which have no caspases or Apaf-1 homologues, Bax targets to mitochondria, induces cyt-*c* release, and causes cell death (18, 19). This cytotoxic effect of Bax on yeast has permitted screens for human antiapoptosis genes that maintain cell survival despite expression of the Bax protein (20). Here we describe the cloning and characterization of human cDNAs encoding an apoptosis regulator identified through such a yeast-based screen. We have termed this protein BAR, for bifunctional apoptosis regulator, because it contains both a DED-like domain capable of suppressing apoptosis signaling through Fas (extrinsic pathway) and another domain that mediates interactions with Bcl-2 family protein and that is required for suppression of Bax-induced cell death in yeast and mammalian cells (intrinsic pathway). BAR thus represents a protein at the intersection of two major pathways controlling apoptosis.

Materials and Methods

Plasmids. A Bgl-II fragment containing the complete ORF of BAR was isolated from a HepG2 library as described (20). cDNAs encoding full-length or fragments of BAR were generated by PCR and subcloned into various plasmids, as indicated.

Yeast Assays. Yeast strain QX95001, containing the *LEU2*-marked mBax-encoding plasmid YEP51-Bax (20), was transformed with the plasmids p424, p424-BAR, p424-BAR(ΔR), and p424-BAR(ΔTM) containing the TRP marker by a lithium acetate method. Transformants were plated on SD-Leu, TRP (leucine-deficient and tryptophan-deficient SD). Protein extracts were prepared as described (18, 20). Yeast two-hybrid assays were performed as described (18, 21), by using Bcl-2 (ΔTM) proteins to avoid problems with nuclear targeting.

Cell Culture and Transfections. 293, 293T, and HT1080 cells were seeded at 5×10^5 cells per well in six-well plates and were transfected the next day with various combinations of plasmids by using SuperFect (Qiagen, Chatsworth, CA). Both floating and adherent cells (after trypsinization) were collected 24 hr after transfection and analyzed by 4′,6-diamidine-2′-phenylindole dihydrochloride (DAPI) staining for assessing nuclear morphology. Transfection efficiencies were routinely >70% based on cotransfecting a green fluorescent protein (GFP)-encoding plasmid.

Caspase Assays. Cell extracts (25 μg total protein) were prepared from transfected cells and incubated with 100 μM substrate benzyloxycarbonyl-Asp-Glu-Val-Asp-AFC (Z-DEVD-AFC) in

Abbreviations: TNF, tumor necrosis factor; DD, death domain; DED, death effector domain; DAPI, 4′,6-diamidine-2′-phenylindole dihydrochloride; GFP, green fluorescent protein; TM, transmembrane.

*H.Z. and Q.X. contributed equally to this work.

†To whom reprint requests should be addressed at: The Burnham Institute, 10901 North Torrey Pines Road, La Jolla, CA 92037. E-mail: jreed@burnham-inst.org.

The publication costs of this article were defrayed in part by page charge payment. This article must therefore be hereby marked "*advertisement*" in accordance with 18 U.S.C. §1734 solely to indicate this fact.

100 μl caspase buffer (16). Caspase activity was assayed by using a fluorometer plate reader, measuring release of fluorescent AFC.

Subcellular Fractionations. 293T cell lysates were prepared and fractionated to yield cytosolic, light-membrane, heavy-membrane, and nuclear fractions (20).

***In Vitro* Protein-Binding Assays.** GST-fusion proteins (≈3 μM) immobilized on glutathione-Sepharose beads were incubated with 10 μl of reticulocyte lysates (TNT-lysates, Promega) containing *in vitro* translated [^{35}S] methionine-labeled proteins in 0.5 ml binding buffer (142.5 mM KCl/5 mM $MgCl_2$/10 mM Hepes, pH 7.2/1 mM EGTA/0.2% Nonidet P-40) containing protease inhibitors for 3 hr at 4°C. Beads were washed three times in 1.5 ml binding buffer, and bound proteins were eluted by boiling in SDS-loading buffer and subjected to SDS/PAGE.

Coimmunoprecipitation Assays. 293T cells transfected with plasmids encoding Myc-BAR, Bcl-2, Bax, or other proteins were cultured with or without 20 μM MG-132 for 6 hr before lysing in HKME solution (142.5 mM KCl/5 mM $MgCl_2$/10 mM Hepes, pH 7.2/1 mM EGTA) containing 0.4% Nonidet P-40 and protease inhibitors. Lysates were cleared by incubation with the protein G-Sepharose 4B (Zymed) and then incubated with anti-Myc antibody immobilized on agarose gel (Santa Cruz Biotechnology) at 4°C for 2 hr with constant rotation. Beads were then washed 4 times in HKME containing 0.2% Nonidet P-40 before boiling in SDS sample buffer. For analysis of interactions of BAR or BAR mutants with Flag-caspases or Flag-FADD, transfected cells were lysed in modified HKME solution, which contained 400 mM KCl and 0.8% Nonidet P-40. Immunoprecipitations were performed as above, by using either anti-Flag-M2 agarose affinity gel (Sigma) or anti-Myc immobilized agarose gel. SDS/PAGE immunoblotting was performed as described (20).

Antibody Production and Immunohistochemistry. High-titer antisera specific for BAR were generated in rabbits by using a multiple boosting technique and recombinant GST-BAR(1–139) as immunogen, as described (22). Antibody reactivity with BAR was confirmed by immunoblot analysis of *in vitro* translated BAR vs. various control proteins and of lysates from 293T cells transfected with Myc-BAR or various control plasmids, revealing reactivity solely with the expected BAR protein. Specificity of antisera was determined by comparisons of immune and preimmune serum and by preadsorption of anti-BAR antisera with excess immunogen (GST-BAR) at 5 μg per 50 μl antiserum.

Computer Analysis. BAR sequence has been analyzed with threading (23) and sensitive profile–profile alignment methods (24) developed at the authors' laboratory, as well as PSI-BLAST (25). Three-dimensional models of identified domains were subsequently built with MODELLER (26) and analyzed for quality by using several structure analysis methods (27).

Results

BAR Is a Multidomain Protein. A screen for cDNAs encoding suppressors of Bax-induced cell death was performed in the yeast *Saccharomyces cerevisiae*, resulting in a cDNA containing an ORF encoding a human protein of 450 amino acids (≈52 kDa), to which we assigned the acronym BAR, for bifunctional apoptosis regulator (GenBank accession no. AF173003). The predicted BAR protein contains several protein domains, including: (*i*) an N-terminal zinc-binding RING domain at residues 24–86; (*ii*) a SAM domain at amino acids 180–254; (*iii*) a DED-like domain at 273–345; and (*iv*) a C-terminal hydrophobic transmembrane (TM) domain at 400–428 (Fig. 1 *A* and *B*). The first two assignments have high statistical significance, with PSI-BLAST *E*-values of E^{-14} and E^{-28}, respectively, indicating high confidence of the prediction. The DED-like domain is not recognized by any of the standard sequence analysis programs and instead was identified by detailed comparison to known DED proteins, as described below. The DED-like domain of BAR was most homologous to the first DED domain of procaspases-10, sharing 21% amino acid sequence identity (39% similarity), respectively, with these proteins (Fig. 1*C*). The BAR DED domain contains 14 of the 21 residues previously recognized to be conserved among DED-family domains based on sequence alignments (28), and 16 of the 19 hydrophobic residues known to be conserved among DED-family domains based on structural considerations (29). A consensus secondary-structure prediction based on PHD (30) and nearest neighbor (31) algorithms suggested the presence of six α-helices, consistent with the known structure of other DED-family proteins (29). The SAM domain of BAR shares greatest homology with the human Ephb2 SAM domain (17% identity) and is predicted by FFAS to adopt a four α-helix bundle structure typical of SAM domains (32), with excellent conservation of the signature residues found in other members of this domain family (Fig. 1*D*).

BAR Is a Membrane-Associated Protein That Suppresses Bax-Induced Cell Death. Expression of full-length BAR protein in yeast rescued cells from Bax-induced death (Fig. 2*A*), despite continued production of the Bax protein (not shown). Deletion of the RING domain from BAR did not interfere with its protective effect on Bax-induced cell death. In contrast, removal of the C-terminal TM domain completely abolished the ability of BAR to rescue against Bax, suggesting that membrane localization of BAR is important for its function as a Bax antagonist. Immunoblot analysis confirmed production of the BAR (ΔTM) protein at levels comparable to full-length BAR (not shown).

To investigate the effects of BAR on Bax-induced cell death in mammalian cells, plasmids encoding wild-type or mutant versions of BAR were cotransfected with a Bax-encoding plasmid into 293T cells, which contain low endogenous levels of BAR. Cells were recovered 24 hr later and analyzed for percentage apoptosis by staining with DAPI (18). Both BAR and BAR(ΔR) suppressed Bax-induced apoptosis (Fig. 2*B*), without interfering with Bax protein production (Fig. 2*C*). In contrast, the BAR(ΔTM) protein was ineffective at suppressing Bax-induced apoptosis, even though the protein was produced at levels similar to full-length BAR in 293T cells. We conclude therefore that BAR suppresses Bax-induced cell death in both yeast and mammalian cells, requiring the TM but not the RING domain for its Bax antagonistic function.

The BAR(ΔR) protein consistently accumulated to higher levels in cells compared with full-length BAR (Fig. 2 *C* and *D*), though no difference in plasmid-derived BAR and BAR(ΔR) mRNAs was observed (not shown). Similar to several other RING-containing proteins that are subject to proteosome-dependent degradation (33–35), the 26S proteosome protease inhibitor MG-132 markedly increased accumulation of BAR protein (Fig. 2*D*). Thus, steady-state levels of the BAR protein may be controlled by proteosome-dependent degradation, mediated by the N-terminal RING domain of this protein, explaining the greater suppression of apoptosis by BAR(ΔR) compared with BAR. Though deletion of the RING domain from BAR was helpful for enhancing accumulation of this protein in 293 cells, high levels of full-length BAR were found endogenously in some tumor cell lines such as MCF7 breast cancer cells (Fig. 2*E*), LOXIMVI and UACC-257 melanoma, and IGROV1 ovarian cancer cell lines (not shown).

The presence of a candidate TM domain in BAR suggested it could be a membrane-associated protein. Indeed, BAR protein was not extractable from cellular membrane preparations by using alkaline (pH 11.5) solution, consistent with an integral membrane protein (not shown). Subcellular fractionation exper-

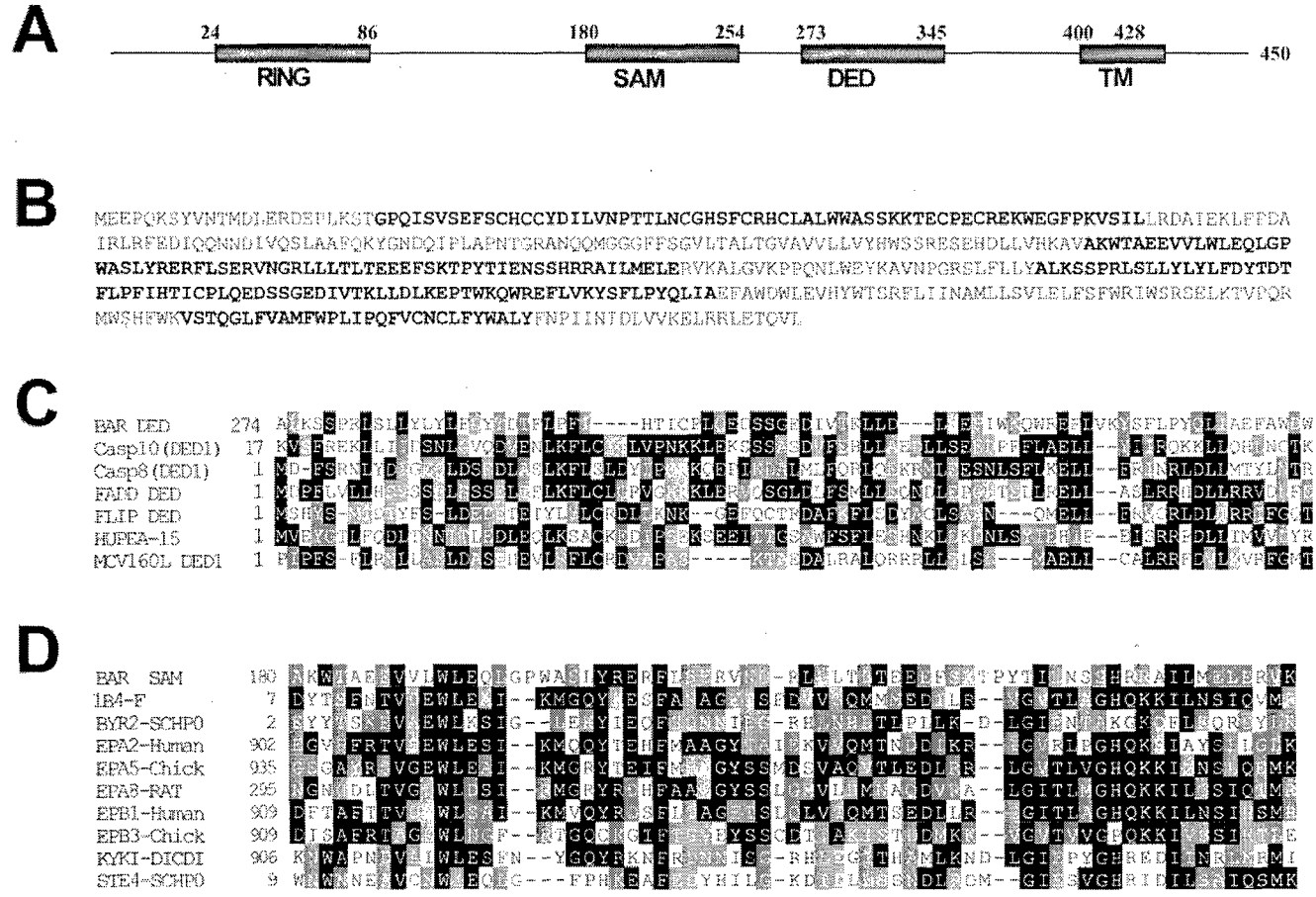

Fig. 1. Sequence and domains of the BAR protein. (*A*) The domains of the human BAR protein are depicted, showing the RING, SAM, DED, and TM segments. (*B*) The predicted amino acid sequence of BAR is presented, with RING, SAM, DED, and TM domains in boldface. (*C*) An alignment of DED domain of BAR with DED domains from other proteins is shown, with identical and similar residues in black and gray, respectively. (*D*) An alignment of the SAM domain of BAR with SAM domains from other proteins is presented as above.

iments (Fig. 2*F*) revealed that BAR resides predominantly in the heavy-membrane (contains mitochondria) and nuclear fractions (presumably representing association with the nuclear envelope; see below), with little BAR present in cytosol or low-density membrane factions. Reprobing the same blots with antibodies to mitochondrial (COX-IV), cytosolic (caspase-3), and nuclear (poly-ADP ribosyl polymerase) proteins validated the fractionation procedure (not shown). BAR also cofractionated with Bcl-2 (Fig. 2*F*). When examined by immunohistochemistry by using normal human tissue sections and monospecific anti-BAR antisera, BAR was present in an organellar pattern within the cytosol of most cells (Fig. 2*G* and data not shown). Preimmune serum and anti-BAR antiserum preadsorbed with recombinant BAR protein resulted in negligible immunostaining, confirming the specificity of these results (not presented). Microscopy examination of cells expressing GFP-tagged BAR confirmed these findings (not shown). BAR mRNA and protein were widely expressed in human tissues, as determined by Northern and immunoblot analyses (unpublished observations).

BAR Modulates Bax-Induced Apoptosis Through a SAM Domain-Dependent Mechanism. To explore how BAR might modulate Bax-induced cell death pathways, we examined whether the BAR protein can associate with members of the Bcl-2 family. For these experiments, Myc-epitope-tagged or untagged BAR or BAR(ΔR) proteins were coexpressed by transient transfection in 293T cells together with Bcl-2, Bcl-X_L, Bak, or Bax. Coimmunoprecipitation assays determined that BAR can specifically associate with antiapoptotic Bcl-2 and Bcl-X_L proteins (Fig. 3*A*), but not with Bax or Bak (not shown). The efficiency with which Bcl-2 coimmunoprecipitated with BAR was comparable to Bax (Fig. 3*A*) under the conditions of these assays.

The region within BAR required for its interaction with Bcl-2 was mapped by using a series of N- and C-terminal truncation mutants and internal fragments of BAR for *in vitro* protein-binding assays (Fig. 3*B*). Fragments of BAR that lacked the RING, DED, or TM domains retained Bcl-2-binding ability, indicating that none of these domains is necessary. In contrast, all fragments of BAR that retained the SAM domain bound Bcl-2 *in vitro*, whereas all fragments lacking this domain failed to bind Bcl-2. The dependence of the SAM domain for interactions with Bcl-2 was also confirmed by yeast two-hybrid assays (Fig. 3*C*).

We next explored the relevance of the SAM domain of BAR for suppression of Bax-induced cell death in yeast and for Bax-induced caspase activation and apoptosis in human cells. When coexpressed in yeast with Bax, the full-length BAR protein suppressed Bax-induced cell death and permitted growth on selective medium, whereas the BAR (ΔSAM) protein failed to rescue yeast from Bax-induced cell death (Fig. 3*D*). Immunoblot analysis confirmed production of the BAR and BAR (ΔSAM) proteins at comparable levels in yeast (not shown). For

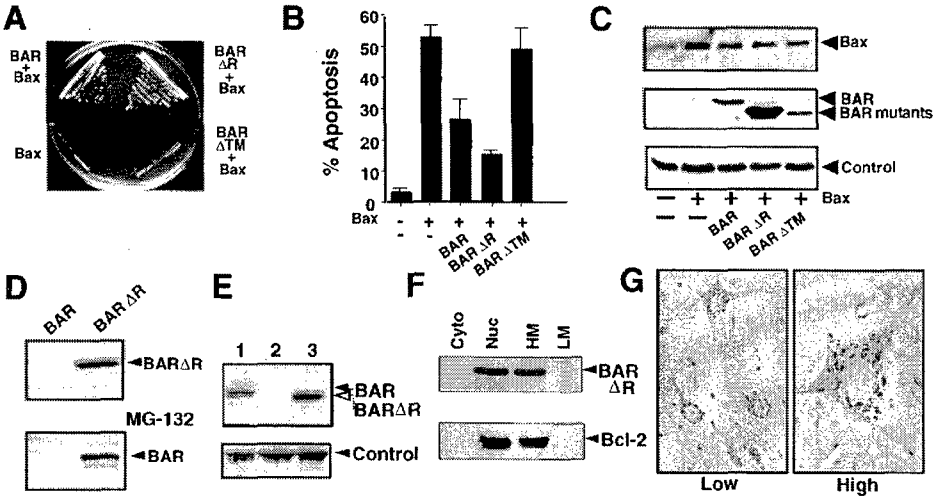

Fig. 2. BAR inhibits Bax-induced cell death in yeast and mammalian cells. (*A*) Plasmids encoding BAR, BAR(ΔR), BAR(ΔTM), or control plasmid were transformed into a yeast strain harboring YEp51-Bax. Transformants were streaked on galactose-containing synthetic medium lacking tryptophan and leucine and photographed after 4 days at 30°C. (*B*) 293T cells were transiently cotransfected with 0.1 μg of GFP-encoding marker plasmid and 4 μg of either pcDNA3 control (−) or 0.5 μg pcDNA3-Bax (+) plasmids together with 3.5 μg of plasmids encoding BAR, BAR(ΔR), or BAR(ΔTM) or a control plasmid (−). After 1 day, both floating and adherent cells (after trypsinization) were pooled, fixed, and stained with DAPI (18). The percentage of GFP-positive cells with fragmented nuclei or condensed chromatin (apoptotic) was determined (mean ± SD; $n = 3$). (*C*) 293T cell extracts (25 μg total protein) were prepared from the transfected cells shown in *B* and subjected to SDS/PAGE immunoblot analysis. (*D*) 293T cells were transfected with 2 μg of BAR- or BAR(ΔR)-encoding plasmids (*Upper*). Cell extracts (25 μg total protein) were prepared 1 day later and subjected to SDS/PAGE immunoblot analysis, by using anti-BAR antiserum. For determination of the effects of proteosome inhibition on BAR protein accumulation, 293T cells transfected with BAR-producing plasmid as above were cultured for 6 hr with (+) or without (−) 20 μM MG-132 before lysis and immunoblot analysis as above (*Lower*). Exposure times to x-ray film were adjusted to maximize differences. Longer exposures, however, demonstrated the presence of both full-length BAR and BAR(ΔR). (*E*) Immunoblot comparison of BAR levels in lysates (25 μg protein) prepared from MCF7 (1), control-transfected 293T cells (2), and BAR(ΔR)-transfected 293T cells (3), probed with anti-BAR antiserum. A band from the same blot resulting from anti-rabbit secondary antibody reactivity with an unidentified human protein is shown as a control for loading. (*F*) 293T cells were transiently transfected with plasmids encoding BAR(ΔR) and Bcl-2, then lysed 2 days later, and crude subcellular fractions of cytosol (Cyto), nuclei (Nuc), heavy membranes (HM), and light membranes (LM) were prepared (20). Fractions were normalized for cell equivalents and analyzed by SDS/PAGE immunoblotting, by using antisera specific for BAR (*Upper*) and Bcl-2 (*Lower*). (*G*) Immunohistochemistry-based analysis of BAR was performed by using paraffin-embedded tissue sections from multiple human tissues (spinal cord is shown here) and anti-BAR antiserum with DAB-colorimetric detection. Representative photomicrographs show neurons at lower (*Left*) and higher (*Right*) magnification, demonstrating punctate organelle-like distribution of BAR.

mammalian cell experiments, 293T (Fig. 3) cells were cotransfected with a Bax-producing plasmid together with plasmids encoding either BAR or BAR (ΔSAM) proteins. Cells were recovered 1 day later, and either cell lysates were prepared for assaying caspase activity by using the fluorigenic substrate Asp-Glu-Val-Asp-aminofluorocoumarin (DEVD-AFC) (Fig. 3*E*) or the percentage of apoptotic cells was quantified based on DAPI staining (Fig. 3*F*). Overexpression of Bax induced caspase activation and apoptosis, which were both markedly suppressed by coexpression of full-length BAR but not by BAR (ΔSAM) (Fig. 3 *E* and *F*). Immunoblot analysis confirmed that neither BAR nor BAR(ΔSAM) interfered with Bax protein production and demonstrated that the BAR and BAR (ΔSAM) proteins were produced at roughly equivalent levels in these transfected cells (Fig. 3*F* and data not presented). Taken together, the results demonstrate that the SAM domain of BAR is required both for its interactions with Bcl-2 and its ability to suppress Bax-induced cell death.

BAR Binds DED-Containing Caspases and Suppresses Fas-Induced Apoptosis. The presence of a DED-like domain in the BAR protein suggested that it might interact with other DED-containing proteins. Indeed, BAR and BAR(ΔR) specifically interacted with procaspase-8 and -10 in coimmunoprecipitation assays by using lysates from transfected 293T cells (Fig. 4*A* and data not shown). In contrast, BAR and BAR(ΔR) did not coimmunoprecipitate with Fadd (Fig. 4*A*), even though interactions of Fadd with procaspases-8 and 10 were detectable under the same experimental conditions (not shown). Thus, BAR associates with some but not all DED-family proteins. Mutagenesis studies confirmed a role for the DED domains of BAR, procaspase-8 and -10 for mediating their interactions (Fig. 4 *B* and *C*).

Because caspase-8 is essential for Fas-induced apoptosis (36, 37), we sought evidence that BAR could modulate this apoptotic pathway. For these experiments, 293 (Fig. 4) or HT1080 (not shown) cells were transfected with plasmids encoding Fas in combination with either a control plasmid or plasmids producing the BAR, BAR(ΔR) and BAR(ΔDED) proteins. Caspase activity and apoptosis were then assayed after 1 day. 293 and HT1080 cells were chosen for these studies because overexpression of Fas triggers apoptosis in these cells through a Bcl-2-independent mechanism (20, 38), thus avoiding any contributions that BAR might make with respect to modulation of Bcl-2 family proteins. As shown, Fas stimulated activation of DEVD-cleaving caspases and triggered apoptosis (Fig. 4 *D* and *E*), both of which were partially blocked by coexpression of BAR or BAR(ΔR). In contrast, BAR(ΔDED) and BAR (ΔR/ΔDED), which failed to bind procaspase-8, were ineffective at blocking Fas-induced activation of caspases and apoptosis (Fig. 4 *D* and *E*). Thus, BAR requires the DED domain to interact with procaspase-8 and to suppress Fas-induced apoptosis. Immunoblot analysis also revealed correlations with Fas-induced processing of procaspase-8, with BAR reducing the amount of processed procaspase-8 produced as a result of Fas overexpression (Fig. 4*F*).

BAR Can Mediate Association of Bcl-2 and Procaspase-8. Recognizing that BAR is capable of interacting with both Bcl-2 and procaspase-8, we determined whether BAR bridges these two proteins together in a complex. Accordingly, Bcl-2 and Flag-

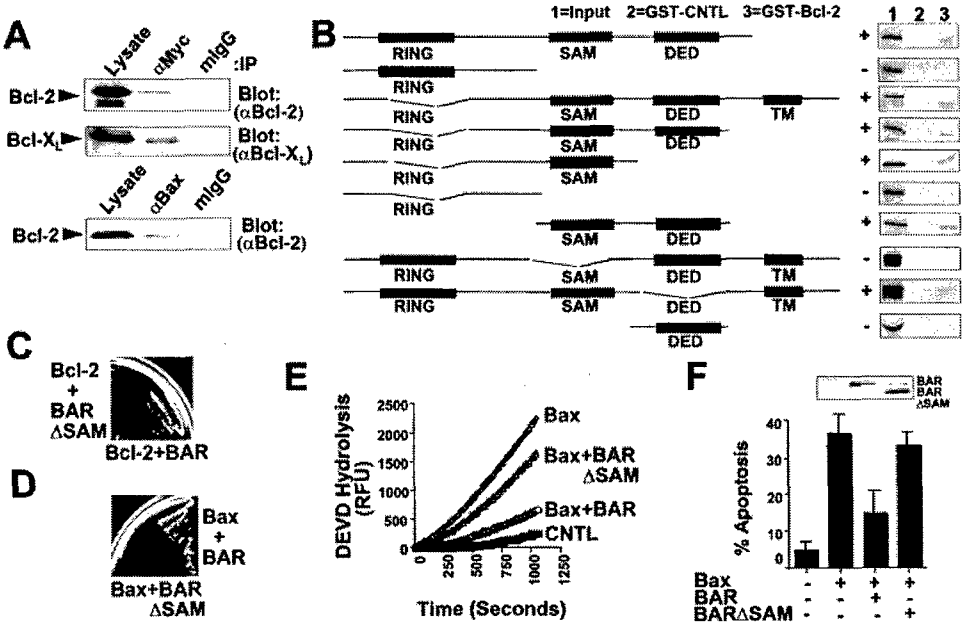

Fig. 3. SAM Domain of BAR Is Required for Interaction with Bcl-2 and Inhibition of Bax-Induced Apoptosis. (*A*) 293T cells were transiently transfected with plasmids encoding Myc-BAR(ΔR) and either Bcl-2 or Bcl-X_L (*Upper*) or with plasmids encoding Bax and Bcl-2 (*Lower*). Cells were lysed 2 days later in buffer containing 0.4% Nonidet P-40, and immunoprecipitations were performed by using anti-Myc or anti-Bax antibodies or by using mouse IgG_1 as a control. Immune complexes and lysates (representing ≈5% of input) were subjected to SDS/PAGE and immunoblot analysis by using antisera for detection of Bcl-2 or Bcl-X_L. (*B*) For *in vitro* binding studies, *in vitro* translated ^{35}S-labeled BAR mutant proteins were incubated with 10 μg of either GST-Bcl-2 or GST (control; CNTL) recombinant proteins, and protein complexes were recovered on glutathione-Sepharose and analyzed by SDS/PAGE followed by autoradiography. *In vitro* translation mixes (10% input) were run directly in gels as a control. A wide variety of control GST proteins were tested, thus confirming specificity of BAR interactions with Bcl-2 (not shown). All BAR fragments shown were >50% intact when produced by *in vitro* translation in reticulocyte lysates, but others attempted could not be produced without extensive degradation, such as SAM only. (*C*) For yeast two-hybrid assay, 1 μg pGilda-Bcl-2(ΔTM) was cotransformed into EGY191 cells with 1 μg pJG4–5-BAR or pJG4–5-BAR(ΔSAM). Transformants were initially selected on glucose-containing medium lacking histidine and tryptophan. Two-hybrid interactions were assayed by streaking onto galactose plates lacking leucine, histidine, and tryptophan. Use of various positive and negative control proteins in yeast two-hybrid assays confirmed the validity of these observations (not shown). (*D*) For cytotoxicity assays in yeast, plasmids encoding BAR or BAR(ΔSAM) were transformed into a yeast strain harboring YEp51-Bax. Transformants were then streaked on galactose-containing synthetic medium lacking tryptophan and leucine. Photograph was taken after 4 days at 30°C. (*E*) For caspase assays, 293T cells were transfected with either 4 μg of vector control plasmid (CNTL) or with 0.5 μg Bax-encoding plasmid together with 3.5 μg of either vector control plasmid or plasmids encoding BAR or BAR(ΔSAM). Cell extracts were prepared 24 hr after transfection, normalized for protein content (25 μg), and incubated with 100 μM DEVD-AFC. Enzyme activity was determined by the release of the AFC fluorophore (expressed as relative fluorescence units, RFU). (*F*) A portion of the transfected 293T cells described in *E* were stained with DAPI, and the percentage of GFP-positive cells with fragmented or condensed nuclei (apoptotic) was determined (mean ± SD; $n = 3$). *Inset* shows immunoblot analysis of lysates from transfected cells using anti-BAR antiserum with enhanced chemiluminescence-based detection.

procaspase-8 were coexpressed in 293T cells by transient transfection, in the presence or absence of cotransfected BAR. Coimmunoprecipitation assays revealed that Bcl-2 was readily detected in caspase-8-containing immune complexes when using lysates from cells overexpressing BAR but not in lysates of control transfected 293T cells (Fig. 4*G*), which contain relatively little endogenous BAR protein. Coexpression of Bax prevented BAR-mediated coimmunoprecipitation of Bcl-2 and procaspase-8 (not shown), suggesting that Bcl-2 cannot simultaneously bind Bax and BAR. We therefore conclude that BAR can bridge Bcl-2 and procaspase-8, at least when overexpressed, thus bringing together members of two important families of proteins involved in apoptosis regulation.

Discussion

BAR represents an apoptosis regulator having unique features heretofore not seen in other modulators of cell death pathways. This protein has a multidomain structure, which includes RING, SAM, DED, and TM domains, thus suggesting it may serve as a scaffold protein that integrates interactions and communication between two types of apoptosis-regulatory proteins—namely, the DED-containing initiator caspases and Bcl-2 family proteins. Though the extrinsic (e.g., Fas/death receptor) and intrinsic (e.g., Bax/mitochondrial) pathways for apoptosis are capable of operating independently, crosstalk between these two major pathways for apoptosis also occurs (2, 3, 12, 13). In this regard, overexpression of Bcl-2 or Bcl-X_L can protect some cell lines *in vitro* and some tissues *in vivo* from Fas-induced apoptosis (39–43), but not others. Sensitivity to Bcl-2 protection from Fas-induced apoptosis correlates with reduced activation of procaspase-8 after Fas crosslinking (44), requiring a mitochondrial amplification step to achieve sufficient activation of downstream caspases for triggering apoptosis (45). Antiapoptotic DED-containing proteins such as BAR, Bap31 (46), and Flip (7) may compete with adaptor proteins such as Fadd for binding to procaspases-8 and -10, thus reducing the amount of caspase processing and activation (9).

At present, it remains unclear why BAR suppressed Bax-induced cell death in yeast, given that we have been unable to demonstrate interaction of BAR with Bax by coimmunoprecipitation or yeast two-hybrid assays. However, the observation that the SAM and TM domains of BAR are required for suppression of Bax-induced cell death in both yeast and mammalian cells suggests a conserved mechanism.

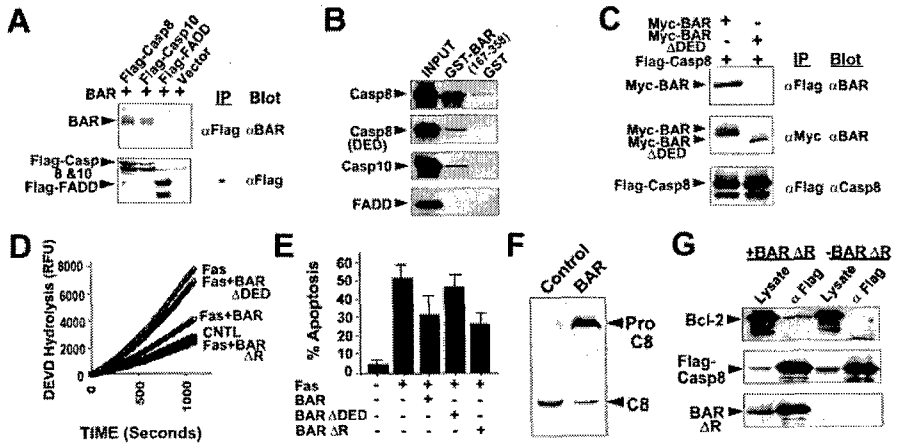

Fig. 4. DED Domain of BAR Is Required for Interactions with Procaspases-8 and -10 and for Inhibition of Fas-induced Apoptosis. (*A*) Coimmunoprecipitation assays were performed as described above by using 293T cells transfected with plasmids encoding Myc-BAR and either Flag-procaspase-8 (cys/ala), procaspase-10 (cys/ala), or Fadd. (*B*) For *in vitro* binding studies, *in vitro* translated ^{35}S-labeled procaspase-8, procaspase-8 domain (DED), procaspase-10, and FADD proteins were incubated with 10 μg of either GST or GST-BAR-DED (residues 167–358) recombinant proteins. Protein complexes were recovered on glutathione-Sepharose beads, followed by analysis by SDS/PAGE autoradiography. *In vitro* translation mixes (10% input) were run directly in gels as a control. A wide variety of control GST proteins were tested, thus confirming specificity of BAR interactions with procaspases-8 and -10 (not shown). (*C*) 293T cells were cotransfected with 5 μg of either BAR- or BAR(ΔDED)-encoding plasmids and 5 μg of a plasmid encoding Flag-procaspase-8. Cell extracts were prepared 2 days later, and immunoprecipitates were prepared by using either anti-Flag or anti-Myc monoclonal antibodies. Immune complexes were subjected to SDS/PAGE immunoblot analysis, by using anti-BAR and anti-procaspase-8 antibodies. (*D*) For caspase activity assays, 293T cells were transfected with either control plasmid or cotransfected with 0.3 μg of Fas-encoding plasmid and 3.7 μg of either control plasmid or plasmids encoding BAR, BAR(ΔDED) or BAR(ΔR). Cell extracts were prepared 1 day later, normalized for total protein (25 μg), and incubated with 100 μM DEVD-AFC. Enzyme activity was determined by the release of the AFC fluorophore. (*E*) A portion of the transfected 293T cells described above were stained with DAPI, and the percentage of GFP-positive cells with fragmented or condensed nuclei (apoptotic) was determined (mean ± SD; $n = 3$). (*F*) 293T cells were transfected with plasmids encoding procaspase-8 and either pcDNA3 (control) or pcDNA3-Myc-BAR. Cell lysates were prepared 1 day later, normalized for protein content (50 μg), and analyzed by SDS/PAGE immunoblotting by using anti-caspase-8 antiserum. The positions of the unprocessed procaspase-8 and the large subunit of processed caspase-8 are indicated by arrows. (*G*) 293T cells were cotransfected with 5 μg each of plasmids encoding Bcl-2, Flag-Procaspase-8 and either 10 μg of BAR encoding plasmid (+BAR) or control plasmid (−BAR). Cell extracts were prepared 2 days later and immunoprecipitates were prepared by using anti-Flag antibody. Immune complexes were analyzed by SDS/PAGE immunoblotting, probing the same blot sequentially with anti-Bcl-2 antiserum (*Top*), anti-Flag monoclonal antibody (*Middle*), and anti-BAR antiserum (*Bottom*), with antibody stripping between each detection. Data are representative of several experiments and include a wide variety of control transfections and immunoprecipitations that further confirmed specificity of the observed interactions.

Though gene transfer-mediated overexpression of BAR was used here for assaying its effects on apoptosis pathways, the levels of BAR produced by transfection of 293T and HT1080 cells were similar to the endogenous levels of BAR found in a variety of human tumor cell lines, based on comparisons by immunoblotting (unpublished observations). Thus, levels of BAR sufficient to impact apoptosis pathways can occur at least within the context of cancer. Further analysis of BAR in other cellular contexts and ultimately by gene ablation experiments in mice is required to understand the overall importance of this protein for the *in vivo* regulation of apoptosis.

We thank E. Smith, R. Cornell, and S. Farrar for manuscript preparation; F. Pio for computer analysis; S. Matsuzawa (The Burnham Institute), D. Sykes (Buffalo General Hospital, Buffalo, NY), and S. Torii (Gunma University, Gunma, Japan), for plasmids; and the National Institutes of Health (NIH)/National Institutes on Aging (AG15393), A.G. and K.P. under NIH Grant GM60049, CaP-CURE, and the Department of Defense Breast Cancer Research Program (Q.X. and H.Z.) for generous support.

1. Wallach, D., Boldin, M., Varfolomeev, E., Beyaert, R., Vandenabeele, P. & Fiers, W. (1997) *FEBS Lett.* **410**, 96–106.
2. Salvesen, G. S. & Dixit, V. M. (1997) *Cell* **91**, 443–446.
3. Ashkenazi, A. & Dixit, V. (1998) *Science* **281**, 1305–1308.
4. Chinnaiyan, A. M., O'Rourke, K., Tewari, M. & Dixit, V. M. (1995) *Cell* **81**, 505–512.
5. Boldin, M. P., Varfolomeev, E. E., Pancer, Z., Mett, I. L., Camonis, J. H. & Wallach, D. (1995) *J. Biol. Chem.* **270**, 7795–7798.
6. Bertin, J., Armstrong, R., Ottilie, S., Martin, D., Wang, Y., Banks, S., Wang, G., Senkevich, T., Alnemri, E., Moss, B., *et al.* (1997) *Proc. Natl. Acad. Sci. USA* **94**, 1172–1176.
7. Irmler, M., Thome, M., Hahne, M., Schneider, P., Hofmann, K., Steiner, V., Bodmer, J.-L., Schröter, M., Burns, K., Mattmann, C., *et al.* (1997) *Nature (London)* **388**, 190–195.
8. Thome, M., Schneider, P., Hofmann, K., Fickenscher, H., Meinl, E., Neipel, F., Mattmann, C., Burns, K., Bodmer, J.-L., Schroter, M., *et al.* (1997) *Nature (London)* **386**, 517–521.
9. Tschopp, J., Irmler, M. & Thome, M. (1998) *Curr. Opin. Immunol.* **10**, 552–558.
10. Zou, H., Henzel, W. J., Liu, X., Lutschg, A. & Wang, X. (1997) *Cell* **90**, 405–413.
11. Li, P., Nijhawan, D., Budihardjo, I., Srinivasula, S., Ahmad, M., Alnemri, E. & Wang, X. (1997) *Cell* **91**, 479–489.
12. Adams, J. & Cory, S. (1998) *Science* **281**, 1322–1326.
13. Green, D. & Reed, J. (1998) *Science* **281**, 1309–1312.
14. Schendel, S., Montal, M. & Reed, J. C. (1998) *Cell Death Differ.* **5**, 372–380.
15. Narita, M., Shimizu, S., Ito, T., Chittenden, T., Lutz, R. J., Matsuda, H. & Tsujimoto, Y. (1998) *Proc. Natl. Acad. Sci. USA* **95**, 14681–14686.
16. Jurgensmeier, J. M., Xie, Z., Deveraux, Q., Ellerby, L., Bredesen, D. & Reed, J. C. (1998) *Proc. Natl. Acad. Sci. USA* **5**, 4997–5002.
17. Finucane, D. M., Bossy-Wetzel, E., Cotter, T. G. & Green, D. R. (1998) *J. Biol. Chem.* **274**, 2225–2233.
18. Zha, H., Fisk, H. A., Yaffe, M. P., Mahajan, N., Herman, B. & Reed, J. C. (1996) *Mol. Cell. Biol.* **16**, 6494–6508.
19. Manon, S., Chaudhuri, B. & Buérin, M. (1997) *FEBS Lett.* **415**, 29–32.
20. Xu, Q. & Reed, J. C. (1998) *Mol. Cell* **1**, 337–346.
21. Wang, H. G., Rapp, U. R. & Reed, J. C. (1996) *Cell* **87**, 629–638.
22. Krajewski, S., Krajewska, M., Shabaik, A., Wang, H.-G., Irie, S., Fong, L. & Reed, J. C. (1994) *Cancer Res.* **54**, 5501–5507.
23. Jaroszewski, L., Rychlewski, B., Zhang, B. & Godzik, A. (1998) *Protein Sci.* **7**, 1431–1440.
24. Rychlewski, L., Jaroszewski, L., Li, W. & Godzik, A. (2000) *Protein Sci.* **9**, 232–241.
25. Altschul, S. F., Madden, T. L., Schaeffer, A. A., Zhang, J., Zhang, Z., Miller, W. & Lipman, D. J. (1997) *Nucleic Acids Res.* **25**, 3389–3402.
26. Sali, A. & Blundell, T. L. (1993) *J. Mol. Biol.* **234**, 779–815.
27. Jaroszewski, L., Pawłowski, K. & Godzik, A. (1998) *J. Mol. Model.* **4**, 294–309.
28. Peter, M., Medema, J. & Krammer, P. (1997) *Cell Death Differ.* **4**, 523–525.
29. Eberstadt, M., Huang, B., Chen, Z., Meadows, R., Ng, S., Zheng, L., Lenardo, M. & Fesik, S. (1998) *Nature (London)* **392**, 941–945.
30. Rost, B. (1996) *Methods Enzymol.* **266**, 525–539.
31. Rychlewski, L. & Godzik, A. (1997) *Protein Eng.* **10**, 1143–1153.
32. Thanos, C., Goodwill, K. & Bowie, J. (1999) *Science* **283**, 833–836.
33. Kubbutat, M. H., Jones, S. N. & Vousden, K. H. (1997) *Nature (London)* **387**, 299–303.
34. Hu, G. & Fearon, E. R. (1999) *Mol. Cell. Biol.* **19**, 724–732.
35. Kamura, T., Koepp, D., Conrad, M., Skowyra, D., Moreland, R., Iliopoulos, O., Lane, W., Kaelin, W. J., Elledge, S., Conaway, R., *et al.* (1999) *Science* **284**, 657–661.
36. Muzio, M., Chinnaiyan, A. M., Kischkel, F. C., O'Rourke, K., Shevchenko, A., Ni, J., Scaffidi, C., Bretz, J. D., Zhang, M., Gentz, R., *et al.* (1996) *Cell* **85**, 817–827.
37. Nagata, S. (1997) *Cell* **88**, 355–365.
38. Frisch, S. M., Vuori, K., Kelaita, D. & Sicks, S. (1996) *J. Cell Biol.* **135**, 1377–1382.
39. Srinivasan, A., Li, F., Wong, A., Kodandapani, L., Smidt, R., Krebs, J., Fritz, L., Wu, J. & Tomaselli, K. (1998) *J. Biol. Chem.* **273**, 4523–4529.
40. Medema, J., Scaffidi, C., Krammer, P. & Peter, M. (1998) *J. Biol. Chem.* **273**, 3388–3393.
41. Torigoe, T., Millan, J. A., Takayama, S., Taichman, R., Miyashita, T. & Reed, J. C. (1994) *Cancer Res.* **54**, 4851–4854.
42. Lacronique, V., Mignon, A., Fabre, M., Viollet, B., Rouquet, N., Molina, T., Porteu, A., Henrion, A., Bouscary, D., Varlet, P., *et al.* (1996) *Nat. Med.* **2**, 80–86.
43. Rodriguez, I., Matsuura, K., Khatib, K., Reed, J. C., Nagata, S. & Vassalli, P. (1996) *J. Exp. Med.* **183**, 1031–1036.
44. Scaffidi, C., Fulda, S., Srinivasan, A., Friesen, C., Li, F., Tomaselli, K., Debatin, K.-M., Krammer, P. & Peter, M. (1998) *EMBO J.* **17**, 1675–1687.
45. Kuwana, T., Smith, J. J., Muzio, M., Dixit, V., Newmeyer, D. D. & Kornbluth, S. (1998) *J. Biol. Chem.* **273**, 16589–16594.
46. Ng, F. W. H., Nguyen, M., Kwan, T., Branton, P. E., Nicholson, D. W., Cromlish, J. A. & Shore, G. C. (1997) *J. Cell Biol.* **39**, 327–338.

Cell Death and Differentiation (2003) 10, 1178–1187

www.nature.com/cdd

Bifunctional apoptosis inhibitor (BAR) protects neurons from diverse cell death pathways

W Roth[1,3], P Kermer[1,3,4], M Krajewska[1], K Welsh[1], S Davis[2], S Krajewski[1] and JC Reed*[,1]

[1] The Burnham Institute, 10901 N. Torrey Pines Road, La Jolla, CA 92037, USA
[2] Isis Pharmaceuticals, Inc., Carlsbad, CA, USA
[3] WR and PK contributed equally to this work.
[4] Current address: Department of Neurology, University of Goettingen, Germany.
* Corresponding author: JC Reed, Tel: 858-646-3140; Fax: 858-646-3194; E-mails: jreed@burnham.org, reedoffice@burnham.org

Received 24.2.03; revised 10.4.03; accepted 07.5.03

Abstract

The bifunctional apoptosis regulator (BAR) is a multidomain protein that was originally identified as an inhibitor of Bax-induced apoptosis. Immunoblot analysis of normal human tissues demonstrated high BAR expression in the brain, compared to low or absent expression in other organs. Immunohistochemical staining of human adult tissues revealed that the BAR protein is predominantly expressed by neurons in the central nervous system. Immunofluorescence microscopy indicated that BAR localizes mainly to the endoplasmic reticulum (ER) of cells. Overexpression of BAR in CSM 14.1 neuronal cells resulted in significant protection from a broad range of cell death stimuli, including agents that activate apoptotic pathways involving mitochondria, TNF-family death receptors, and ER stress. Downregulation of BAR by antisense oligonucleotides sensitized neuronal cells to induction of apoptosis. Moreover, the search for novel interaction partners of BAR identified several candidate proteins that might contribute to the regulation of neuronal apoptosis (HIP1, Hippi, and Bap31). Taken together, the expression pattern and functional data suggest that the BAR protein is involved in the regulation of neuronal survival.
Cell Death and Differentiation (2003) **10,** 1178–1187. doi:10.1038/sj.cdd.4401287

Keywords: apoptosis; BAR; neurodegeneration; neurons; astrocytoma

Abbreviations: Bap31, B-lymphocyte receptor-associated protein 31; BAR, bifunctional apoptosis regulator; BID, BH3 interacting domain death agonist; CNS, central nervous system; DED, death effector domain; ER, endoplasmic reticulum; FADD, Fas-associated death domain; FITC, fluorescein isothiocyanate; GFP, green fluorescent protein; HIP1, Huntingtin-interacting protein; Hippi, HIP1 protein interactor; kDa, kilo Dalton; MPTP, 1-methyl-4-phenyl-1,2,3,6-tetrahydropyridine; PBS, phosphate-buffered saline; kb, kilobase pairs; PDI, protein disulfide isomerase; PEA15, phosphoprotein enriched in astrocytes 15; STS, staurosporine; XIAP, X-linked inhibitor of apoptosis

Introduction

Tight regulation of signalling pathways controlling neuronal death and survival is crucial for the normal development and function of the nervous system. In contrast to most cell types, neurons survive for the entire lifetime of the organism and therefore need to possess powerful intracellular mechanisms to antagonize cell death stimuli. Dysregulation of apoptotic cell death pathways can lead to several neurological conditions. Neurodegenerative diseases such as Parkinson's or Huntington's disease are characterized by a relative preponderance of proapoptotic intracellular signalling events in certain populations of neurons.[1,2] Similarly, delayed neuronal death in the ischemic penumbra after occurrence of a stroke may be mediated by apoptosis.[3]

Several antiapoptotic proteins are involved in the protection of neurons from damaging influences such as oxidative stress, lack of neurotrophic factors, or toxins. Antiapoptotic members of the Bcl-2 family have been shown to protect neurons from metabolic and oxidative insults by stabilizing mitochondrial functions, thereby inhibiting cytochrome *c* release, Apaf-1 oligomerization, and activation of Caspase 9.[4] Inhibitor of apoptosis proteins (IAPs) may play an important role in neuronal cell survival mechanisms by directly binding to and inhibiting Caspases 3, 7, or 9.[5,6] Compared to the regulation of mitochondrial apoptosis, the relevance of death receptor- and Caspase-8-mediated apoptosis in neurons is far less well documented. However, TNFα may induce neuronal death after nerve growth factor withdrawal[7] and HIV-1 infection.[8,9] Further, neuronal death in Huntington's disease may involve Caspase-8 activation dependent on a protein complex comprising HIP1, Hippi, and Caspase-8.[10]

The bifunctional apoptosis inhibitor (BAR) is a multidomain protein that was first discovered as an inhibitor of Bax-induced cell death.[11] BAR is capable of inhibiting apoptosis induced by TNF-family death receptors ('extrinsic pathway') as well as mitochondria-dependent apoptosis ('intrinsic pathway'). Interaction of BAR with Bcl-2 or Bcl-X_L via a SAM domain may contribute to the antiapoptotic properties of BAR. Moreover, the BAR protein contains a domain that shares similarity with classical death effector domains (termed 'pseudo DEDs'), which mediates Caspase-8 binding. Therefore, BAR was suggested to act as a scaffold protein that can bridge components of extrinsic and intrinsic apoptosis pathways. This theory was supported by the finding that active Caspase-8 subunits are sequestered to Bcl-X_L/BAR complexes, thereby preventing further cleavage of Caspase-8 substrates and subsequent cell death in the context of Fas-induced apoptosis.[12]

In this report, we provide evidence that BAR is mainly expressed *in vivo* by neurons in the central and peripheral

nervous systems. Overexpressed BAR protects neuronal cell lines from a broad range of cell death stimuli, while down-regulation of endogenous BAR leads to sensitization to apoptosis. Our findings suggest that the biological functions of the BAR protein *in vivo* are likely to be relevant to suppression of cell death and maintenance of survival of neurons.

Results

BAR is predominantly expressed in neurons

The physiological functions of the BAR protein are largely unknown. To investigate the possible roles of BAR *in vivo*, we studied the expression pattern of this protein in human organs. To this end, we performed an immunoblot analysis of human normal tissue samples using a BAR-specific rabbit antiserum, previously described.[11] BAR expression was highest by far in brain, with moderate expression in small intestine, weak expression in testes, and only faint expression in liver and skeletal muscle (Figure 1a). No signal was detected in heart, kidney, lung, and spleen.

To demonstrate antibody specificity, we analyzed tissue lysates of brain, heart, and small intestine side by side with lysates of SK-N-BE(2) neuroblastoma cells that had been transfected with BAR-specific antisense oligonucleotides (Figure 1b). Treatment of SK-N-BE(2) cells with BAR-specific antisense oligonucleotides resulted in a significant decrease in signal intensity of an ~50 kDa protein band that comigrates in gels with the same immunoreactive band as present endogenously in tissue lysates, confirming that this band is BAR.

Owing to the distinct expression pattern in various organs, we studied the anatomic distribution of BAR in greater detail by performing immunohistochemical staining of paraffin-embedded, human tissue specimens. The staining pattern was generally organellar or diffuse cytosolic. Staining for BAR was present in keratinizing epithelium in the upper layers of the epidermis (Figure 2a), but not in nonkeratinizing squamous epithelium of the esophagus (Figure 2b), cervix, stomach, intestine, and lung (not shown). Moreover, BAR expression was found in seminiferous tubules (secondary spermatocytes and early spermatids; Figure 2c), in endometrial glands, the fallopian tubes, and in plasma cells in the colonic lamina propria (not shown). Multiple tissues were entirely negative for BAR staining including prostate (Figure 2d), spleen, bone marrow, smooth and skeletal muscle, hypophysis, thyroid, liver, and pancreas.

Overall, BAR staining was most prominent in the nervous system. Highest signal intensities were observed in neurons in the central and peripheral nervous systems. Both the cell bodies and axons of neurons were stained with anti-BAR antibody. Among neuronal types, the strongest BAR immunostaining was found in pyramidal neurons located in cortical layers III–V (Figure 2e–h) and in the neurons of the nuclei of pontomedullary reticular formation, such as the principal olivary nucleus (Figure 2i,j) and the facial (Figure 2k) and hypoglossal nuclei, and in the red nucleus in the mesencephalon. Purkinje cells, granular neurons, and the synapses of the mossy fibers on granule cells in the cerebellum were strongly positive (Figure 2l).

Within the peripheral nervous system, neurons in the sympathetic ganglia and dorsal root ganglia (Figure 2m–o) exhibited strong staining. Moreover, peripheral neurons showed intense staining in ganglion cells of Meissner's plexus, interspersed among negative smooth muscle adjoining unstained gastrointestinal epithelium (not shown). In contrast to the adrenal cortex, where no staining was observed, neuroendocrine chromaffin cells in the adrenal medulla were positive for BAR staining (Figure 2p–r). Strong BAR signal was also observed in pinealocytes, but not in the glial compartment (Figure 2s,t).

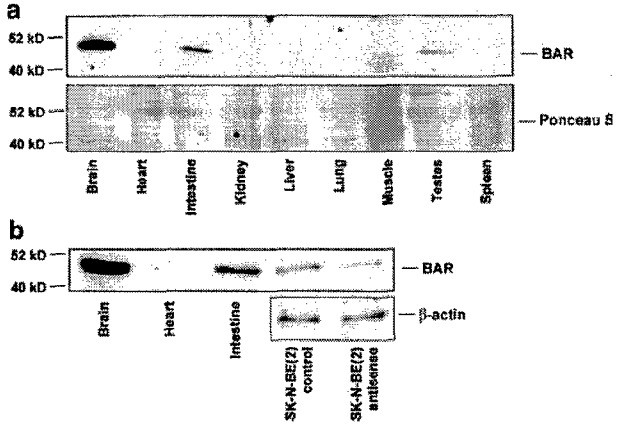

Figure 1 Expression of BAR in human adult tissues. (**a**) Immunoblot analysis of BAR in human tissues. Human tissue lysates (25 μg) were analyzed by SDS-PAGE/immunoblot using anti-BAR antiserum (1 : 3000) and HRP-coupled secondary antibody (top panel). As a protein loading control, the membrane was stained with Ponceau S solution (bottom panel). (**b**) Specificity of the polyclonal anti-BAR antibody was demonstrated by including cell lysates from anti-BAR antisense oligonucleotide-treated SK-N-BE(2) cells during immunoblot analysis of human tissue samples. The BAR protein migrates at a molecular weight of ~50 kDa

BAR localizes to the endoplasmic reticulum (ER)

Since immunohistochemistry showed an organellar-like staining pattern for BAR in neuronal cells, we examined the subcellular localization of the BAR protein in cells of neural origin. First, we sought to confirm the staining pattern observed in immunohistochemistry by performing immunofluorescence staining of SK-N-BE(2) neuroblastoma cells that had been shown to express endogenous BAR (Figure 1b). In accordance with the immunohistochemical findings, staining of these cells with anti-BAR antiserum produced a perinuclear and organellar-like fluorescence signal, whereas staining with preimmune serum produced no signal (Figure 3a,b). To examine BAR localization in more detail, we stably transfected the rat nigrostriatal cell line CSM 14.1 and the human astrocytoma cell line LN18 with a truncated version of BAR lacking its N-terminal RING domain, BAR(ΔR). Removal of the RING domain of BAR has been shown to prevent proteasome-dependent degradation of the protein,[11] allowing greater protein accumulation. The generation of these cell lines served as a useful model for expression and functional studies since: (i) BAR-transfected CSM cells allow the study of BAR localization and function in cells of neuronal origin, while

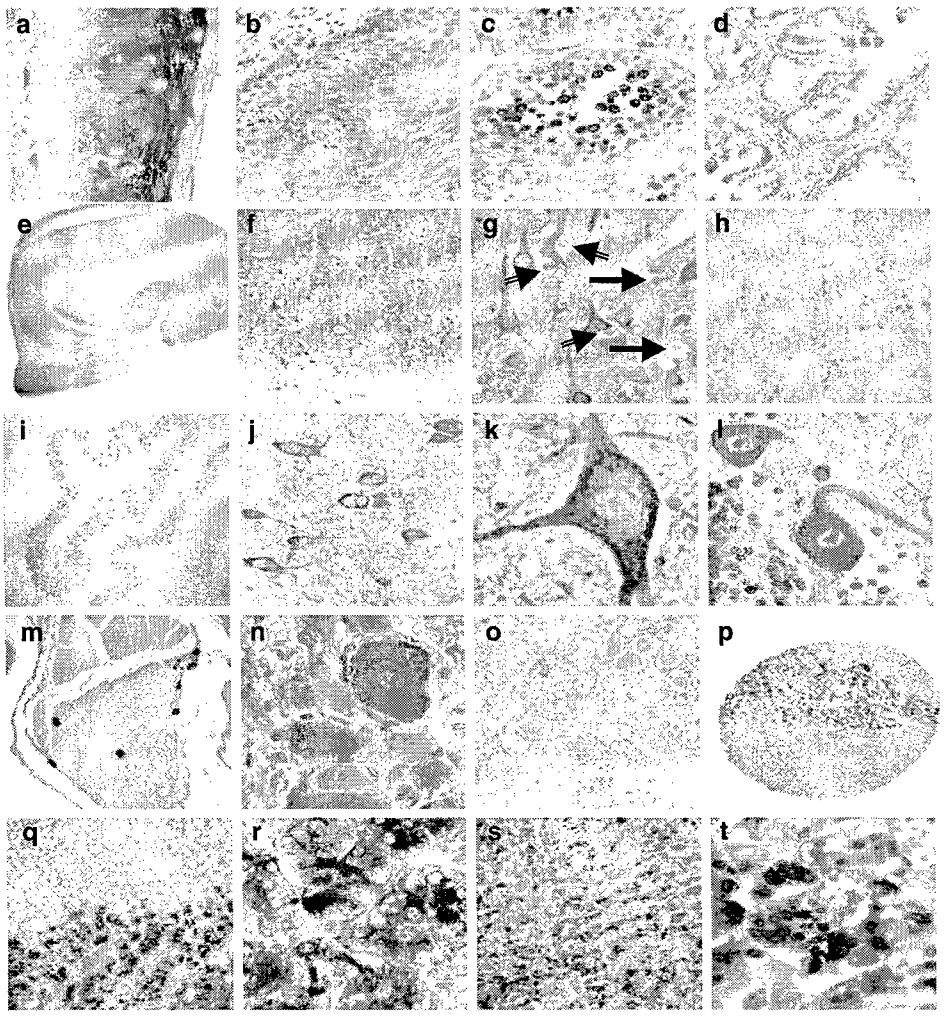

Figure 2 Immunohistochemical analysis of BAR expression. Expression of the BAR protein in normal human tissues is demonstrated in epidermis ((**a**) × 400), esophageal squamous, nonkeratinizing epithelium ((**b**) × 200), testis ((**c**) × 400), and prostate ((**d**) × 200). In the central nervous system, BAR expression was exclusively neuronal as shown in the examples from the occipital cortex ((**e**) × 40; (**f**) × 100; (**g**) × 400). The subcellular pattern in neurons is organellar and fine granular cytoplasmic in perikaryon and dendrites. The negative astroglia (long arrows) and satellite oligodendroglia (short arrows) are clearly visible in panel (**g**). The specificity control of the antibody preabsorbed with BAR recombinant protein is demonstrated in (**h**) (× 100) and (**o**) (× 400). BAR immunoreactivity in other parts of the CNS is shown in examples of olivary nucleus ((**i**) × 100 and (**j**) × 400), motoneurons in the facial nucleus of the brain stem ((**k**) × 1000), and Purkinje cells in the cerebellum ((**l**) × 1000). In the peripheral nervous system, ganglion cells in dorsal root ganglia were strongly positive for BAR staining ((**m**) × 100 and (**n**) × 1000), whereas nerve fibers and myelin were negative. Moreover, prominent BAR immunoreactivity was detected in adrenal medulla ((**p**) × 80; (**q**) × 200; (**r**) × 1000) and in pinealocytes ((**s**) × 200; (**t**) × 1000)

BAR-transfected astrocytic LN18 cells serve as a control cell line for possible neuron-specific effects; and (ii) the epitope-tagged, ectopically expressed BAR protein allows detection by two independent antibodies, anti-BAR and anti-myc. For each cell line, several subclones of BAR transfectants were generated (Figure 3c). Cells stably transfected with empty expression vectors served as controls. The subcellular localization of the epitope-tagged BAR in these transfected cells was then accomplished by immunofluorescence and organelles were simultaneously colocalized using a mitochondrial marker (Mitotracker) or an ER marker (anti-protein disulfide isomerase, PDI). As shown in Figure 3, BAR exhibited clear colocalization with PDI (Figure 3d–f), whereas only partial overlap was detected with the mitochondrial marker (Figure 3g–i). Similar findings were obtained in LN18 cells, as well as in transiently transfected COS-7 cells (data not shown), suggesting that BAR resides mainly in association with the ER, independent of cell type.

BAR protects neuronal cells from a broad range of cell death stimuli

The prominent expression of BAR in neurons together with its distinct subcellular localization suggests that BAR might be relevant for survival pathways, particularly in CNS cells. Therefore, we sought to characterize BAR functions in CSM neuronal cells and to compare these results with BAR-induced effects in other, non-neuronal CNS cells. Since BAR was initially identified as an apoptosis regulator that inhibits intrinsic as well as extrinsic apoptotic signalling, we first

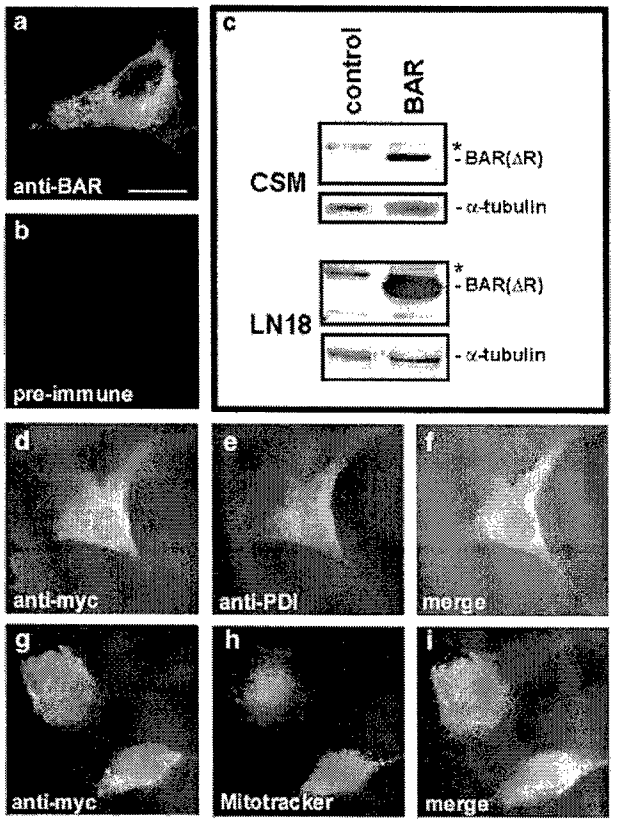

Figure 3 Subcellular localization of BAR. (**a,b**) Expression pattern of endogenous BAR protein in SK-N-BE(2) human neuroblastoma cells. After fixation and permeabilization, cells were stained with anti-BAR antiserum (1 : 1000) and Alexa 594 anti-rabbit secondary antibody. As a negative control, cells were incubated with pre-immune serum. (**c**) Expression control for BAR(ΔR) stably transfected cell lines. Whole-cell lysates (20 μg per lane) of control cells and transfectants were subjected to immunoblot analysis (*=unspecific band). Reprobing the blot with anti-α-tubulin antibody served as a loading control. (**d–i**) Coimmunostaining of BAR and ER or mitochondria. CSM cells were differentiated to neurons, fixed, and permeabilized as outlined in the *Methods* section. Ectopic BAR expression was detected by staining with anti-myc antibody (**d,g**). Anti-PDI was used as an ER marker (**e**), and Mitotracker was used as a mitochondrial marker (**h**). Merged pictures are shown in (**f**) and (**i**)

treated neuronal and astrocytoma cells with staurosporine (STS), an inducer of the intrinsic apoptotic pathway. While BAR overexpressing CSM cells were substantially protected from STS-induced cell death, LN18 cells were not (Figure 4a,b). To evaluate the extent of BAR-mediated protection in CSM cells compared to other antiapoptotic proteins, we performed identical experiments with CSM cells stably transfected with Bcl-2.[13] BAR conferred significant resistance to STS, but the extent of protection was not as large as that afforded by Bcl-2.

These cells were also subjected to serum deprivation as another type of stimulus thought to operate primarily through the mitochondrial cell death pathway. BAR-expressing CSM cells clearly resisted serum withdrawal, whereas the differences in cell survival of LN18 astrocytoma cells did not achieve statistical significance (Figure 4c,d). Again, protection afforded by Bcl-2 was more potent than BAR in CSM cells subjected to serum deprivation.

Next, we tested the extrinsic signalling pathways that are normally induced by activation of death receptors. CSM cells were treated with TNFα, whereas TNFα-resistant LN18 cells were treated with anti-Fas antibody CH11. In this cell death model, BAR expression resulted in substantial protection in both CSM and LN18 cells (Figure 4e,f). Interestingly, protection mediated by BAR and Bcl-2 was of similar potency in CSM cells.

Since BAR predominantly localizes to the ER, and because ER stress is an important cell death stimulus in normal and diseased CNS cells,[14] we treated the cell lines with thapsigargin, a specific antagonist of the ER Ca^{2+}-ATPase. CSM cells, but not LN18 cells, were significantly protected from thapsigargin-induced cell death by overexpression of BAR (Figure 4g,h). The protection conferred against ER stress by BAR was somewhat weaker than by Bcl-2.

We have previously shown that the wild-type BAR protein and the BARΔR mutant have similar antiapoptotic activity in 293 T cells.[11] To confirm that protection of neuronal cells from diverse cell death stimuli can be achieved by full-length BAR as well as BARΔR, we transiently transfected CSM cells with a plasmid encoding wildtype BAR or the empty expression vector together with a GFP-encoding plasmid. After performing similar treatments as shown in Figure 4, apoptosis was assessed by counting GFP-positive cells exhibiting apoptotic morphology of DAPI-stained nuclei. The percentages (±S.D.) of apoptosis of CSM cells transfected with full-length BAR or control vector were 24(±4) *versus* 37(±6)% after treatment with staurosporine (0.01 μM, 12 h); 19(±2) *versus* 42(±6)% after serum deprivation (16 h); 7(±3) *versus* 20(±4)% after incubation with TNFα (50 ng/ml; 12 h); and 16(±5) *versus* 32(±3)% after treatment with thapsigargin (0.3 μM; 12 h). These experiments confirmed that overexpressed wild-type BAR and BARΔR have similar antiapoptotic effects in neuronal cells.

In addition to cell death, we examined the effects of BAR expression on caspase activation. After treatment of BAR-transfected or control LN18 cells with anti-Fas antibody CH11, Caspase-3-like protease activity was measured by incubation of lysates with Caspase-3 substrate DEVD-AFC. While control cells showed a prominent increase in DEVD-AFC cleavage, Caspase activity in BAR transfectants remained low (Table 1). In parallel experiments, pro-Caspase-8 cleavage was examined by detection of the active p18 subunit by immunoblot analysis. Cleavage of pro-Caspase-8 into active subunits was readily detected in control cells even at low concentrations of CH11 antibody (0.08 μg/ml), while BAR-overexpressing cells showed cleavage of pro-Caspase-8 only at 25-fold higher concentrations of anti-Fas antibody (Figure 5).

Next, we tested if neuronal-lineage cells could be sensitized to apoptosis by downregulating endogenous BAR expression using antisense oligonucleotides. Lipid-mediated transfection of two different antisense oligonucleotides specific for human BAR into SK-N-BE(2) neuroblastoma cells resulted in almost complete loss of BAR mRNA, as assessed by quantitative RT-PCR methods after 24 h (Figure 6a and data not shown). Since the adapter protein FADD and the cell death protease Caspase-8 participates in the death receptor-induced apoptosis pathways, we tested the effects of downregulating

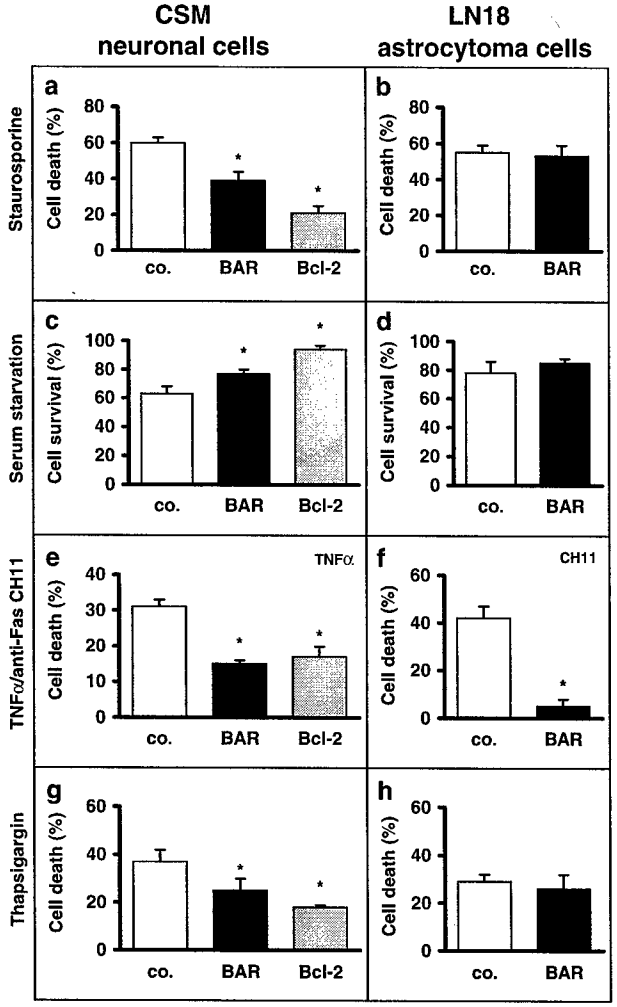

Figure 4 Antiapoptotic activity of BAR in neuronal and astrocytoma cells. The neuronal cell line CSM and the astrocytoma cell line LN18 were treated with various cell death stimuli. For these assays, cells were seeded in 12- or 96-well-plates and treated as outlined below. Cell death was assessed by counting living *versus* dead cells by Trypan blue exclusion assay or, alternatively, by crystal violet assay (see *Methods* section). All data are derived from at least four independent experiments and represent mean ± standard deviation (S.D.) (P=0.05, t-test). **(a,b)** As a model for intrinsic apoptosis, cells were treated with staurosporine (0.01 μM) for 16 h. **(c,d)** For serum starvation, cells were seeded, allowed to adhere for 24 h, washed twice with PBS, and incubated with serum-free medium for 48 h. **(e,f)** To trigger death receptor-dependent (extrinsic) apoptosis, CSM cells were treated with TNFα (50 ng/ml) for 16 h, and LN18 cells were treated with anti-Fas antibody CH11 (0.2 μg/ml) for 16 h. **(g,h)** ER stress-dependent cell death was induced by incubating cells with thapsigargin (0.3 μM) for 16 h. Asterisks indicate statistically significant results (P=0.05)

endogenous BAR on apoptosis induced as a result of transient overexpression of these proteins in SK-N-BE(2) cells. In control SK-N-BE(2) cells, little apoptosis was induced by overexpression of FADD or Caspase-8. In contrast, FADD and Caspase-8 were effective at inducing apoptosis in cells treated with BAR antisense (Figure 6a). Thus, we conclude that BAR is an intrinsic suppressor of Caspase-8-mediated apoptosis in these cells of neuronal lineage. In contrast to human SK-N-BE(2) neuroblastoma cells, endogenous BAR in rat CSM cells cannot be downregulated by the antisense

Table 1 Caspase-3-like activity in BAR-overexpressing versus control-transfected cells

	Control		BAR	
Min	Co.	+CH11	Co.	+CH11
1	51±8	108±2	73±1	74±2
5	38±5	358±3	64±4	79±7
10	28±2	586±11	50±5	108±9
15	17±1	753±10	46±7	116±6

LN18 cells were incubated without ('Co.') or with anti-Fas antibody CH11 (0.5 μg/ml) for 6 h. Cell lysates were generated from equivalent numbers of cells and incubated with DEVD-AFC. Cleavage of DEVD-AFC substrate was monitored by measuring fluorescence intensity. Data are presented as mean ± standard deviation of four consecutive measurements at the indicated times

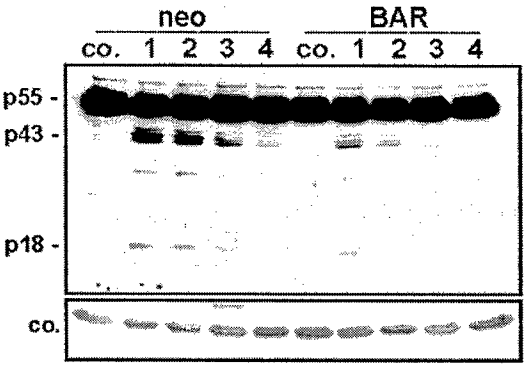

Figure 5 Role of BAR in extrinsic apoptosis. Caspase-8 cleavage after treatment with anti-Fas antibody. LN18 cells were treated with anti-Fas antibody CH11 for 16 h using (1) 2 μg/ml; (2) 0.4 μg/ml; (3) 0.08 μg/m; or (4) 0.016 μg/ml. Cell lysates were subjected to immunoblot analysis with mouse monoclonal anti-Caspase-8 antibody (Upstate Biotechnology)

oligonucleotides that are specific for the human BAR sequence. However, antisense-mediated downregulation of the ectopically expressed human BAR protein resulted in re-sensitization of CSM cells to apoptosis, thereby confirming that the resistant phenotype of BAR-transfected CSM cells was specifically caused by BAR (Figure 6b).

Novel candidate interaction partners of BAR

BAR protein contains a pseudo-DED, similar to Huntingtin-interacting protein (HIP1), HIP1 protein interactor (Hippi), and B-lymphocyte receptor-associated protein 31 (Bap31). We therefore tested BAR for interactions with HIP1, Hippi, and Bap31 by coimmunoprecipitation assays. For these experiments, candidate interacting proteins were transiently coexpressed with BAR in 293T cells and subsequently coimmunoprecipitated. No interaction was detectable for the DED-containing proteins FADD and PEA15, or for non-DED proteins such as XIAP and Bid (Figure 7a and data not shown). In contrast, HIP1, Hippi, and Bap31 were readily detected in BAR-containing immune complexes (Figure 7a).

Since physiological protein interactions require that the binding partners share the same intracellular compartments, we tested whether the interacting proteins colocalize in immunofluorescence experiments. COS-7 cells were transiently cotransfected with plasmids encoding a GFP-BAR

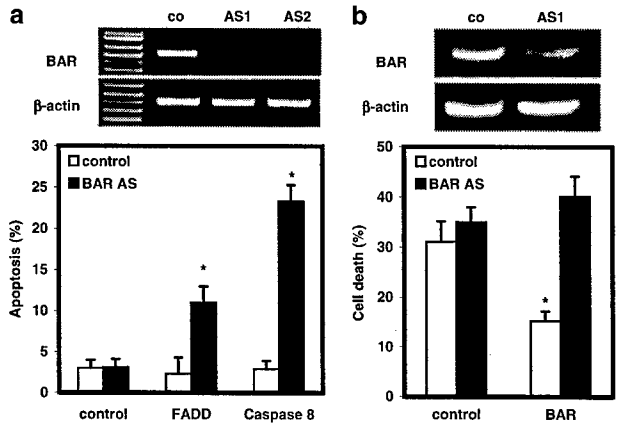

Figure 6 Antisense-mediated reductions in BAR sensitize cells to apoptosis. (**a**) SK-N-BE(2) human neuroblastoma cells were transfected with two different BAR-specific antisense oligonucleotides (AS1, AS2; 150 nM). After 24 h, the cells were transiently transfected with FADD or Caspase-8 (1 μg/ml), and apoptotic cell death was assessed after 16 h by DAPI staining. The data shown are derived from samples treated with antisense oligonucleotide AS1 (n=4, P=0.05), and represent mean ± S.D. Transfecting cells with AS2 produced similar results (not shown). (**b**) Downregulation of BAR reverses the resistant phenotype in BAR-overexpressing cells. BAR-overexpressing CSM cells were transfected with antisense oligonucleotide AS1 (150 nM) or control oligonucleotide ('co'). After 24 h, cells were cultured with TNFα (50 ng/ml) for 16 h. Cell death was assessed by trypan blue exclusion assay (n=4, mean ± S.D.; P=0.05)

fusion protein (pEGFP-BAR full-length) and FLAG-tagged HIP1, Hippi, Bap31, or FADD. After staining the cells with anti-FLAG antibody, the intracellular localization of the proteins was examined by confocal laser-scanning microscopy (Figure 7b). The fluorescence signal of GFP-BAR coincided well with the staining patterns for HIP1, Hippi, and Bap31. In contrast, only a partial overlap between GFP-BAR and FADD (bottom panel) or FLIP (not shown) was observed.

Discussion

The preservation of neurons is crucial for the functional integrity of the central nervous system. Since cells of neuronal origin are in general irreplaceable, loss of substantial amounts of brain tissue often results in permanent neurological deficits. On a cellular basis, the conservation of neurons for the entire lifespan of the organism is a considerable task, given the many diverse damaging stimuli that can impact neurons throughout life. Since apoptosis is believed to play an important role in the pathological loss of neurons, the expression of proteins that block apoptotic signalling may be decisive for the prevention of neuronal death. Dysregulated apoptotic cell death is held accountable for several diseases of the nervous system, and particularly within the group of neurodegenerative diseases, apoptosis has been implicated as a potentially crucial pathogenetic mechanism.[1,15–18] Despite the considerable progress in the knowledge about pathological features of neurological diseases, the therapeutic options are currently limited. Therefore, a need exists for additional insight into the mechanisms of how life and death decisions are regulated in adult neurons.

Two major routes of induction of apoptosis are the intrinsic and extrinsic pathways. The intrinsic pathway depends mainly on mitochondrial events, such as release of cytochrome *c*, leading to oligomerization of the CARD-containing protein Apaf-1 and activation of the CARD-carrying protease Caspase 9, and then subsequent activation of downstream caspases.[19] In contrast, the extrinsic cell death pathway is induced by TNF-family death receptors and involves the formation of membrane-bound signalling complexes consisting of the cytosolic death domains (DDs) of death receptors, adaptor proteins, and DED-containing caspases.[20]

BAR was described as a protein at the crossroads of intrinsic and extrinsic apoptosis pathways.[11] Evidence has been presented that complexes of Bcl-2/Bcl-X_L and BAR can sequester active Caspase-8 subunits on intracellular membranes, thereby neutralizing the active Caspase-8 fragments and preventing cleavage of substrates.[12] Despite these insights into the possible molecular mechanism of BAR, little has been known regarding the physiological functions of this protein *in vivo*. Therefore, we sought to define the anatomic location of the BAR protein and to interrogate its function as a suppressor of variant apoptotic stimuli. Interestingly, tissue expression of BAR is highly restricted, with brain tissue representing the predominant site of expression, followed by intestine, epidermis, testis, and little or no expression in other organs. Furthermore, immunohistochemical analysis revealed that BAR is expressed almost exclusively by neurons, but not by astrocytes or other cells in the brain, such as microglia. Interestingly, peripheral neuronal cells such as sympathetic ganglion cells also expressed high levels of BAR, suggesting that BAR expression is a general feature of neuronal cells and independent of their anatomical location. The staining of BAR in autonomic ganglion cells within the bowel wall and the absence of BAR in intestinal epithelial or stromal cells provides an explanation for the moderate BAR expression observed in small intestine by immunoblotting.

Immunofluorescence studies indicated that BAR predominantly localizes to the ER. Interestingly, only a minor fraction of the total BAR colocalized with mitochondria in neural cell lines, although it has been reported that the BAR-mediated sequestration of active Caspase-8 takes place at mitochondrial membranes in MCF-7 cells.[12] Thus, BAR distribution between ER and mitochondria could differ depending on the cell type, particularly because the ER and the mitochondrial network can coalesce into a continuous membrane structure.[21] An ER-localization for BAR is also consistent with its ability to coimmunoprecipitate with Bap31, which is an ER-resident protein.[22] It is conceivable that BAR could have ER-specific cytoprotective functions, given its ability to suppress cell death induced by ER stress.

For our studies of BAR in neuronal cells, we took advantage of the cell line CSM14.1. These cells originate from rat nigral neurons immortalized by expression of temperature-sensitive SV40 large T antigen. CSM cells show a high proliferative rate at permissive temperature (32°C), while inactivation of large T antigen at nonpermissive temperature (39°C) induces neuronal differentiation.[13,23] Overexpression of Bcl-2 in these cells resulted in protection from a variety of death stimuli.[13] Similarly, overexpression of wild-type BAR as well as BARΔR rendered CSM cells more resistant to a broad range of

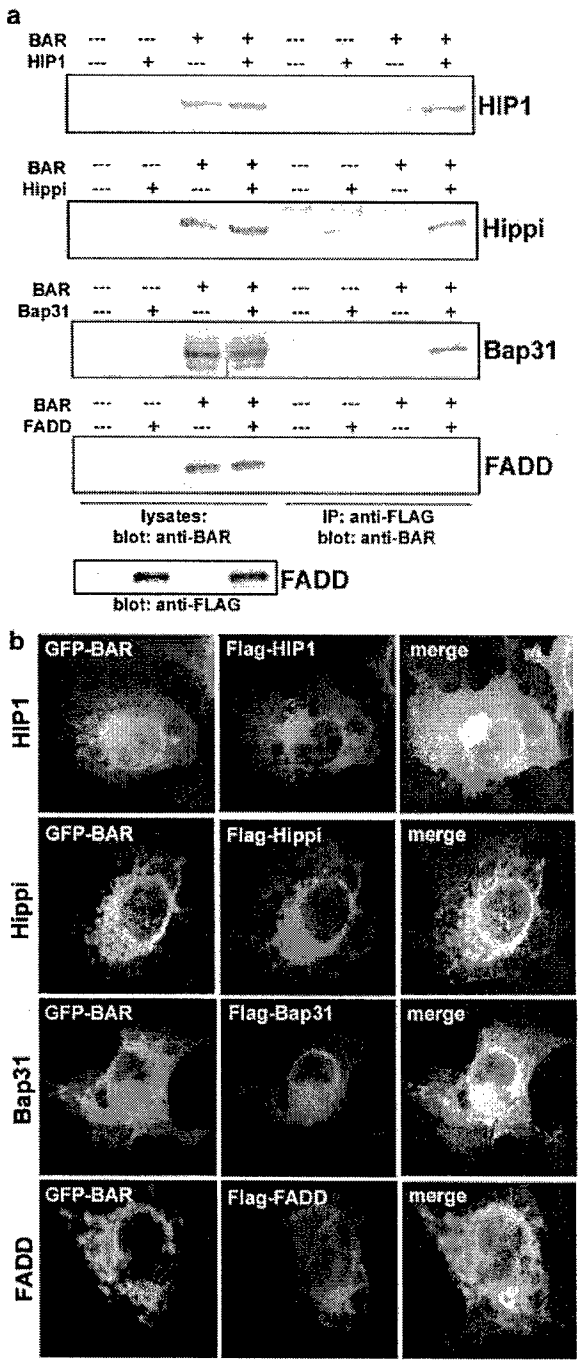

Figure 7 Interaction of BAR with HIP1, Hippi, and Bap31. (**a**) Myc-BAR and FLAG-tagged HIP1, Hippi, Bap31, and FADD were expressed in 293 T cells by transient transfection. After immunoprecipitation of FLAG-tagged proteins, protein complexes were resolved by SDS-PAGE and transferred to nitrocellulose. The membrane was incubated with BAR-specific antiserum (1 : 3000). Shown are the expression controls for BAR in cell lysates (left four lanes) and immunoprecipitates (right four lanes). Membranes were reprobed with anti-FLAG antibody to demonstrate sufficient and equal expression of FLAG-tagged proteins as demonstrated for FADD (bottom panel and not shown). (**b**) Colocalization of BAR with HIP1, Hippi, and Bap31. COS-7 cells were transfected with plasmids encoding GFP-BAR, FLAG-HIP1, FLAG-Hippi, FLAG-Bap31, and FLAG-FADD. At 20 h post-transfection, cells were fixed in 2% formaldehyde, stained with a monoclonal antibody recognizing the FLAG epitope followed by an Alexa 594-labelled secondary antibody, and visualized by laser confocal microscopy. The overlay of the images is shown in the right column

cytotoxic stimuli. We chose several cell death assays to model various types of stress and injury known to affect neurons *in vivo*. Staurosporine and TNFα were used to trigger the intrinsic and extrinsic pathways for apoptosis, respectively. For example, intrinsic, mitochondria-dependent apoptosis could play an important role in the pathogenesis of Parkinson's disease, since Bax gene ablation inhibited neuronal apoptosis in an MPTP mouse model of Parkinson's disease.[24] Similarly, extrinsic apoptosis pathways triggered by TNFα could play a role during the progression phase of stroke, where cytokine elaboration occurs in the peri-infarct zone after a focal ischemia.[25] Moreover, ER stress leading to induction of cell death in the brain has gained more attention in recent years. In the case of Alzheimer's disease, increasing evidence suggests that mutations in the presenilin-1 gene and perturbed ER calcium homeostasis render neurons more susceptible to damaging insults.[26] In this regard, BAR expression in CSM cells conferred resistance to thapsigargin, which is an irreversible inhibitor of Ca^{2+}-ATPase of the ER.[27] Finally, serum deprivation is a well-described and common experimental *in vitro* model for a nonsupportive microenvironment. Pathological conditions such as stroke and cerebral edema might result in an undersupply of essential nutrients.

In contrast to neuronal cells, BAR-overexpressing LN18 astrocytoma cells were only protected from death receptor-mediated cell death but not from the other cytotoxic stimuli. Similar effects were seen with a second astrocytoma cell line, LN229 (not shown). Differences in the expression of interaction partners of BAR or variations in the BAR-relevant pathways may account for the varying effects of BAR overexpression in these cell lines. Future investigations are needed to pinpoint the responsible proteins and to test a wider panel of cell lines for responsiveness to BAR-mediated protection.

Interestingly, BAR expression resulted not only in an inhibition of Caspase-3 activation but also in a decrease of the Caspase-8 active subunits (Table 1; Figure 5). BAR has been shown to sequester active Caspase-8 subunits,[12] but this does not inhibit the generation of the p43 and p18 cleavage products as seen in our experiments (Figure 5). Therefore, our findings suggest that BAR additionally affects the further processing of Caspase-8. It is known that active Caspase-8 can induce the mitochondrial apoptosis pathway via cleavage of Bid, resulting in cytochrome *c* release and Apaf1-mediated oligomerization of Caspase-9. These mitochondrial events, however, can in turn lead to cleavage and activation of Caspase-8, which establishes a positive amplification loop.[28] Thus, BAR-mediated sequestration of Caspase-8 active subunits could prevent the mitochondrial-dependent amplification of Caspase-8 activation.

In addition to overexpression experiments, we interrogated the function of BAR using antisense oligonucleotides to reduce endogenous BAR expression. Since the available antisense oligonucleotides were specific for human BAR, they could not be used to sensitize rat CSM cells by down-regulating endogenous BAR, and thus we chose a human neuroblastoma cell line that contains high levels of BAR protein. Transfection of neuroblastoma cells with antisense oligonucleotides downregulated BAR mRNA almost completely. By monitoring the BAR protein levels after antisense

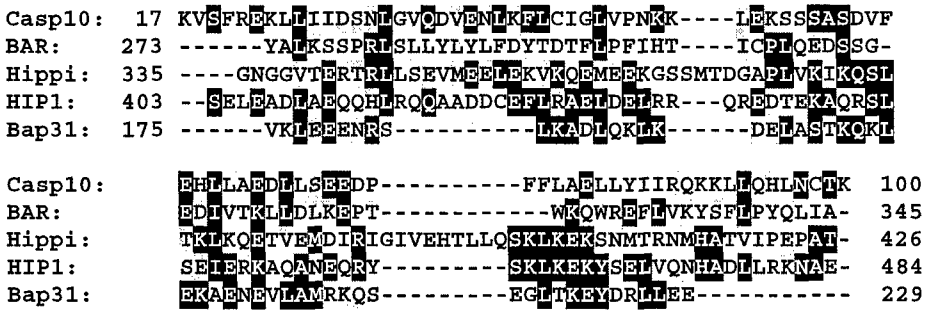

Figure 8 Comparison of pseudo-DEDs. An alignment is presented of the classical DED(1) of Caspase-10 and the pseudo-DEDs of BAR, Hippi, HIP1, and Bap31. At the beginning and the end of each sequence, the relative position of the domain in the molecule is shown. The amino-acid sequences were obtained from GenBank (NCBI) and aligned using the ClustalX program. Identical and similar residues are indicated in black and gray, respectively

oligonucleotide treatment, the half-life of the BAR protein was ~6 h (not shown). Antisense-mediated BAR suppression sensitized neuroblastoma cells to proapoptotic stimuli, including transfection with FADD or Caspase-8. These experiments thus confirm the antiapoptotic properties of BAR by an independent method.

Given the broad range of antiapoptotic activity of BAR, it is entirely possible that interactions with proteins other than Bcl-2 and Caspase-8 are important for its cytoprotective functions. Since BAR contains a variant DED domain similar to those found in HIP1, Hippi, and Bap31 (Figure 8), we tested BAR for interactions with these and selected other apoptosis-related proteins by coimmunoprecipitation assays. Interestingly, the three proteins containing pseudo-DEDs exhibit binding to BAR: HIP1, Hippi, and Bap31. In contrast, no interaction was detected with the classical DED-containing proteins, FADD and PEA15. Moreover, BAR showed extensive colocalization with HIP1, Hippi, and Bap31 in confocal microscopy studies, whereas FADD or FLIP did not clearly overlap with BAR. These findings raise the intriguing possibility that BAR interacts with other pseudo-DED-containing proteins, some of which are reported to be involved in regulating neuronal cell death. The 110 kDa protein HIP1, for example, binds to Huntingtin, which suffers poly-glutamine expansions in Huntington's disease.[29,30] Recently, it has been suggested that mutated Huntingtin releases the HIP1 protein, which then is free to interact with another novel protein, Hippi. HIP1 and Hippi reportedly form a complex together with pro-Caspase-8, thereby triggering caspase activation and cell death.[10] In addition, Bap31 is a transmembrane protein that resides mainly in the ER and which also contains a pseudo-DED.[22] Similar to BAR, Bap31 reportedly binds Bcl-2 as well as pro-Caspase-8.[22] Interestingly, Bap31 expression is highest in neurons, lymphocytes, and endocrine cells.[31] Future investigations will reveal to what extent the interactions of these variant DED-containing proteins are relevant for BAR-mediated neuroprotection.

Materials and Methods

Transfections

The rat nigrostriatal cell line CSM 14. 1, immortalized by introduction of the temperature-sensitive SV40 large T antigen, and a stably Bcl-2-transfected subline of these cells were kindly provided by Dale Bredesen.[13] Cells were maintained in Dulbecco's modified Eagle's medium (DMEM) supplemented with 10% fetal bovine serum (FBS), 1 mM L-glutamine, 100 U/ml penicillin, and 100 μg/ml streptomycin sulfate either at a permissive temperature of 32°C or nonpermissive temperature of 39°C.[13] For stable transfection, 50–70% confluent CSM cells in six-well plates were transfected with pcDNA3-myc-BARΔR and pBabe *puro* using Gene Porter II (Gene Therapy Systems). LN-18 human glioblastoma cells were transfected with pcDNA3 *neo* (control), or pcDNA3-myc-BARΔR[11] plasmids using Lipofectamine PLUS (Life Technologies). After 2 days, complete medium containing puromycin (4 μg/ml) (Sigma) or G418 (700 μg/ml) (Omega Scientific), respectively, was used to select stably transfected cells. Single clones were obtained 4–8 weeks after transfection by limiting-dilution cloning. For transient transfections, 293 T, SK-N-BE(2), COS-7, and CSM 14.1 cells were transfected using Lipofectamine PLUS (Life Technologies) with plasmid DNA encoding myc-BAR (full-length), myc-BARΔR, FADD, or pro-Caspase-8, and, in some experiments, green fluorescent protein (GFP) marker plasmid pEGFP (Clontech). In each experiment, the total amount of DNA was normalized using pcDNA3.

Immunohistochemistry

The distribution of BAR protein expression in human organ tissues was assessed in single paraffin sections or tissue microarray slides derived from human biopsy and autopsy material. Dewaxed tissue sections were exposed to a 1 : 3000 (v/v) dilution of polyclonal antiserum raised against an immunogen consisting of a recombinant N-terminal portion (1–139 aa) of the human BAR protein (AR-48). In addition, a rabbit polyclonal antibody was raised against an N-terminal peptide (3–21 aa: CEPQK-SYVNTMDLERDEPLK) conjugated with carrier proteins (AR-47). Specificity was confirmed by using preimmune serum or anti-BAR antiserum preadsorbed with recombinant BAR immunogen (10 μg/ml) or the N-terminal peptide, respectively. The sections were immunostained using a diaminobenzidine (DAB)-based detection method, employing either an avidin–biotin complex reagent (Vector Laboratories) or the Envision-Plus-Horse Radish Peroxidase (HRP) system (DAKO) using an automated immunostainer (Dako Universal Staining System).

Immunofluorescence and confocal microscopy

For immunofluorescence, control and stably transfected CSM cells expressing myc-BARΔR were cultured in eight-well, covered chamber slides (Nalge Nunc) at 32 or 39°C. After incubation with 25 nM Mitotracker Red (Molecular Probes), cells were washed and fixed in PBS containing

4% paraformaldehyde for 15 min at room temperature, followed by several washing steps in PBS. Permeabilization was performed in 0.3% Triton X-100/PBS for 5 min with subsequent preblocking in PBS containing 2% normal goat serum. Cells were incubated for 1 h at 4°C in blocking solution containing the following primary antibodies: anti-BAR (1 : 1000; AR-48), anti-myc (1 : 100; Santa Cruz), or anti-protein disulfide isomerase (PDI, 1 : 250; Stressgene). After washing three times in PBS and incubation with FITC-conjugated secondary anti-mouse or anti-rabbit antibody (1 : 50; Dako) or Alexa 594 goat anti-rabbit IgG $F(ab')_2$ secondary antibody (1 : 200; Molecular Probes) for 1 h at room temperature, slides were covered with Vectashield mounting medium with or without 1.5 μg/ml 4,6-diamidino-2-phenylindole (DAPI) (Vector Laboratories) and sealed with Cytoseal 60 mounting medium (Stephens Scientific). For confocal microscopy, COS-7 cells were cultured in eight-well, covered chamber slides (Nalge Nunc) (10^4 cells per chamber), transfected with various plasmids (pEGFP-BAR, pEGFP, pcDNA3-FLAG-HIP1, pcDNA3-FLAG-Hippi, pcDNA3-FLAG-Bap31, and pcDNA3-FLAG-FADD) using Lipofectamine PLUS reagent, and incubated at 37°C for 20 h. After staining with a monoclonal mouse anti-FLAG M2 antibody (Sigma) and Alexa 594 goat anti-mouse secondary antibody, the cells were imaged by confocal microscopy using a Bio-Rad MRC 1024 instrument.

Immunoblot analysis

Lysates from adult human tissues were purchased from Imgenex (San Diego, CA, USA). Lysates from LN18 cells and CSM cells were generated by resuspending cell pellets in lysis buffer (150 mM NaCl, 20 mM Tris (pH 7.4), 0.2% NP-40) containing 1 mM phenylmethylsulfonyl fluoride, and a protease inhibitor mixture (Roche). Proteins were resolved by SDS-PAGE and transferred onto nitrocellulose membranes. After blocking with 5% skim milk in PBS at room temperature for 1 h, blots were incubated with various primary antibodies including polyclonal antisera against BAR (AR-48; 1 : 3000), Bap31 (1 : 3000; kindly provided by Gordon Shore), and monoclonal antibodies against Caspase-8 (1 : 1000; clone 5F7, Upstate Biotechnology), myc (1 : 100; Santa Cruz), and FLAG (1 : 1000; Sigma), followed by HRP-conjugated anti-mouse or anti-rabbit IgG (Biorad) secondary antibodies. Bound antibodies were visualized using an enhanced chemiluminescence (ECL) detection system (Amersham).

Cell death assays

For cytotoxicity assays, cells were plated in 96-well plates, cultured for 24 h, and then incubated for 16 h with staurosporine (0.01 μM), TNFα (50 ng/ml), anti-Fas antibody CH11 (0.2 μg/ml) (MBL), or thapsigargin (0.3 μM). Cell death was assessed by Trypan blue exclusion assay. Additionally, the percentage of surviving cells was assessed by staining with crystal violet, as previously described in detail.[32] Cell death by serum deprivation was induced as published previously.[13] Cell survival was assessed by crystal violet staining after 2 days of serum starvation. Experiments were repeated four times.

Synthesis and transfection of antisense oligonucleotides

Second-generation 2′-*O*-methoxyethyl/DNA chimeric phosphorothioate oligonucleotides that inhibit BAR expression were identified following evaluation of 78 different oligonucleotides designed to bind to human BAR mRNA. Oligonucleotides were synthesized and purified as previously described.[33] A549 cells were plated in 96-well plates and treated with 150 nM oligonucleotide in the presence of 3.75 μg/ml Lipofectin reagent (Life Technologies) for 4 h at 37°C. Cells were incubated overnight in the absence of oligonucleotide. Total RNA was extracted using an RNeasy Mini prep kit (Qiagen) according to the manufacturer's protocol. Gene expression was analyzed using quantitative RT-PCR. The following primer/probe sets were used. Forward primer: 5′-GTGGAGA-GAGTTCCTGGTCAAATAC-3′, reverse primer: 5′-CCAACCAGTCC-CAAGCAAA-3′. Several oligonucleotides were identified that inhibited BAR expression by greater than 70%. Isis 143770 (AS1; 5′-TCCAGCCGCCGGAGTTCCTT-3′) and Isis 143780 (AS2; 5′-TCTCTATGCCTATGACAGAA-3′) were selected for additional studies. (Underlined text represents nucleosides containing the 2′-*O*-methoxyethyl modifications.) Isis 129689 (5′-GAGGTCTCGACTTACCCGCT-3′) was used as a control. SK-N-BE(2) or CSM cells were transfected with antisense oligonucleotides prior to inducing cell death as above. Antisense oligonucleotides or the control oligonucleotide were transfected at a concentration of 150 nM according to the Lipofectin method (Life Technologies). After 24 h, CSM cells were treated with TNFα (50 ng/ml) for 16 h and cell death was measured by trypan blue exclusion assay. SK-N-BE(2) cells were transiently transfected with FADD or Caspase-8 (1 μg/ml), and 0.2 μg/ml of GFP marker plasmid pEGFP (Clontech). At 16 h post-transfection, both adherent and floating cells were collected, fixed, and stained with 0.1 μg/ml DAPI. The percentage of apoptotic cells was determined by counting the GFP-positive cells exhibiting nuclear condensation and/or fragmentation.

Caspase activity assay

Caspase-3-like activity was measured by DEVD-AFC cleavage. Briefly, 10^4 cells were plated in 96-well plates, adhered for 24 h, and incubated for 6 h with anti-Fas antibody CH11 (0.5 μg/ml; MBL). The cells were suspended in lysis buffer (60 mM NaCl, 5 mM Tris/HCl, 2.5 mM EDTA, 0.25% NP40) for 10 min. Subsequently, the fluorogenic Caspase-3 substrate acetyl-aspartyl-glutamyl-valinyl-aspartyl-7-amino-4-trifluoro-methyl-coumarin (Ac-DEVD-AFC; 100 μM) was added to the lysates. Caspase activity was assayed by using a fluorometer plate reader, measuring release of fluorescent AFC.

Co-immunoprecipitation assays

Cell lysates were precleared and incubated with 20 μl anti-FLAG antibody M2-conjugated agarose (Sigma) at 4°C for 8 h.[32] Controls included immunoprecipitations (IPs) performed using an equivalent amount of normal mouse IgG in combination with Protein G-Sepharose 4B. After extensive washing with lysis buffer, immune complexes were fractionated by SDS-PAGE and transferred to nitrocellulose for immunoblotting using polyclonal antisera against BAR (1 : 3000; AR-48) or monoclonal mouse anti-FLAG (1 : 1000; Sigma) antibody, followed by HRPase-conjugated antibodies.

Acknowledgements

This work was supported by a fellowship from the Emmy-Noether-Programm of the Deutsche Forschungsgemeinschaft to W. Roth (Ro 2270/1-1) and by grants from the NIH (AG15393 and NS 36821). We thank D. Bredesen for providing CSM 14.1 and CSM 14.1-Bcl-2 cells, M. Weller for glioma cell lines LN18 and LN229, G. Shore for anti-Bap31 antibody, M. Hayden for the HIP1 plasmid, and F. Bennett for antisense oligonucleotides.

References

1. Mattson MP (2000) Apoptosis in neurodegenerative disorders. Nat. Rev. Mol. Cell. Biol. 1: 120–129
2. Robertson GS, Crocker SJ, Nicholson DW and Schulz JB (2000) Neuroprotection by the inhibition of apoptosis. Brain Pathol. 10: 283–292
3. Dirnagl U, Iadecola C and Moskowitz MA (1999) Pathobiology of ischaemic stroke: an integrated view. Trends Neurosci. 22: 391–397
4. Yuan J and Yankner BA (2000) Apoptosis in the nervous system. Nature 407: 802–809
5. Deveraux QL, Roy N, Stennicke HR, Van Arsdale T, Zhou Q, Srinivasula SM, Alnemri ES, Salvesen GS and Reed JC (1998) IAPs block apoptotic events induced by caspase-8 and cytochrome *c* by direct inhibition of distinct caspases. Embo J. 17: 2215–2223
6. Perrelet D, Ferri A, Listen P, Muzzin P, Korneluk RG and Kato AC (2002) IAPs are essential for GDNF-mediated neuroprotective effects in injured motor neurons *in vivo*. Nat. Cell. Biol. 4: 175–179
7. Barker V, Middleton G, Davey F and Davies AM (2001) TNFalpha contributes to the death of NGF-dependent neurons during development. Nat. Neurosci. 4: 1194–1198
8. New DR, Maggirwar SB, Epstein LG, Dewhurst S and Gelbard HA (1998) HIV-1 Tat induces neuronal death via tumor necrosis factor-alpha and activation of non-*N*-methyl-D-aspartate receptors by a NFkappaB-independent mechanism. J. Biol. Chem. 273: 17852–17858
9. Kaul M, Garden GA and Lipton SA (2001) Pathways to neuronal injury and apoptosis in HIV-associated dementia. Nature 410: 988–994
10. Gervais FG, Singaraja R, Xanthoudakis S, Gutekunst CA, Leavitt BR, Metzler M, Hackam AS, Tam J, Vaillancourt JP, Houtzager V, Rasper DM, Roy S, Hayden MR and Nicholson DW (2002) Recruitment and activation of caspase-8 by the Huntingtin-interacting protein Hip-1 and a novel partner Hippi. Nat. Cell. Biol. 4: 95–105
11. Zhang H, Xu Q, Krajewski S, Krajewska M, Xie Z, Fuess S, Kitada S, Godzik A and Reed JC (2000) BAR: an apoptosis regulator at the intersection of caspases and Bcl-2 family proteins. Proc. Natl. Acad. Sci. USA 97: 2597–2602
12. Stegh AH, Barnhart BC, Volkland J, Algeciras-Schimnich A, Ke N, Reed JC and Peter ME (2002) Inactivation of caspase-8 on mitochondria of Bcl-xL-expressing MCF7-Fas cells: role for the bifunctional apoptosis regulator protein. J. Biol. Chem. 277: 4351–4360
13. Zhong LT, Sarafian T, Kane DJ, Charles AC, Mah SP, Edwards RH and Bredesen DE (1993) bcl-2 inhibits death of central neural cells induced by multiple agents. Proc. Natl. Acad. Sci. USA 90: 4533–4537
14. LaFerla FM (2002) Calcium dyshomeostasis and intracellular signalling in Alzheimer's disease. Nat. Rev. Neurosci. 3: 862–872
15. Masliah E, Mallory M, Alford M, Tanaka S and Hansen LA (1998) Caspase dependent DNA fragmentation might be associated with excitotoxicity in Alzheimer disease. J. Neuropathol. Exp. Neurol. 57: 1041–1052
16. Sawa A, Wiegand GW, Cooper J, Margolis RL, Sharp AH, Lawler Jr JF, Greenamyre JT, Snyder SH and Ross CA (1999) Increased apoptosis of Huntington disease lymphoblasts associated with repeat length-dependent mitochondrial depolarization. Nat. Med. 5: 1194–1198
17. Martin LJ, Price AC, Kaiser A, Shaikh AY and Liu Z (2000) Mechanisms for neuronal degeneration in amyotrophic lateral sclerosis and in models of motor neuron death (review). Int. J. Mol. Med. 5: 3–13
18. Friedlander RM (2003) Apoptosis and caspases in neurodegenerative diseases (review). N. Engl. J. Med. 348: 1365–1375
19. Green DR and Reed JC (1998) Mitochondria and apoptosis. Science 281: 1309–1312
20. Ashkenazi A and Dixit VM (1998) Death receptors: signaling and modulation. Science 281: 1305–1308
21. Rizzuto R, Pinton P, Carrington W, Fay FS, Fogarty KE, Lifshitz LM, Tuft RA and Pozzan T (1998) Close contacts with the endoplasmic reticulum as determinants of mitochondrial Ca^{2+} responses. Science 280: 1763–1766
22. Ng FW, Nguyen M, Kwan T, Branton PE, Nicholson DW, Cromlish JA and Shore GC (1997) p28 Bap31, a Bcl-2/Bcl-XL- and procaspase-8-associated protein in the endoplasmic reticulum. J. Cell. Biol. 139: 327–338
23. Kermer P, Krajewska M, Zapata JM, Takayama S, Mai J, Krajewski S and Reed JC (2002) Bag1 is a regulator and marker of neuronal differentiation. Cell Death Differ. 9: 405–413
24. Vila M, Jackson-Lewis V, Vukosavic S, Djaldetti R, Liberatore G, Offen D, Korsmeyer SJ and Przedborski S (2001) Bax ablation prevents dopaminergic neurodegeneration in the 1-methyl-4-phenyl-1,2,3,6-tetrahydropyridine mouse model of Parkinson's disease. Proc. Natl. Acad. Sci. USA 98: 2837–2842
25. Hallenbeck JM (2002) The many faces of tumor necrosis factor in stroke. Nat. Med. 8: 1363–1368
26. Vito P, Lacana E and D'Adamio L (1996) Interfering with apoptosis: Ca(2+)-binding protein ALG-2 and Alzheimer's disease gene ALG-3. Science 271: 521–525
27. Thastrup O, Cullen PJ, Drobak BK, Hanley MR and Dawson AP (1990) Thapsigargin, a tumor promoter, discharges intracellular Ca2+ stores by specific inhibition of the endoplasmic reticulum Ca2(+)-ATPase. Proc. Natl. Acad. Sci. USA 87: 2466–2470
28. Slee EA, Harte MT, Kluck RM, Wolf BB, Casiano CA, Newmeyer DD, Wang HG, Reed JC, Nicholson DW, Alnemri ES, Green DR and Seamus JM (1999) Ordering the cytochrome *c*-initiated caspase cascade: hierarchical activation of caspases-2, -3, -6, -7, -8, and -10 in a caspase-9-dependent manner. J. Cell. Biol. 144: 281–292
29. Kalchman MA, Koide HB, McCutcheon K, Graham RK, Nichol K, Nishiyama K, Kazemi-Esfarjani P, Lynn FC, Wellington C, Metzler M, Goldberg YP, Kanazawa I, Gietz RD and Hayden MR (1997) HIP1, a human homologue of *S. cerevisiae* Sla2p, interacts with membrane-associated huntingtin in the brain. Nat. Genet. 16: 44–53
30. Wanker EE, Rovira C, Scherzinger E, Hasenbank R, Walter S, Tait D, Colicelli J and Lehrach H (1997) HIP-I: a huntingtin interacting protein isolated by the yeast two-hybrid system. Hum. Mol. Genet. 6: 487–495
31. Manley HA and Lennon VA (2001) Endoplasmic reticulum membrane-sorting protein of lymphocytes (BAP31) is highly expressed in neurons and discrete endocrine cells. J. Histochem. Cytochem. 49: 1235–1243
32. Roth W, Stenner-Liewen F, Pawlowski K, Godzik A and Reed JC (2002) Identification and characterization of DEDD2, a death effector domain-containing protein. J. Biol. Chem. 277: 7501–7508
33. McKay RA, Miraglia LJ, Cummins LL, Owens SR, Sasmor H and Dean NM (1999) Characterization of a potent and specific class of antisense oligonucleotide inhibitor of human protein kinase C-alpha expression. J. Biol. Chem. 274: 1715–1722

Molecular Cell, Vol. 15, 355–366, August 13, 2004, Copyright ©2004 by Cell Press

BI-1 Regulates an Apoptosis Pathway Linked to Endoplasmic Reticulum Stress

Han-Jung Chae,[1] Hyung-Ryong Kim,[1] Chunyan Xu,[1] Beatrice Bailly-Maitre,[1] Maryla Krajewska,[1] Stan Krajewski,[1] Steven Banares,[1] Janice Cui,[1] Murat Digicaylioglu,[1] Ning Ke,[1] Shinichi Kitada,[1] Edward Monosov,[1] Michael Thomas,[1] Christina L. Kress,[1] Jeremy R. Babendure,[3] Roger Y. Tsien,[2,3] Stuart A. Lipton,[1] and John C. Reed[1,*]

[1]The Burnham Institute
10901 North Torrey Pines Road
La Jolla, California 92037

[2]Department of Chemistry and Biochemistry
University of California, San Diego

[3]Howard Hughes Medical Institute
University of California, San Diego
310 CMM West
9500 Gilman
La Jolla, California 92093

Summary

Bax inhibitor-1 (BI-1) is an evolutionarily conserved endoplasmic reticulum (ER) protein that suppresses cell death in both animal and plant cells. We characterized mice in which the *bi-1* gene was ablated. Cells from BI-1-deficient mice, including fibroblasts, hepatocytes, and neurons, display selective hypersensitivity to apoptosis induced by ER stress agents (thapsigargin, tunicamycin, brefeldin A), but not to stimulators of mitochondrial or TNF/Fas-death receptor apoptosis pathways. Conversely, BI-1 overexpression protects against apoptosis induced by ER stress. BI-1-mediated protection from apoptosis induced by ER stress correlated with inhibition of Bax activation and translocation to mitochondria, preservation of mitochondrial membrane potential, and suppression of caspase activation. BI-1 overexpression also reduces releasable Ca^{2+} from the ER. In vivo, *bi-1*$^{-/-}$ mice exhibit increased sensitivity to tissue damage induced by stimuli that trigger ER stress, including stroke and tunicamycin injection. Thus, BI-1 regulates a cell death pathway important for cytopreservation during ER stress.

Introduction

Apoptosis dysregulation represents an underlying cause or contributor to many diseases. Activation of caspase-family proteases is at the core of apoptotic cell death, representing a common point of intersection (Nicholson and Thornberry, 2003). Several pathways leading to caspase activation and apoptosis have been elucidated, including pathways triggered by: (i) TNF/Fas-family cytokine receptors; (ii) mitochondrial release of cytochrome c and other proteins; and (iii) granzyme B-mediated cleavage of caspases in the context of cytolytic T cell responses (Salvesen, 2002). However, damage or stress in many organelles (besides mitochondria) may trigger apoptosis, though mechanisms remain unclear.

In this regard, a pathway for caspase activation and apoptosis induction has been linked to stress in the endoplasmic reticulum (ER). Evidence is emerging that the ER participates in the initiation of apoptosis induced by the unfolded protein response (UPR) and by aberrant Ca^{2+} signaling (Kaufman, 1999; Patil and Walter, 2001; Demaurex and Distelhorst, 2003). Damage to the ER can trigger caspase activation, and indeed certain members of the caspase family reportedly are associated with the ER (e.g., caspase-12) or the Golgi (e.g., caspase-2) (Mancini et al., 2000; Nakagawa et al., 2000). ER stress pathways linked to apoptosis may be important in ischemia-reperfusion injury, where Ca^{2+} escapes from the organelle during times of ATP deficiency, and in neurodegenerative diseases such as Alzheimer's and Parkinson's, where abnormalities have been identified in protein folding or secretion in the Golgi-ER compartment.

Bax inhibitor-1 (BI-1) is an antiapoptotic protein that contains several transmembrane domains, localizes to ER membranes, and is conserved in both animal and plant species (Chae et al., 2003; Xu and Reed, 1998). The cytoprotective function of BI-1 was originally discovered in cDNA library screens for human proteins capable of suppressing death of yeast induced by ectopic expression of mammalian Bax protein, a pro-apoptotic member of the Bcl-2 family (Xu and Reed, 1998). Overexpressed BI-1 also provides protection against apoptosis induced by some types of stimuli in mammalian cells, while BI-1 antisense can promote apoptosis of some tumor lines (Xu and Reed, 1998). Plant homologs of BI-1 appear to be at least partly conserved with the human counterpart, given that BI-1 orthologs of tomato (*Lycopersicon*), rice (*Oryza*), and mustard (*Arabidopsis*) also rescue in the yeast-based Bax-lethality assay (Chae et al., 2003; Kawai et al., 1999; Sanchez et al., 2000). In culture, BI-1 homologs of oilseed rape and tobacco rescue against Bax-induced apoptosis in human cells (Bolduc et al., 2003), and At-BI-1 protects rice cells against cytotoxic stimuli (Matsumura et al., 2003). Conversely, antisense-mediated knockdown of BI-1 in tobacco cells results in accelerated cell death during carbon starvation (Bolduc and Brisson, 2002). Importantly, BI-1 from *Arabidopsis thaliana* (At) has been shown to protect transgenic plants against cell death induced by ectopic expression of mammalian Bax (Kawai-Yamada et al., 2001), indicating an in vivo role for BI-1 in cytoprotective pathways in planta and further suggesting that the biochemical mechanism regulated by BI-1 is evolutionarily conserved. Thus, BI-1 regulates cell death in both plant and animal cells.

In this report, we investigated the cytoprotective mechanism of mammalian BI-1 protein by using gene ablation and gene transfer approaches.

Results

Generation of *bi-1* Knockout Mice

We identified an ES cell clone in the Lexigen database containing a single proviral insertion in reverse orienta-

*Correspondence: reedoffice@burnham.org

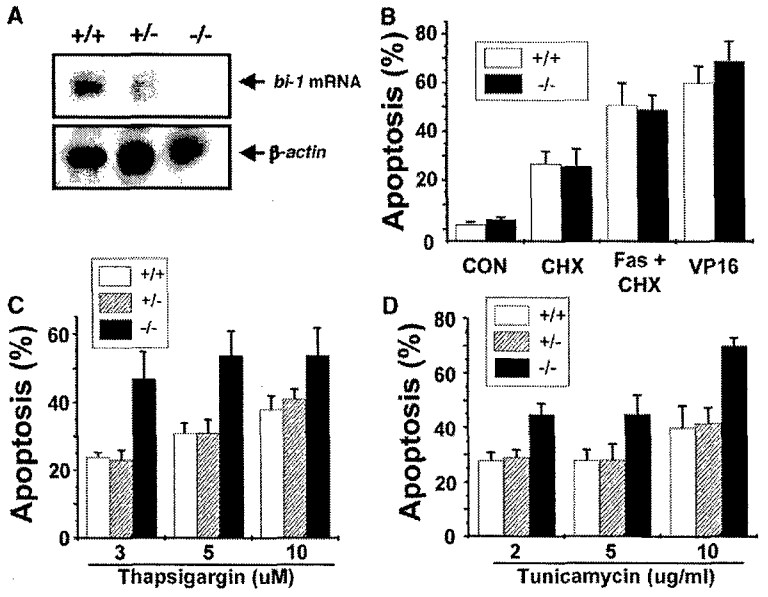

Figure 1. BI-1-Deficient MEFs Display Increased Sensitivity to ER Stress Agents

Early-passage MEFs were obtained from wild-type (+/+), heterozygous (+/−), and homozygous (−/−) *bi-1* knockout embryos.

(A) Total RNA was isolated from MEFs, and 10 μg was analyzed by Northern blotting with a ^{32}P-*bi-1* cDNA probe. The blot was striped and reprobed with a ^{32}P-β-actin probe.

(B–D) MEFs from wild-type (+/+) (white bars), heterozygous (+/−) (gray bars), and homozygous (−/−) (black bars) *bi-1* knockout embryos were cultured for 2 days without or with cycloheximide (20 μg/ml), anti-Fas antibody (Jo2) (1 μg/ml), VP16 (50 μM), various concentrations of thapsigargin (THPS) or tunicamycin (TUN), or combinations of selected reagents. Both floating and adherent cells were recovered from cultures, fixed, and stained with Hoechst 33258 dye. Apoptotic cells were identified by UV-microscopy, counting a minimum of 200 total cells, and data were expressed as a percentage relative to the total number of cells counted (mean ± SD; n = 3 determinations).

tion between exons 7 and 8 of the mouse *bi-1* gene (see the Supplemental Data at http://www.molecule.org/cgi/content/full/15/3/355/DC1). These ES cells were used to create mice containing the targeted *bi-1* gene and were bred to homozygosity. Homozygous *bi-1*$^{-/-}$ mice displayed no gross abnormalities, indicating that *bi-1* is a nonessential gene. Histological inspection of tissues revealed no apparent abnormalities in *bi-1*$^{-/-}$ mice (data not shown). Northern blotting showed the presence of a truncated *bi-1* transcript, which was present at very low levels in most tissues, estimated at a few percent (at most) compared to the amount of full-length *bi-1* mRNA present in wild-type tissues including liver, brain, kidney, and testis. Exceptions were thymus and lung, where truncated *bi-1* transcripts were more significant (see Supplemental Data). Thus, *bi-1* gene expression was successfully knocked out in several tissues (~99%), with only a low abundance of truncated transcript remaining.

BI-1-Deficient Cells Display Increased Sensitivity to ER Stress

Mouse embryo fibroblasts (MEFs) with normal (+/+), heterozygous (+/−), and homozygous (−/−) genotypes were exposed to various types of cell death stimuli. Analysis of *bi-1* mRNA levels in these MEFs by RT-PCR revealed a reduction in *bi-1* expression in heterozygous MEFs and a complete absence of detectable *bi-1* mRNA in homozygous *bi-1*$^{-/-}$ MEF cells (Figure 1A).

We first tested the effects of BI-1 deficiency on apoptosis induced by classical intrinsic (mitochondrial) and extrinsic (TNF family) stimuli. BI-1-deficient MEFs displayed normal sensitivity to apoptosis induced by intrinsic pathway stimulus VP16 (etoposide), a DNA-damaging anticancer drug, and to anti-Fas antibody (plus cycloheximide) (Figure 1B).

Since the BI-1 protein localizes to ER, we next tested the effects of BI-1 deficiency on apoptosis induced by ER stress stimuli. Thapsigargin (THPS) is a selective inhibitor of the Ca^{2+}-ATPase of the ER, which induces cell death due to leakage of Ca^{2+} from the ER into cytosol (Berridge et al., 2000). Treatment of MEFs with various concentrations of THPS revealed a significant difference in the sensitivity of *bi-1*$^{-/-}$ knockout cells compared to heterozygous (+/−) and wild-type (+/+) MEFs, particularly at lower doses of THPS (Figure 1C).

Tunicamycin (TUN) is an inhibitor of N-linked glycosylation that causes defects in glycoprotein trafficking between ER and Golgi, producing ER stress and inducing apoptosis (Patil and Walter, 2001). Treatment of *bi-1*$^{-/-}$ MEFs with TUN at 2–10 μM revealed increased sensitivity to this agent, compared to treatment of *bi-1*$^{+/-}$ and *bi-1*$^{+/+}$ MEFs (Figure 1D).

We extended these studies to other types of cells and other types of apoptotic stimuli. Though *bi-1* is ubiquitously expressed at the mRNA level in mammalian tissues (Jean et al., 1999), the highest levels of *bi-1* mRNA are found in liver, kidney, and testes (see Supplemental Data). We therefore tested effects of BI-1 deficiency on hepatocytes. In primary cultures of hepatocytes derived from *bi-1*$^{-/-}$, *bi-1*$^{+/-}$, and *bi-1*$^{+/+}$ adult mice, increased sensitivity to THPS and TUN was observed for BI-1-deficient cells, with markedly higher percentages of *bi-1*$^{-/-}$ hepatocytes undergoing apoptosis (Figure 2A). In contrast, sensitivity to the broad-spectrum kinase inhibitor, staurosporine (STS), was increased to a lesser extent in *bi-1*$^{-/-}$ cells, primarily occurring at higher concentrations of this drug known to induce apoptosis through a mitochondria-dependent pathway (Green and Reed, 1998). Also, apoptosis induced by anti-Fas antibody was not as extensively impacted by BI-1 deficiency, compared to ER stress stimuli in hepatocytes (Figure 2A). These observations regarding the relative sensitivity of BI-1-deficient hepatocytes to apoptosis-inducing agents were paralleled by corresponding differences in caspase activity, as measured in cell lysates by using fluorigenic substrate Ac-DEVD-AFC (Figure 2B).

Finally, we explored the effects of BI-1 deficiency in neurons. Cortical neurons were isolated from *bi-1*$^{-/-}$,

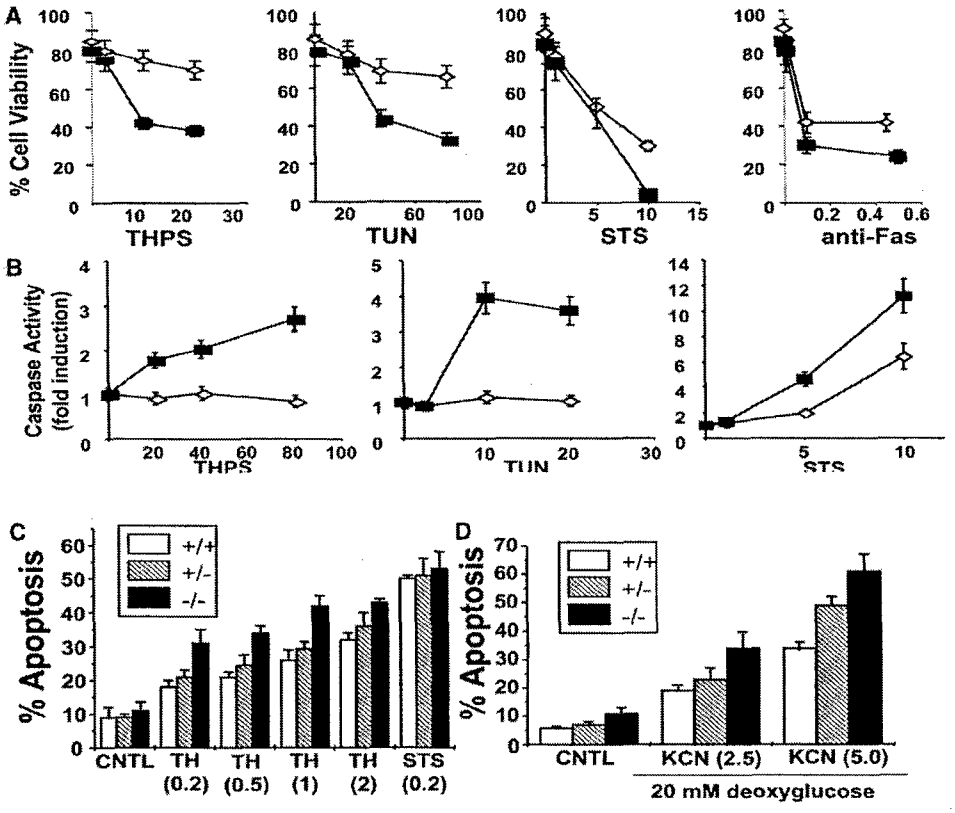

Figure 2. Increased Sensitivity of BI-1-Deficient Hepatocytes and Neurons to Apoptosis Induction by ER Stress

(A and B) Hepatocytes were isolated from adult wild-type (+/+) (open symbols) and knockout (−/−) (closed symbols) *bi-1* mice. (A) Hepatocytes were treated with (from right to left) anti-Fas mAb (10, 100, 500 ng/ml), staurosporine (STS) (1, 5, and 10 μM), TUN (20, 40, and 80 μg/ml), or THPS (2.5, 10, and 20 μM) for 12 hr (Fas; STS) or 72 hr (THPS; TUN). The percentage of TUNEL-positive cells was determined (mean ± SD; n = 5). (B) Hepatocytes were treated as above and lysed, and caspase activity was measured by using the fluorigenic substrate, after normalizaion for total protein content; data was expressed as a fold-increase above untreated cells (mean ± SD; n = 5).

(C and D) Cortical neurons were isolated from E15-E16 *bi-1*$^{+/+}$ (white bars), *bi-1*$^{-/+}$ (gray bars), and *bi-1*$^{-/-}$ (black bars) embryos (Rose et al., 1993). (C) Neurons were cultured for 2 days in medium alone (CNTL) or with 0.2–0.5 μM THPS, 1–2 μg/ml TUN, or 0.2 μM STS. (D) Neurons were cultured for 50 min in normal medium (CNTL) or in medium containing 20 mM deoxyglucose and either 2.5 or 5.0 mM KCN, then washed and cultured for 1 day in normal medium, essentially as described. After treatments, cells were fixed and stained with Hoechst 33258, and the percentage of neurons with apoptotic features was determined (mean ± SD; n = 3).

bi-1$^{+/-}$, and *bi-1*$^{+/+}$ embryos, then cultured with THPS, TUN, or STS, measuring apoptosis of neurons by DAPI staining of fixed cells. BI-1-deficient neurons displayed statistically significant increases in sensitivity to THPS at both doses tested (0.2 and 0.5 μM) and to TUN at lower doses (1 μg/ml) (Figure 2C). In contrast, BI-1 deficiency did not alter the sensitivity of neurons to either low (Figure 2C) or high (data not shown) concentrations of STS, an agent often used to invoke the mitochondrial pathway for apoptosis.

Because ischemia-reperfusion injury is known to cause loss of Ca^{2+} from ER (Lipton, 1999), we also tested the effects of BI-1 deficiency on the sensitivity of primary cortical neurons to culture conditions that mimic this injury. Accordingly, neurons were cultured in medium containing 20 mM deoxyglucose and either 2.5 or 5.0 mM KCN for 1 hr, then washed and placed into fresh medium for 1 day, followed by enumeration of the percentage of apoptotic neurons. BI-1-deficient neurons displayed significant increases in sensitivity to apoptosis induction by these culture conditions, compared to wild-type neurons. Heterozygous neurons exhibited intermediate sensitivity (Figure 2D).

Absence of *bi-1* expression thus correlates with increased sensitivity to apoptosis induced by ER stress and is relatively specific for the ER pathway compared to activators of the mitochondrial (STS) and death receptor (anti-Fas) pathways for apoptosis. Note that the extent of sensitization of *bi-1*$^{-/-}$ cells to apoptosis is of comparable magnitude to knockouts of other well-characterized cell death-regulatory genes, including caspase 12, caspase 2, Bim, and Bid (Bergeron et al., 1998; Nakagawa et al., 2000; Villunger et al., 2003; Yin et al., 1999). While affecting apoptosis of fibroblasts, hepatocytes, and neurons, apoptosis of thymocytes induced by THPS or TUN was not significantly different when using cells isolated from *bi-1*$^{-/-}$ versus *bi-1*$^{+/+}$ mice (data not shown), possibly due to the relatively low basal levels of *bi-1* mRNA expression in normal thymocytes compared to other tissues or because of the presence of *bi-1*-truncated transcripts in the *bi-1*$^{-/-}$ line (see Supplemental Data). Note that no abnormalities in the relative propor-

tions of thymocyte and lymphocyte subsets were observed in *bi-1*$^{-/-}$ mice (data not shown).

BI-1-Deficient Mice Display Increased Sensitivity to ER-Dependent Tissue Injury

Injection of TUN into live animals causes apoptosis of epithelial cells lining the renal tubules (Nakagawa et al., 2000; Zinszner et al., 1998). We tested the sensitivity of age- and sex-matched *bi-1*$^{-/-}$ and *bi-1*$^{+/+}$ mice to low-dose TUN (1 μg/gm). Animals were sacrificed 2 days thereafter, and kidneys were examined. Gross inspection of the kidneys of TUN-treated *bi-1*$^{-/-}$ mice revealed marked necrosis of the cortical areas, adjacent to the corticomedullary junction, while the kidneys of control *bi-1*$^{+/+}$ mice were grossly normal. Histological analysis revealed that the kidneys of *bi-1*$^{-/-}$ mice showed far more damage compared to *bi-1*$^{+/+}$ animals (Figure 3A). Many of the tubules were denuded, indicative of cell loss, and multiple pyknotic nuclei were seen, indicative of apoptosis. Morphometric analysis of the extent of medullary necrosis revealed a statistically significant increase in the area of damage in the *bi-1*$^{-/-}$ mice (Figure 3A).

We also noticed that TUN induced apoptosis of hippocampal neurons in mice. We therefore compared the extent of in vivo neuronal apoptosis in *bi-1*$^{-/-}$ and *bi-1*$^{+/+}$ adult mice at various times (days 1–3) after injection with 1 μg/gm TUN. In contrast to BI-1-expressing animals where only occasional pyknotic neurons were evident in the hippocampus after TUN exposure, apoptotic neurons were abundant in the hippocampus of BI-deficient mice (Figure 3B).

Finally, since BI-1 deficiency was associated with increased sensitivity of cultured neurons to ischemia-reperfusion injury, we compared *bi-1*$^{+/+}$ and *bi-1*$^{-/-}$ mice with respect to stroke injury, by using a model of transient middle cerebral artery occlusion (MCAO) (Kermer et al., 2003; Wang et al., 1998). Accordingly, age-matched *bi-1*$^{-/-}$ and *bi-1*$^{+/+}$ littermates were subjected to 2 hr of MCA occlusion, then blood flow was restored, and after 24 hr of reperfusion, mice were sacrificed, and the brains were removed and analyzed by staining with 2,3,5-triphenyltetrazolium chloride (TTC) (Kermer et al., 2003; Wang et al., 1998). Infarct volumes were significantly larger in *bi-1*$^{-/-}$ mice compared to *bi-1*$^{+/+}$ mice (44.8% ± 1.5% versus 28.9% ± 5.7% hemisphere; $p = 0.007$ by Mann-Whitney test) (Figure 3C). No differences were noted in wild-type and BI-1-deficient mice with respect to anatomy of the cerebral arteries (data not shown) or with respect to cerebral blood flow, arterial blood pressure, blood pH, pCO_2, pO_2, or glucose before or after MCAO (see Supplemental Data). Thus, *bi-1* is required for resistance to brain damage caused by ischemia-reperfusion injury.

Overexpression of BI-1 Protein Protects Cells from Apoptosis Induced by ER Stress

Since loss of *bi-1* expression resulted in increased sensitivity to apoptosis induced by ER stress, we next explored the effects of overexpressing the BI-1 protein. HT1080 fibrosarcoma or CMS14.1 neuronal cells were employed, because preliminary experiments indicated that they undergo apoptosis when treated with ER stress-inducing agents. BI-1 was expressed in these cells with an HA-epitope tag fused to its C terminus, to facilitate detection by immunoblotting (Figure 4A).

BI-1-overexpressing HT1080 cells exhibited marked resistance to cell death induced by ER stress agents TUN and THPS, while displaying a comparatively smaller difference in sensitivity to VP16, Doxorubicin (intrinsic pathway), or anti-Fas (extrinsic pathway) (Figure 4B and Supplemental Data). Similar results were obtained with respect to caspase activation (Figure 4C). BI-1 also prevented cell shrinkage and other morphological manifestations of apoptosis when cells were treated with ER stress agents (see Supplemental Data). Experiments with additional clones of BI-1 stable transfectants produced similar results (see Supplemental Data).

BI-1-transfected CMS14.1 neuronal cells also displayed marked resistance to apoptosis induced by ER stress agents, THPS, TUN, and brefeldin A (BRE), while demonstrating little difference in their sensitivity to low-dose STS (intrinsic pathway) or TNF (extrinsic pathway) (Figure 4D and data not shown). Note that while BI-1 overexpression provided partial protection from apoptosis induced by high-dose STS (data not shown), higher doses of this kinase antagonist appear to provide a mixed picture of both mitochondrial- and ER-induced apoptosis (unpublished data).

BI-1 Overexpression Interrupts Cell Death Signaling between ER and Mitochondria

To attempt to map the point at which BI-1 offers protection in cell death pathways activated by ER stress, we examined several apoptosis-relevant events that occur following treatment of cells with ER stress agents, including induction of ER chaperones associated with unfolded protein responses, alterations in ER/Golgi morphology, caspase activation, Bax conformational changes, Bax translocation from cytosol to mitochondria, dissipation of mitochondrial membrane potential ($\Delta\Psi m$), and alterations in mitochondrial morphology. While BI-1 overexpression did not prevent TUN-induced dilation and disruption of the Golgi and ER as determined by transmission electron microscopy (EM) or TUN-induced expression of ER molecular chaperones (Grp78; Grp94), BI-1 effectively reduced caspase processing and activation, Bax activation, mitochondrial membrane depolarization, and mitochondrial ultrastructural changes induced by the ER stress agents TUN and THPS. For example, while THPS induced proteolytic consumption of pro-caspase-9 and pro-caspase-3 (but not pro-caspase-8) in control-transfectant HT1080-Neo cells, these effects were largely blocked in BI-1-overexpressing cells (Figure 5A). In contrast to ER stress agents, BI-1 overexpression did not alter caspase processing induced by classical extrinsic (anti-Fas) and intrinsic (VP16) pathway stimuli, demonstrating selectivity of BI-1 for suppression of the ER pathway (Figure 5A). Note that while BI-1 reduced caspase processing induced by ER stress agents, and while pharmacological inhibitors of the relevant caspases rescued cells from apoptosis induced by ER stress agents (as did transfection of dominant-negative mutants of caspases) (Figures 5B and 5C), BI-1-mediated protection from cell death was not caspase dependent, as shown by experiments where

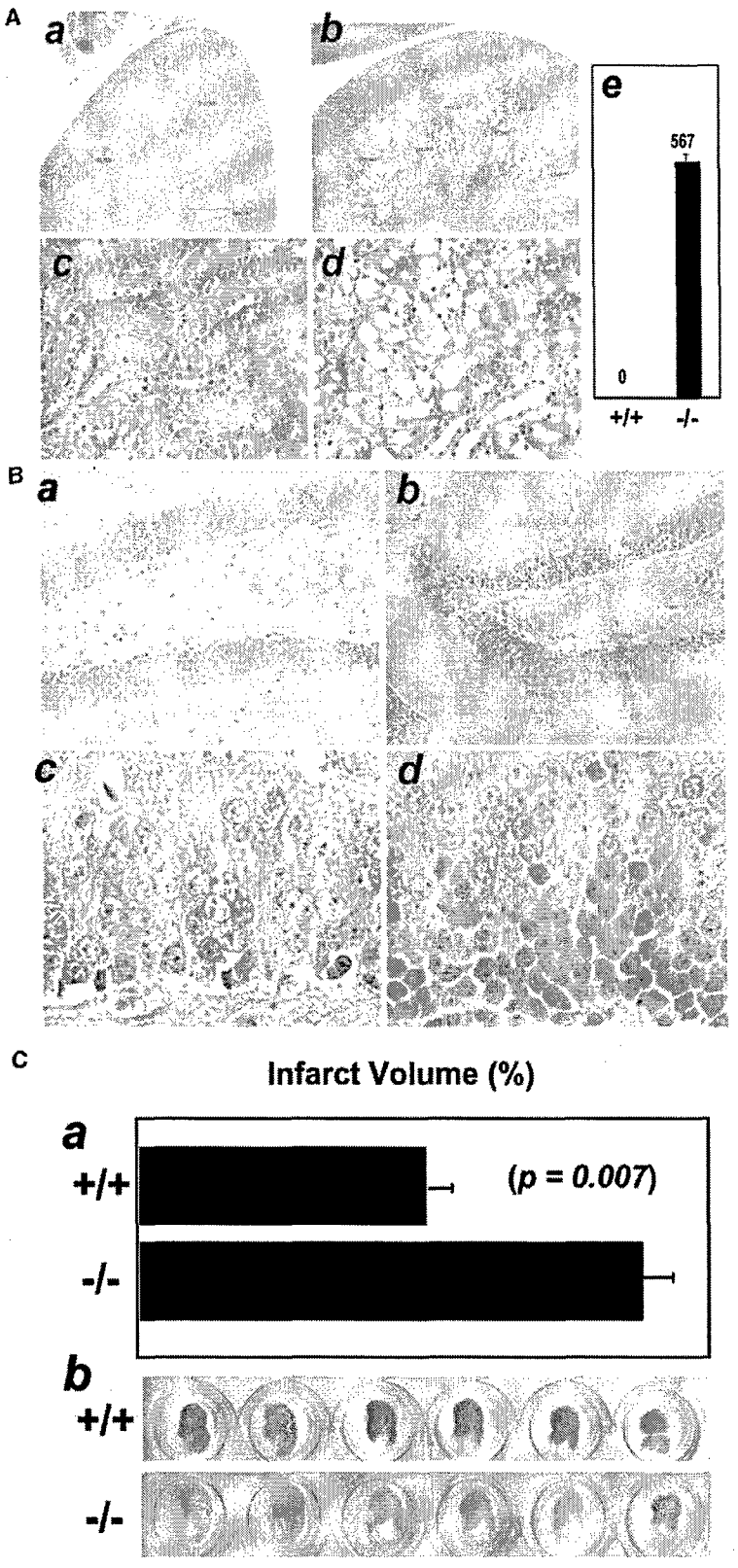

Figure 3. BI-1-Deficient Mice Display Increased Sensitivity to Tunicamyin and Stroke Injury

(A) Age-matched (a and c) *bi-1*$^{+/+}$ and (b and d) *bi-1*$^{-/-}$ littermates were injected intraperitoneally with 1 μg/gm TUN. After 2 days, mice were sacrificed and kidneys were examined by Mason Trichrome staining. The kidneys from the BI-1-deficient animals revealed pronounced tubular degeneration, especially in the corticomedullary region ([b], ×60; [d], ×400). The pathologic alterations range from increased vacuolization of tubular epithelial cells to pyknotic or karyorrhetic nuclei and desquamation of necrotic cells into the tubule lumen. In contrast, only occasional renal tubules display cell degeneration in the wild-type littermates ([a], ×60; [c], ×400). The annotations and red lines in (a) and (b) indicate some of the places from which measurements were taken to assess the region of tubular necrosis relative to the total cortical diameter. In (e), data represent mean length (n = 5 animals) of the damaged zone in μm, normalized for length of cortical radius, based on measurements performed at four locations for each kidney ($p < 0.0001$).

(B) Comparison of hippocampus of *bi-1*$^{+/+}$ and *bi-1*$^{-/-}$ mice after tunicamycin injection. Representative H&E-stained coronal hippocampal sections are presented from (a and c) *bi-1*$^{+/+}$ and (b and d) *bi-1*$^{-/-}$ mice, sacrificed 1 day after tunicamycin injection. Marked neuronal damage was present in the dentate gyrus region in the BI-1-deficient animals ([b], ×200; [d], ×400) compared with the wild-type littermates ([a], ×200; [c], ×400). Note the presence of multiple dark, pyknotic and condensed apoptotic nuclei in the specimen from the *bi-1*$^{-/-}$ animal (shown in [b] and [d]).

(C) Focal ischemic infarcts were created by using a reversible, intraluminal middle cerebral artery occlusion model (Kermer et al., 2003; Wang et al., 1998). At 24 hr reperfusion, after 2 hr of occlusion, mice were sacrificed, and the brains were removed and analyzed by staining with TTC for performing infarct size measurements. (a) Data represent the percentage of the involved hemisphere infracted; the volumes of both hemispheres were used for normalization (mean ± SD for n = 6 [+/+] and n = 7 [−/−] mice). (b) An example of TTC staining data is presented and shows serial coronal sections through brains of a *bi-1*$^{+/+}$ and a *bi-1*$^{-/-}$ mouse.

BI-1-overexpressing cells were cultured with TUN for 3 days in the presence of broad-spectrum caspase inhibitor zVAD-fmk and cell death (rather than apoptosis) was measured by a dye exclusion assay (Figure 5D). Similarly, BI-1 overexpression inhibited TUN-induced conversion of Bax to its active conformation (as determined

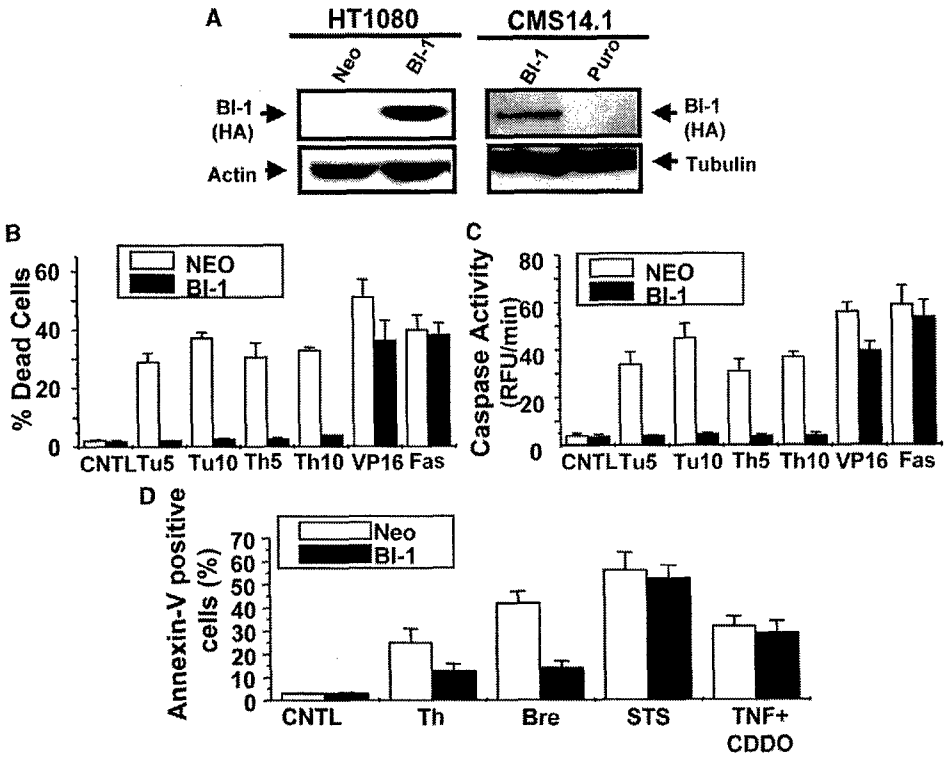

Figure 4. Bl-1 Overexpression Protects Cells from Apoptosis Induced by ER Stress

(A) The Bl-1 protein was overexpressed with a C-terminal HA tag in HT1080 human fibrosarcoma cells and CMS14.1 immortalized rat hippocampal neurons. CMS14.1 is an immortalized rat hippocampal neuronal cell clone that contains temperature-sensitive SV40 large T-antigen. All experiments with CMS14.1 cells were performed, essentially as described, at the nonpermissive temperature (39°C) to shut off SV40 large T-antigen (Kermer et al., 2002). Lysates were normalized for total protein content and were analyzed by SDS-PAGE/immunoblotting with anti-HA antibody (top) or anti-β-actin or anti-tubulin antibodies (bottom).

(B and C) Neo-control and Bl-1-transfected HT1080 cells were cultured for 2 days with 5–10 μM TUN or 5–10 μM THPS or cultured for 1 day with 50 μM VP16 or 0.25 μg/ml anti-Fas antibody CH11. (B) The percentage of apoptotic cells was determined by annexin-V/propidium iodide (PI) staining (mean ± SD; n = 3). (C) Caspase activity was measured in cell lysates by using fluorigenic substrate Ac-DEVD-AFC, normalizing data relative to total protein content. Data represent enzyme rates, expressed as relative fluorescent units (RFU) of fluorescent product generated per minute at 30°C; measurements were taken within the linear portion of the enzyme-progress curves (mean ± SD; n = 3 determinations).

(D) CMS14.1 cells stably transfected with pBabe-PURO parent vector or pBabe-PURO encoding Bl-1-HA were cultured 5 days after differentiation at 39°C with 5 μM THPS for 2 days, 5 μM brefeldin-A for 2 days, 0.3 μM STS for 18 hr, or 50 ng/ml TNF, with 1 μM CDDO (used as a TNF sensitizer) (Kim et al., 2002). The percentage of apoptotoic cells was determined by annexin-V/PI staining (mean ± SD; n = 3).

by immunoprecipitation with an epitope-specific antibody (Nechushtan et al., 1999) and translocation of Bax from cytosol to mitochondria (as determined by subcellular fractionation studies) (Figures 6A and 6B). By comparison, however, STS-induced translocation and activation of Bax was not blocked by Bl-1 overexpression, indicating selectivity (see Supplemental Data; and data not shown). Bl-1 overexpression also blocked dissipation of mitochondrial $\Delta\Psi$ in HT1080 cells treated with THPS or TUN, but not VP16 of anti-Fas, as determined by $DiOC_6$ staining (Figure 6C), indicating that Bl-1-mediated protection occurs upstream of mitochondria.

Bl-1 Alters Regulation of ER Calcium

An important role for alterations in ER handling of Ca^{2+} has been implicated in apoptosis control mechanisms (Baffy et al., 1993; Demaurex and Distelhorst, 2003). We therefore explored the effects of Bl-1 overexpression on ER-based Ca^{2+} regulation. For these experiments, HT1080-Neo and HT1080-Bl-1 cells were loaded with Fura2 and cultured in either Ca^{2+} or Ca^{2+}-free medium. Cells were then treated with THPS to inhibit the ER Ca^{2+}-ATPase and release ER Ca^{2+}, then cytosolic free Ca^{2+} was imaged essentially as described by using ratiometric methods after verifying uptake of comparable amounts of dye by Neo- and Bl-1 transfectants (Grynkiewicz et al., 1985). In both Ca^{2+}-containing and Ca^{2+}-free medium, far less Ca^{2+} was released into the cytosol following THPS treatment of Bl-1-overexpressing cells compared to control transfectants (Figure 7A). Control experiments with ionomycin in Ca^{2+}-containing medium to allow extracellular Ca^{2+} influx confirmed that differences in Neo- and Bl-1 transfectants were not due to differences in dye response to Ca^{2+} in these cells (data not shown).

We then performed similar experiments with *bi-1*$^{-/-}$ MEFs. Dose-response experiments performed in Ca^{2+}-free media showed that more Ca^{2+} was released from internal stores in response to either THPS or TUN in *bi-1*$^{-/-}$ compared to *bi-1*$^{+/+}$ cells (Figure 7B; and data not shown).

Taken together, these observations indicate that Bl-1

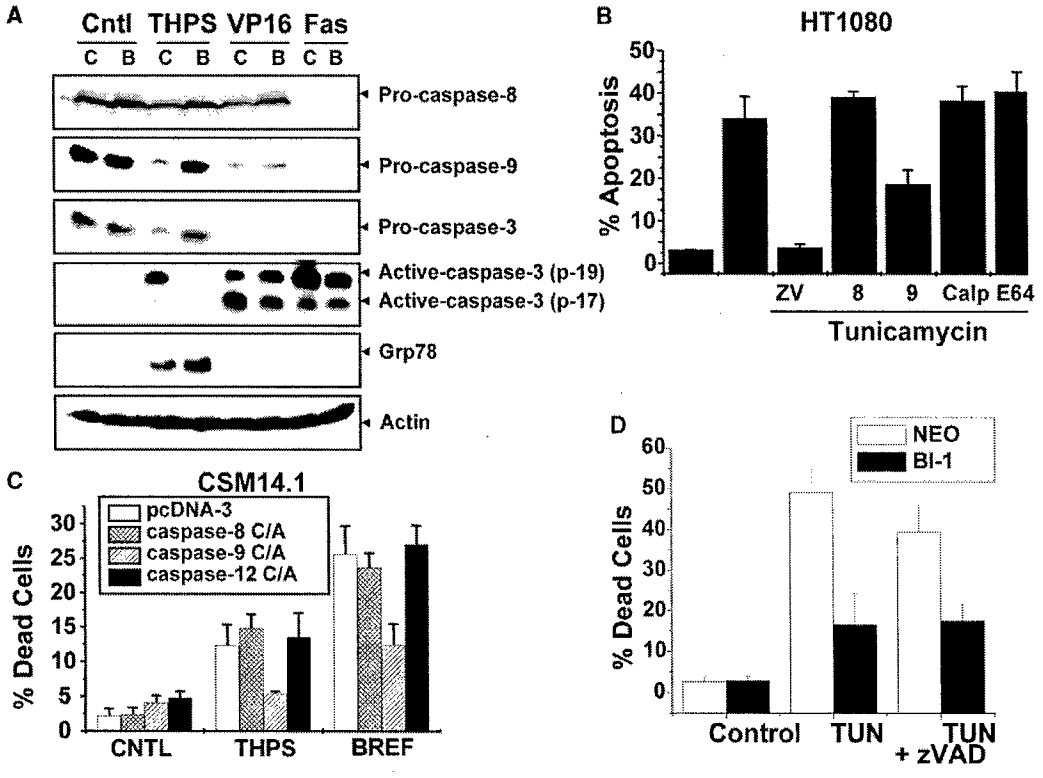

Figure 5. Effects of BI-1 Overexpression on ER Damage and Caspase Processing

(A) HT1080-Neo ("C") and HT1080-BI-1 ("B") stable transfectants were cultured without treatment (CNTL) or for 1 day with 5 μM THPS, 50 μM VP16, or 0.25 μg/ml anti-Fas antibody (CH11). Detergent lysates were prepared, normalized for total protein content, and analyzed by SDS-PAGE/immunoblotting by using antibodies specific for (from top to bottom) caspase-8, caspase-9, caspase-3, large subunit of processed caspase-3, Grp78, or Actin.

(B) HT1080 cells were cultured with 100 μM zVAD-fmk ("ZV"), 100 μM Ac-IETD-fmk ("8") (caspase-8 inhibitor), 100 μM-LEHD-fmk ("9") (caspase-9 inhibitor), 10 μM Calpeptin ("Calp"), or 10 μg/ml E64d (Calpain inhibitors). Cells were then stimulated with 5 μM TUN for 2 days, and the percentage of apoptotic cells was determined by annexin-V/PI staining (mean ± SD; n = 3).

(C) CMS14.1 cells were transiently transfected with control plasmid (pcDNA3) or plasmids encoding cysteine-alanine active site mutants of pro-caspase-8 (stippled bars), pro-caspase-9 (striped bars), or pro-caspase-12 (black bars). After 1 day, cells were cultured in medium without (CNTL) or with 5 μM THPS or 5 μM TUN. The next day, adherent and floating cells were recovered, incubated with 1 μg/ml propidium iodide in PBS, and imaged by UV-microscopy; the percentage of GFP-positive (transfected) cells which took up PI stain (dead) were counted. Data represent mean ± SD; n = 3.

(D) HT1080-Neo and HT1080-BI-1 cells were cultured with 5 μg/ml TUN for 3 days, with or without the addition of 100 μM zVAD-fmk at initiation of culture and again after 1.5 days. The percentage of viable cells was determined by trypan blue dye exclusion (mean ± SD; n = 3).

alters Ca^{2+} handling by the ER, in a manner resembling the effects of overexpressing Bcl-2 or knocking out Bax and Bak (Demaurex and Distelhorst, 2003). Examination of the kinetic profiles for Fura2 fluorescence following treatment with THPS also suggests the possibility that BI-1 may indirectly affect Ca^{2+} reentry after emptying ER stores.

Discussion

Here we show that the BI-1 protein suppresses an apoptosis pathway linked to ER stress in cultured mammalian cells and in mice in vivo. The BI-1 protective mechanism is characterized by suppression of Bax activation and translocation to mitochondria, preservation of mitochondria membrane potential and mitochondrial morphology, and prevention of activation of post-mitochondrial caspases. Thus, BI-1 appears to block the transmission of a death signal or signals from damaged ER/Golgi to mitochondria. However, because tissues of BI-1-deficient mice are histologically normal, BI-1 is presumably not required for physiological regulation of developmental programmed cell death. Rather, the functional importance of BI-1 in vivo is revealed in pathological contexts, when cells are under stress. Similarly, several other genes playing roles in apoptosis regulation principally manifest their essentiality in vivo at times of stress or injury (e.g., *p53, caspase-1, caspase-2, caspase-11, bid, bak*), with knockout mice displaying little or no overt phenotypes under normal conditions.

Precisely how the BI-1 protein functions is unknown. The cytoprotective properties of BI-1 were first discovered in a screen for mammalian cDNAs capable of suppressing Bax-induced death of yeast cells (Xu and Reed, 1998). Since then, BI-1 orthologs and homologs have been identified in insects and numerous plant species by using the same screening method, and all members of the BI-1 protein family tested to date block yeast

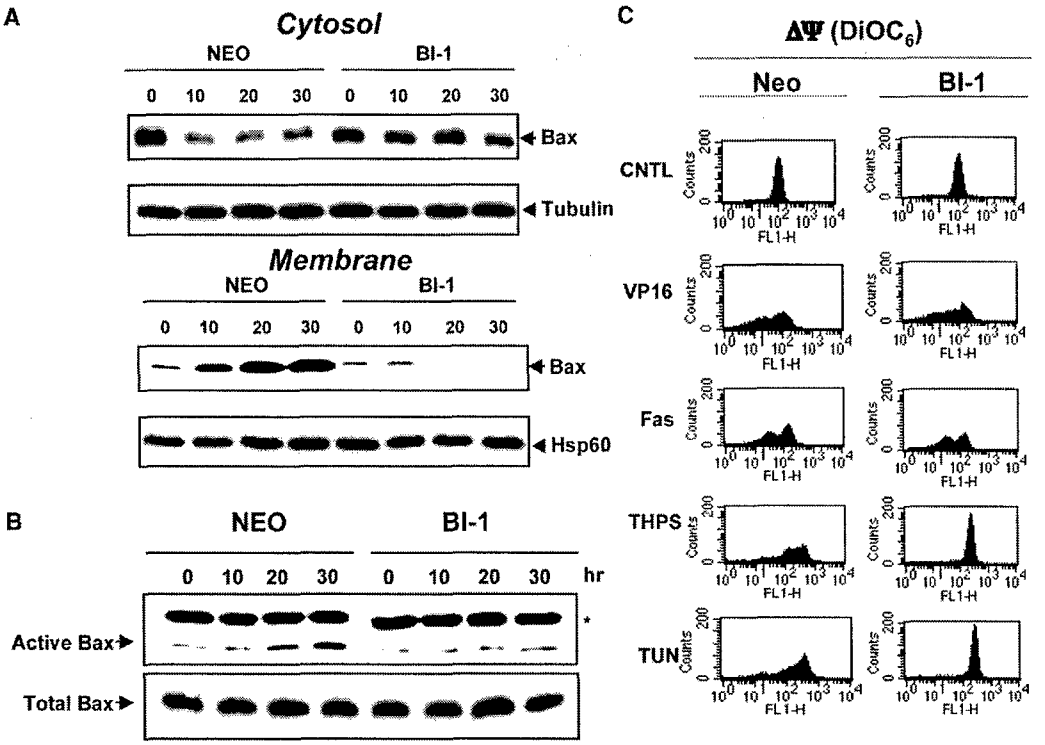

Figure 6. BI-1 Blocks Bax Translocation and Mitochondrial Damage Induced by ER Stress

(A) HT1080-neo and HT1080-BI-1 stable transfectants were cultured for various times (0, 10, 20, 30 hr) with 5 μM TUN. Cytosolic and membrane fractions were prepared as described (Nouraini et al., 2000) and were analyzed by SDS-PAGE/immunoblotting with antibodies specific for Bax (top), the intramitochondrial protein Hsp60, or the cytosolic protein Tubulin, used here as loading controls. Probing blots with anti-Hsp60 and anti-Tubulin antibodies confirmed proper fractionation (i.e., no Hsp60 and no Tubulin contaminating the cytosolic and membrane <mitochondria> fractions, respectively [data not shown]). Total levels of Bax in whole-cell lysates were not changed by TUN treatment (data not shown)

(B) BI-1 blocks conversion of Bax to the active conformation during ER stress. HT1080-neo and HT1080-BI-1 stable transfectants (10^7 cells) were treated for various times (0, 10, 20, 30 hr) with 5 μM tunicamycin. CHAPS lysates were normalized for total protein content, and immunoprecipitations were performed with epitope-specific anti-Bax antibody 6A7 (Nechushtan et al., 1999) and were analyzed by immunoblotting with rabbit anti-Bax antiserum (top). The immunoglobulin light-chain band is indicated by an asterisk (bottom). Total cell lysates were normalized for protein content and were analyzed by immunoblotting to compare total amounts of Bax before and after treatment with Tunicamycin.

(C) Mitochondrial transmembrane potential ($\Delta\Psi$) was measured by $DiOC_6$ staining and flow cytometry analysis. Representative FACS histograms are presented as fluorescence intensity (x axis) versus cell number (y axis) for HT1080-neo and HT1080-BI-1 cells treated with various apoptotic agents, including 50 μM VP16, 5 μM THPS, or 5 μM TUN for 2 days; 0.25 μg/ml anti-Fas antibody for 1 day; or medium control (CNTL) for 2 days.

cell death induced by ectopic expression of mammalian Bax. *Arabidopsis* BI-1 also blocks cell death induced in planta by mammalian Bax (Kawai-Yamada et al., 2001), implying a conserved mechanism. BI-1 orthologs and homologs of animals and plants contain 5–7 predicted membrane-spanning domains.

BI-1 is located predominantly in ER in both mammalian and plant cells (Matsumura et al., 2003; Xu and Reed, 1998). Given that Bax is located in a latent, inactive state in the cytosol of many cells, translocating to mitochondrial membranes in response to various apoptotic stimuli (Hsu et al., 1997; Wolter et al., 1997), it is mysterious that an ER protein should block Bax-induced cell death. However, the mechanisms that trigger activation and translocation of Bax are only partially defined, and emerging evidence of communication between ER and mitochondria in the context of apoptosis regulation (Ghribi et al., 2001; Hacki et al., 2000; Rizzuto et al., 1998) suggests that death signals emanating from the ER may provoke Bax activation. Indeed, we observed Bax activation and translocation to mitochondria following treatment of cells with ER stress agents, with BI-1 overexpression blocking these events. It should be noted, however, that the cell death pathway controlled by BI-1 is evidently Bcl-2/Bax independent in yeast and plants, where no apparent Bcl-2/Bax homologs exist. Thus, while ER stress triggers Bax activation in mammalian cells, and while BI-1 can block that activation, this observation by itself does not imply a causal role for Bax in the cell death mechanism induced by ER stress. However, recent studies of Bax/Bak double knockout mammalian cells have shown that these Bcl-2-family proteins are essential for induction of cell death by the same ER stress agents employed in this study (Scorrano et al., 2003). Thus, *bax* is among the genes required for execution of the cell death pathway blocked by BI-1 in mammalian cells, but the functional equivalents of the ER-initiated cell death pathway in plants and yeast remain unknown.

In addition to protecting against overexpression of

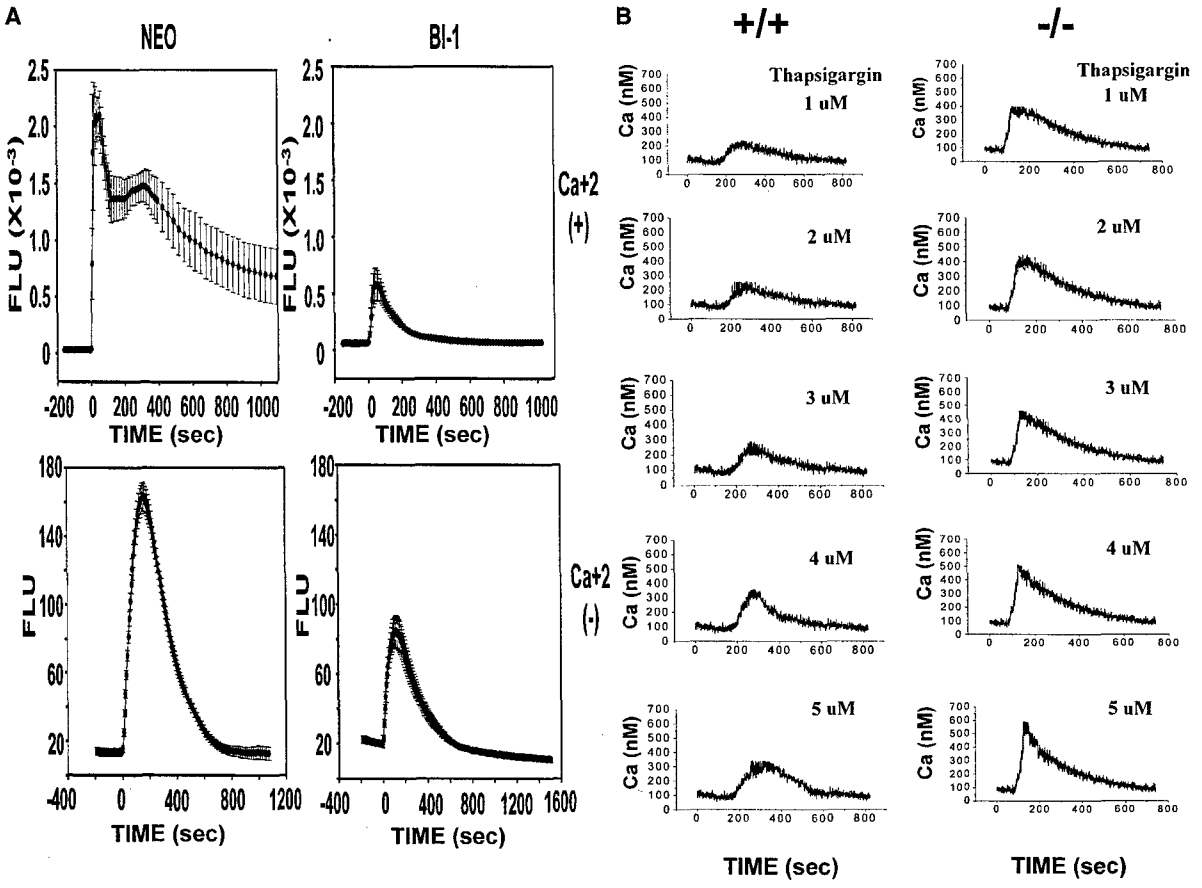

Figure 7. BI-1 Overexpression Alters ER Handling of Calcium

(A) HT1080-neo (left) and HT1080-BI-1 (right) cells were loaded with Fura2, cultured in either Ca^{2+}-containing (top) or Ca^{2+}-free medium (bottom), and incubated with 1 μM THPS at time = 0. Individual cells were imaged (n = 20), and fluorescence intensity was recorded over time. The data presented represent mean ± SEM. Note that the scale of the y axis is different in Ca^{2+}-containing versus Ca^{2+}-free medium. (B) Fura2 imaging was performed by using MEFs from *bi-1*$^{-/-}$ and *bi-1*$^{+/+}$ embryos cultured in Ca^{2+}-free medium and stimulated with various concentrations of THPS. Similar data were obtained for several independently imaged cells.

Bax, the BI-1 orthologs of animals and plants can reduce yeast cell death induced by oxidative stress (e.g., H_2O_2) (Chae et al., 2003). Oxidative stress may predominantly activate an ER pathway for cell death (Scorrano et al., 2003). Moreover, ablation of the *bi-1* gene in mice increased susceptibility to stroke injury in a model of ischemia-reperfusion injury, where oxidative stress is a recognized culprit in cell death (Lipton, 1999), and also increased sensitivity of cultured neurons to death caused by conditions mimicking ischemia-reperfusion. Thus, BI-1 possesses evolutionarily conserved functions that allow it to intercede during cell stress involving ER damage, oxidative stress, or Bax activation. While a caspase activation pathway linked to stress in the ER and Golgi has been suggested (Nakagawa et al., 2000), we obtained evidence only for involvement of post-mitochondrial caspases in our studies where ER stress was induced by agents such as TUN, brefeldin A, and THPS. Thus, caspase activation is a downstream concomitant of the ER stress pathways studied here, but not a requirement for BI-1's cytoprotective mechanism or for cell death induced by these ER stress agents.

Indirect activation of ER-based cell death mechanisms by stimuli not classically associated with ER stress may explain why overexpressed BI-1 can partly suppress apoptosis induced by several types of cytotoxic agents (Xu and Reed, 1998). Crosstalk between ER and the mitochondrial cell death pathway may allow the ER death pathway to amplify cell death signals initiated via the mitochondria pathway, thus explaining why BI-1 overexpression reduces apoptosis induced by mitochondria pathway stimuli in some types of cells (Xu and Reed, 1998). This concept is analogous to the crosstalk between the TNF/Fas death receptor (extrinsic) and mitochondrial (intrinsic) cell death pathways, which has resulted in the discovery of type I versus type II cells, where Bcl-2 overexpression blocks TNF/Fas-initiated cell death in type II but not type I cells because of the requirement for mitochondrial amplification of death receptor-initiated signals (Scaffidi et al., 1998). Thus, in some cells, such as HT1080 and CMS14.1 cells, little crosstalk with the ER pathway may occur, while in others, crosstalk pathways may be operative, thus allowing BI-1 to have a protective effect.

Damage to the ER can trigger several potential parallel pathways contributing to cell death, including distur-

bances in Ca^{2+} regulation (Lipton, 1999), release of apoptogenic proteins from the lumen of the ER (Tenev et al., 2002), and activation of ER-associated caspases (Nakagawa et al., 2000). Among these, the Bcl-2-family proteins have been most clearly linked to the Ca^{2+}-mediated cell death pathway (Demaurex and Distelhorst, 2003). BI-1 also appears to be linked to this pathway, based on results showing that BI-1 modulates ER Ca^{2+} regulation in manners resembling the actions of overexpressing Bcl-2 or knocking out Bax and Bak.

ER stress is relevant to ischemic and degenerative diseases associated with cell loss, including stroke, Parkinson's disease, Alzheimer's disease, and HIV-associated dementia. Further studies will determine whether BI-1 regulates ER stress pathways of relevance to these diverse pathologies, and whether conserved events unify these death stimuli into a common BI-1-suppressible pathway that might be exploited for preserving cells during a variety of disease situations.

Experimental Procedures

Cell Lines and Transfections

Human HT1080 fibrosarcoma cells were maintained in DMEM medium supplemented with 10% heat-inactivated fetal bovine serum (FBS), penicillin G (100 IU/ml), streptomycin (100 μg/ml), and L-glutamate (2 mM) and incubated at 37°C in a humidified atmosphere containing 5% CO_2 and 95% air. Exponentially growing HT1080 cells were seeded at 1×10^6 per 6-well plate or at 1×10^7 per 100-mm dish, prior to exposure to various agents. CSM14.1 cells were maintained in the same medium at 32°C, then plated at low density, cultured at 39°C, and allowed to differentiate for 7–10 days before challenge with apoptosis agents.

Exponentially growing HT1080 and CSM14.1 cells were stably transfected with pcDNA3 or pcDNA3-BI-1-HA plasmids (Xu and Reed, 1998), by using SuperFect transfection reagent (Qiagen), and culturing the cells in 1 mg/ml G418 (Invitrogen) for 3 weeks. Several independent clones were isolated and tested for BI-1-HA expression by immunoblotting.

Primary Cell Cultures

Mouse embryonic fibroblasts (MEFs) were generated from *bi-1*$^{+/+}$, *bi-1*$^{+/-}$, and *bi-1*$^{-/-}$ embryos (E15.5–E16.5). The embryonic sac was separated from fetal material, and cell suspensions were generated from the whole fetus in FGM-2 (Cambrex Life Sciences Company) by mincing. A portion of whole-cell suspension was taken for genotyping, and the rest was plated in embryo fibroblast culture medium (FGM-2) containing 10% FBS, penicillin G (100 IU/ml), streptomycin (100 μg/ml), and L-glutamate (2 mM).

Mouse cortical neuron cultures were prepared as described previously (Choi et al., 1987). Neocorticies of E14–E15 embryos were dissociated; plated on poly-D-lysine- and laminin-coated 24-well plates at a density of $\sim 5 \times 10^4$ cells per well, in minimum essential medium (MEM, Earle's salts) supplemented with 5% horse serum, 5% FBS, 2 mM glucose, and 2 mM L-glutamine; and then maintained for 3 days in a humidified incubator with 5% CO_2 at 37°C, before adding 10 μM cytosine arabinofuranoside for 3 days to halt proliferation of nonneuronal cells. Cells were washed and cultured for an additional 2–3 days in the same medium lacking FBS. Hepatocytes were isolated from liver exactly as described previously (Bailly-Maitre et al., 2002). Cells were cultured at 2×10^5 cells in 24-well plates in 500 μl medium.

Cell Death and Caspase Activity Assays

Cell viability was assessed by propidium iodide (PI) exclusion, where cells were suspended in phosphate-buffered saline (PBS) containing 10 μg/ml PI and analyzed by flow cytometry (FACS Caliber; Becton Dickinson). For apoptosis assessments, cells were analyzed in suspension after trypsinization by using an Annexin V-FITC/PI apoptosis detection kit (Bioversion). Alternatively, cells were fixed on glass coverslips for 5 min in PBS containing 3% paraformaldehyde, air-dried, stained for 10 min in Hoechst 33258 (10 μg/ml), before mounting in 50% glycerol containing 20 mM citric acid and 50 mM orthophosphate, then stored at −20°C before analysis. Nuclear morphology was evaluated by fluorescence microscopy. For TUNEL assays, cells were cultured on 13 mm glass coverslips in 24-well plates. After various experimental procedures, cells were fixed (4% paraformaldehyde, 30 min) on coverslips and permeabilized (PBS 0.1% Triton X-100 and 0.1% sodium citrate, 2 min). After washing, the coverslips were incubated at 37°C for 1 hr in a humidified chamber with the TUNEL reaction mixture containing 0.4 IU/μl TdT, 2.5 mM $CoCl_2$, and 2 μM Bodipy FL-14-dUTP (Gavrieli et al., 1992), washed in PBS, mounted in "anti-fade" medium, and analyzed under a fluorescence microscope, as described previously (Bailly-Maitre et al., 2002).

Caspase activity was measured in cell lysates by using 25 μg of total protein with 100 μM Ac-DEVD-AFC in 100 μl of 10 mM HEPES (pH 7.4), 220 mM mannitol, 68 mM sucrose, 2 mM NaCl, 2.5 mM KH_2PO_4, 0.5 mM EGTA, 2 mM $MgCl_2$, 5 mM pyruvate, 0.1 mM PMSF, and 1 mM DTT. Production of fluorigenic substrate was measured continuously at 30°C by using a spectrofluorimeter.

RNA and DNA Analysis

See the Supplemental Experimental Procedures.

Immunoblotting and Immmunoprecipitations

For immunoblot analysis, cells were lysed in 1% Nonidet P-40, 50 mM HEPES (pH 7.5), 100 mM NaCl, 2 mM EDTA, 1 mM pyrophosphate, 10 mM sodium orthovanadate, 1 mM phenylmethylsulfonyl fluoride, and 100 mM sodium fluoride. Lysates were normalized for total protein content by using a BCA kit (Pierce, Inc), and 40–50 μg aliquots were suspended in an equal volume of 2× Laemmli buffer containing 2-mercaptoethanol, then either boiled for 5 min before performing SDS-PAGE or loaded directly without boiling when analyzing BI-1 protein. Proteins were transferred to Immobilon-P membranes (Millipore), blocked with skim milk (5%), and incubated with various primary antibodies recognizing HA, Grp78, or actin (Santacruz), cleaved caspase-3 (Cell Signaling), Bax (Trevegen), Hsp60 (Stressgen), or caspases-3, -8, or -9 (Krajewski et al., 1999). Antibody detection was accomplished via horseradish peroxidase-conjugated protein A or goat anti-rabbit immunoglobulin G (Bio-Rad) and a chemiluminescence substrate (Amersham) and exposure to X-ray film (Kodak).

Immunoprecipitations of Bax were performed as described (Nechushtan et al., 1999) with CHAPS-containing lysis solution and anti-Bax antibody (6A7: Trevigen). Relative amounts of protein recovered from protein content-normalized lysates were analyzed by SDS-PAGE/immunoblotting with rabbit anti-Bax antibody (Krajewski et al., 1999).

Subcellular Fractionation

Cells were suspended in 150 mM KCl, 25 mM Tris-HCl (pH 7.4), 2 mM EDTA, 10 mM KH_2PO_4, 0.1% (w/v) bovine serum albumin, and 0.02% digitonin. After a 5-min incubation at 37°C, cells were pelleted by centrifugation at 16,000 × g for 20 min, and the resulting supernatants (cytosol) and pellets (membranes) were analyzed by SDS-PAGE/immunoblotting with antibodies specific for Bax, (Krajewski et al., 1999), Hsp 60 (Stressgene), and Tubulin (Santacruz).

Electron Microscopy

For information on electron microscopy, see the Supplemental Experimental Procedures.

Ca^{2+} Imaging

The cells were plated on glass-bottom plates (MatTek), loaded with 4 μM Fura-2 (Molecular Probe) at room temperature for 30 min in HBSS. The cells were then imaged on a Zeiss Axiovert microscope with a cooled CCD camera, controlled by MetaFluor software (Universal Imaging).

Animal Experiments and Tissue Analysis

Mice of 8 weeks of age were injected intrapesitioneally with 1–2 μg/gm tunicamyin, then anesthetized 1–3 days later by intraperito-

neal injection of 0.9 ml Avertin and perfused transcardially with cold heparinized PBS (pH 7.2) containing 10% formaldehyde. Tissues were recovered, post-fixed in Bouin's solution (Sigma), embedded in paraffin, sectioned (0.4 μm), and stained with either H&E or Mason's trichrome reagent.

For morphometric analysis, tissue sections were photographed with a CCD Spot 3.1 camera (Diagnostic Instruments). After importing images into the Image-Pro plus 4.1 program (Media Cybernetics LP), morphometry analysis was performed, measuring the dimensions of the damaged tissue at the corticomedullary region of kidneys relative to the diameter of the renal cortex.

Stroke experiments were performed as described previously (Kermer et al., 2003).

Acknowledgments

We thank J. Yuan and D. Bredesen for reagents; R. Cornell, M. Lamie, and J. Valois for manuscript preparation; and the National Institutes of Health (AG15393; NS36821; HD29587; EY05477; NS27177; NS47855) and Foundation pour la Recherche Medicale for support.

Received: October 22, 2003
Revised: May 26, 2004
Accepted: May 28, 2004
Published: August 13, 2004

References

Baffy, G., Miyashita, T., Williamson, J.R., and Reed, J.C. (1993). Apoptosis induced by withdrawal of interleukin-3 (IL-3) from an IL-3-dependent hematopoietic cell line is associated with repartitioning of intracellular calcium and is blocked by enforced Bcl-2 oncoprotein production. J. Biol. Chem. *268*, 6511–6519.

Bailly-Maitre, B., de Sousa, G., Zucchini, N., Gugenheim, J., Boulukos, K.E., and Rahmani, R. (2002). Spontaneous apoptosis in primary cultures of human and rat hepatocytes: molecular mechanisms and regulation by dexamethasone. Cell Death Differ. *9*, 945–955.

Bergeron, L., Perez, G., Macdonald, G., Shi, L., Sun, Y., Jurisicova, A., Varmuza, S., Latham, K., Flaws, J., Salter, J., et al. (1998). Defects in regulation of apoptosis in caspase-2-deficient mice. Genes Dev. *12*, 1304–1314.

Berridge, M.J., Lipp, P., and Bootman, M.D. (2000). The versatility and universality of calcium signalling. Nat. Rev. *1*, 11–21.

Bolduc, N., and Brisson, L.F. (2002). Antisense down regulation of NtB1–1 in tobacco BY-2 cells induces accelerated cell death upon carbon starvation. FEBS Lett. *532*, 111–114.

Bolduc, N., Ouellet, M., Pitre, F., and Brisson, L.F. (2003). Molecular characterization of two plant BI-1 homologues which suppress Bax-induced apoptosis in human 293 cells. Planta *216*, 377–386.

Chae, H.-J., Ke, N., Chen, S., Kim, H.-R., Godzik, A., Dickman, M., and Reed, J.C. (2003). Evolutionarily conserved cytoprotection provided by Bax Inhibitor-1 (BI-1) homologs from animals, plants, and yeast. Gene *323*, 101–113.

Choi, D.W., Maulucci-Gedde, M., and Kriegstein, A.R. (1987). Glutamate neurotoxicity in cortical cell culture. J. Neurosci. *7*, 357–368.

Demaurex, N., and Distelhorst, C. (2003). Apoptosis–the calcium connection. Science *300*, 65–67.

Gavrieli, Y., Sherman, Y., and Ben-Sasson, S.A. (1992). Identification of programmed cell death in situ via specific labelling of nuclear DNA fragmentation. J. Cell Biol. *119*, 493–501.

Ghribi, O., DeWitt, D.A., Forbes, M.S., Herman, M.M., and Savory, J. (2001). Co-involvement of mitochondria and endoplasmic reticulum in regulation of apoptosis: changes in cytochrome c, Bcl-2, and Bax in the hippocampus of aluminum treated rabbits. Brain Res. *903*, 66–73.

Green, D.R., and Reed, J.C. (1998). Mitochondria and apoptosis. Science *281*, 1309–1312.

Grynkiewicz, G., Poenie, M., and Tsien, R.Y. (1985). A new generation of Ca2+ indicators with greatly improved fluorescence properties. J. Biol. Chem. *260*, 3440–3450.

Hacki, J., Egger, L., Monney, L., Conus, S., Rosse, T., Fellay, I., and Borner, C. (2000). Apoptotic crosstalk between the endoplasmic reticulum and mitochondria controlled by Bcl-2. Oncogene *19*, 2286–2295.

Hsu, Y.-T., Wolter, K.G., and Youle, R.J. (1997). Cytosol-to-membrane redistribution of members of Bax and Bcl-X_L during apoptosis. Proc. Natl. Acad. Sci. USA *94*, 3668–3672.

Jean, J.C., Oakes, S.M., and Joyce-Brady, M. (1999). The Bax inhibitor-1 gene is differentially regualted in adult testis and developing lung by tow alternative TATA-less promoters. Genomics *57*, 201–208.

Kaufman, R.J. (1999). Stress signaling from the lumen of the endoplasmic reticulum: coordination of gene transcriptional and translational controls. Genes Dev. *13*, 1211–1233.

Kawai, M., Pan, L., Reed, J.C., and Uchimiya, H. (1999). Evolutionally conserved plant homologue of the Bax inhibitor-1 (BI-1) gene capable of suppressing Bax-induced cell death in yeast. FEBS Lett. *464*, 143–147.

Kawai-Yamada, M., Jin, L., Yoshinaga, K., Hirata, A., and Uchimiya, H. (2001). Mammalian Bax-induced plant cell death can be down-regulated by overexpression of *Arabidopsis Bax Inhibitor-1 (AtBI-1)*. Proc. Natl. Acad. Sci. USA *98*, 12295–12300.

Kermer, P., Krajewska, M., Zapata, J.M., Takayama, S., Mai, J., Krajewski, S., and Reed, J.C. (2002). BAG1 is a regulator and marker of neuronal differentiation. Cell Death Differ. *9*, 405–413.

Kermer, P., Digicaylioglu, M.H., Kaul, M., Zapata, J.M., Krajewska, M., Stenner-Liewen, F., Takayama, S., Krajewski, S., Lipton, S.A., and Reed, J.C. (2003). BAG1 over-expression in brain protects against stroke. Brain Pathol. *13*, 495–506.

Kim, Y., Suh, N., Sporn, M., and Reed, J.C. (2002). An inducible pathway for degradation of FLIP protein sensitizes tumor cells to TRAIL-induced apoptosis. J. Biol. Chem. *277*, 22320–22329.

Krajewski, S., Krajewska, M., Ellerby, L.M., Welsch, K., Xie, Z., Deveraux, Q.L., Salvesen, G.S., Bredesen, D.E., Rosenthal, R.E., Fiskum, G., et al. (1999). Release of caspase-9 from mitochondria during neuronal apoptosis and cerebral ischemia. Proc. Natl. Acad. Sci. USA *96*, 5752–5757.

Lipton, P. (1999). Ischemic cell death in brain neurons. Physiol. Rev. *79*, 1431–1568.

Mancini, M., Machamer, C.E., Roy, S., Nicholson, D.W., Thornberry, N.A., Casciola-Rosen, L.A., and Rosen, A. (2000). Caspase-2 is localized at the golgi complex and cleaves golgin-160 during apoptosis. J. Cell Biol. *149*, 603–612.

Matsumura, H., Nirasawa, S., Kiba, A., Urasaki, N., Saitoh, H., Ito, M., Kawai-Yamada, M., Uchimiya, H., and Terauchi, R. (2003). Overexpression of Bax inhibitor suppresses the fungal elicitor-induced cell death in rice (*Oryza sativa L*) cells. Plant J. *33*, 425–434.

Nakagawa, T., Zhu, H., Morishima, N., Li, E., Xu, J., Yankner, B.A., and Yuan, J. (2000). Caspase-12 mediates endoplasmic-reticulum-specific apoptosis and cytotoxicity by amyloid-β. Nature *403*, 98–103.

Nechushtan, A., Smith, C., Hsu, Y.-T., and Youle, R. (1999). Conformation of the Bax C-terminus regulates subcellular location and cell death. EMBO J. *18*, 2330–2341.

Nicholson, D.W., and Thornberry, N.A. (2003). Apoptosis. Life and death decisions. Science *299*, 214–215.

Nouraini, S., Six, E., Matsuyama, S., Krajewski, S., and Reed, J.C. (2000). The putative pore forming-domain of bax regulates mitochondrial localization and interaction with bcl-X_L. Mol. Cell. Biol. *20*, 1604–1615.

Patil, C., and Walter, P. (2001). Intracellular signaling from the endoplasmic reticulum to the nucleus: the unfolded protein response in yeast and mammals. Curr. Opin. Cell Biol. *13*, 349–355.

Rizzuto, R., Pinton, P., Carrington, W., Fay, F.S., Fogarty, K.E., Lifshitz, L.M., Tuft, R.A., and Pozzan, T. (1998). Close contacts with the endoplasmic reticulum as determinants of mitochondrial Ca^{2+} responses. Science *280*, 1763–1766.

Rose, K., Goldberg, M.P., and Choi, D.W. (1993). In vitro biological

methods. In Methods in Toxicology, C.A. Tyson and J.M. Frazier, eds. (San Diego: Academic Press), pp. 46–60.

Salvesen, G.S. (2002). Caspases: opening the boxes and interpreting the arrows. Cell Death Differ. *9*, 3–5.

Sanchez, P., de Torres, M., and Grant, M. (2000). AtBI-1, a plant homologue of Bax inhibitor-1, suppresses Bax-induced cell death in yeast and is rapidly upregulated during wounding and pathogen challenge. Plant J. *21*, 393–399.

Scaffidi, C., Fulda, S., Srinivasan, A., Friesen, C., Li, F., Tomaselli, K., Debatin, K.-M., Krammer, P., and Peter, M. (1998). Two CD95 (APO-1/Fas) signaling pathways. EMBO J. *17*, 1675–1687.

Scorrano, L., Oakes, S.A., Opferman, J.T., Cheng, E.H., Sorcinelli, M.D., Pozzan, T., and Korsmeyer, S.J. (2003). BAX and BAK regulation of endoplasmic reticulum Ca2+: a control point for apoptosis. Science *300*, 135–139.

Tenev, T., Zachariou, A., Wilson, R., Paul, A., and Meier, P. (2002). Jafrac2 is an IAP antagonist that promotes cell death by liberating Dronc from DIAP1. EMBO J. *21*, 5118–5129.

Villunger, A., Scott, C., Bouillet, P., and Strasser, A. (2003). Essential role for the BH3-only protein Bim but redundant roles for Bax, Bcl-2, and Bcl-w in the control of granulocyte survival. Blood *101*, 2393–2400.

Wang, Y.F., Tsirka, S.E., Strickland, S., Stieg, P.E., Soriano, S.G., and Lipton, S.A. (1998). Tissue plasminogen activator (tPA) increases neuronal damage after focal cerebral ischemia in wild-type and tPA-deficient mice. Nat. Med. *4*, 228–231.

Wolter, K.G., Hsu, Y.T., Smith, C.L., Nechushtan, A., Xi, X.G., and Youle, R.J. (1997). Movement of Bax from the cytosol to mitochondria during apoptosis. J. Cell Biol. *139*, 1281–1292.

Xu, Q., and Reed, J.C. (1998). BAX inhibitor-1, a mammalian apoptosis suppressor identified by functional screening in yeast. Mol. Cell *1*, 337–346.

Yin, X.M., Wang, K., Gross, A., Zhao, Y., Zinkel, S., Klocke, B., Roth, K.A., and Korsmeyer, S.J. (1999). Bid-deficient mice are resistant to Fas-induced hepatocellular apoptosis. Nature *400*, 886–891.

Zinszner, H., Kuroda, M., Wang, X., Batchvarova, N., Lightfoot, R.T., Remotti, H., Stevens, J.L., and Ron, D. (1998). CHOP is implicated in programmed cell death in response to impaired function of the endoplasmic reticulum. Genes Dev. *12*, 982–995.

Available online at www.sciencedirect.com
SCIENCE DIRECT®
Gene 323 (2003) 101–113
GENE
AN INTERNATIONAL JOURNAL ON GENES AND GENOMES
www.elsevier.com/locate/gene

Evolutionarily conserved cytoprotection provided by Bax Inhibitor-1 homologs from animals, plants, and yeast

Han-Jung Chae[a,1], Ning Ke[a,1], Hyung-Ryong Kim[a,1], Shaorong Chen[b,1], Adam Godzik[a], Martin Dickman[b], John C. Reed[a,*]

[a] *The Burnham Institute, La Jolla, CA 92037, USA*
[b] *Department of Plant Pathology, The University of Nebraska, Lincoln, NE 68583, USA*

Received 6 May 2003; received in revised form 17 July 2003; accepted 10 September 2003

Received by D.A. Tagle

Abstract

Programmed cell death (PCD) plays important roles in the development and physiology of both animals and plants, but it is unclear whether similar mechanisms are employed. Bax Inhibitor-1 (BI-1) is an intracellular multi-membrane-spanning protein and cell death inhibitor, originally identified by a function-based screen for mammalian cDNAs capable of suppressing cell death in yeast engineered to ectopically express the pro-apoptotic protein Bax. Using this yeast assay, we screened expression libraries for cDNAs from the plant, *Lycopersicon esculentum* (tomato), and the invertebrate animal *Drosophila melanogaster* (fruit fly), identifying close homologs of BI-1 as Bax-suppressors. We studied the fly and tomato homologs of BI-1, as well as BI-1 homologs identified in *Arabidopsis thaliana*, *Oryza sativa* (rice), and *Saccharomyces cerevisiae* (budding yeast). All eukaryotic homologs of BI-1 blocked Bax-induced cell death when expressed in yeast. Eukaryotic BI-1 homologs also partially rescued yeast from cell death induced by oxidative stress (H_2O_2) and heat shock. Deletion of a C-terminal domain from BI-1 homologs abrogated their cytoprotective function in yeast, demonstrating conserved structure–function relations among these proteins. Expression of tomato BI-1 by agroinfiltration of intact plant leaves provided protection from damage induced by heat-shock and cold-shock stress. Altogether, these findings indicate that BI-1 homologs exist in multiple eukaryotic species, providing cytoprotection against diverse stimuli, thus implying that BI-1 regulates evolutionary conserved mechanisms of stress resistance that are germane to both plants and animals.

Keywords: BI-1; Cell death; Cytoprotection; Evolution

1. Introduction

Programmed cell death (PCD) plays critical roles in a wide variety of normal physiological processes in multicellular animal species. The genes that control programmed cell death in animals are conserved across wide evolutionary distances, defining a core set of biochemical reactions that are regulated in diverse ways by inputs from myriad upstream pathways (Metzstein et al., 1998). These genes encode either anti-apoptotic and pro-apoptotic proteins, which do battle with each other in making cell life–death decisions.

Programmed cell death (PCD) plays normal physiological roles in a variety of processes in plants, including (a) deletion of cells with temporary functions such as the aleurone cells in seeds and the suspensor cells in embryos; (b) removal of unwanted cells, such as the root cap cells found in the tips of elongating plant roots and the stamen primoridia cells in unisexual flowers; (c) deletion of cells during sculpting of the plant body and formation of leaf lobes and perforations; (d) death of cells during plant specialization, such as the death of TE cells which creates channels for water transport in vascular plants; (e) leaf senescence; and (f) responses to plant pathogens (Danon et

Abbreviations: BI-1, Bax Inhibitor-1; PCD, programmed cell death; ER, endoplasmic reticulum; TM, transmembrane; gal, galactose; glu, glucose; ECL, enhanced chemiluminescence; OD, optical density.

* Corresponding author. Tel.: +1-858-646-3140; fax: +1-858-646-3194.
E-mail addresses: jreed@burnham.org, reedoffice@burnham.org (J.C. Reed).

[1] These four individuals contributed equally to the results of this paper.

0378-1119/$ - see front matter © 2003 Elsevier B.V. All rights reserved.
doi:10.1016/j.gene.2003.09.011

al., 2000; Pennell and Lamb, 1997). Some elements of the same cell suicide mechanisms used in animal cells may be functionally conserved in plants. Though the biochemical mechanisms responsible for cell suicide in plants are largely unknown, a variety of reports suggest similarities to the PCD that occurs in animal species. For example, PCD in plants typically requires new gene expression and thus can be suppressed by cycloheximide and similar inhibitors of protein or RNA synthesis. The morphological characteristics of plant cells undergoing PCD also bear some striking similarities to apoptosis in animals, though the presence of a cell wall around plant cells imposes certain differences. Akin to animal cells, PCD in plants is associated with internucleosomal DNA fragmentation (DNA ladders) and the activation of proteases (Del Pozo and Lam, 1998; Richael et al., 2001; Solomon et al., 1999). Moreover, ectopic expression of certain animal anti-apoptosis genes in transgenic plants has been demonstrated to provide protection from crop-pathogens and other insults as a result of cell death suppression (Dickman et al., 2001; Mitsuhara et al., 1999). Conversely, expression of animal pro-apoptotic proteins such as Bax in plants can induce cell death mechanisms similar to endogenous programs for cell suicide (Lacomme and Cruz, 1999). However, to date, few endogenous plant genes have been identified that share sequence homology with the apoptosis genes of animal cells.

Bax Inhibitor-1 (BI-1) is an anti-apoptotic protein which is conserved in both animal and plant species. Though transcripts encoding this protein were known from unrelated experiments, the cytoprotective function of BI-1 was discovered in cDNA library screens for human proteins capable of suppressing death of yeast induced by ectopic expression of mammalian Bax protein, a pro-apoptotic member of the Bcl-2 family of apoptosis-regulating proteins (Perfettini et al., 2002; Xu and Reed, 1998). When overexpressed in mammalian cells, BI-1 provides protection against apoptosis induced by several types of stimuli, including Bax overexpression, growth factor deprivation, and Ca^{2+} mobilizing agents (Xu and Reed, 1998). Moreover, BI-1 protects certain types of cells against TRAIL, a member of the tumor necrosis factor (TNF) family of cytokines (Burns and El-Deiry, 2001). Antisense experiments in which BI-1 expression was knocked down suggested that the endogenous BI-1 protein can be important for suppressing apoptosis in some types of tumor cell lines (Xu and Reed, 1998). Immunolocalization and subcellular fractionation studies demonstrated that BI-1 is located predominantly in the endoplasmic reticulum (ER) (Xu and Reed, 1998).

How the BI-1 protein functions is unknown. A Kyte–Doolittle plot of protein hydrophobicity revealed six predicted membrane-spanning domains in mammalian BI-1 proteins (Xu and Reed, 1998). Similar proteins have been identified in several plant species, including *Oryza sativa* (rice), *Arabidopsis thaliana* (*At*), *Hordeum vulgare* (barley), *Brassica napus* (oilseed rape), and *Nicotiana tabacum* (tobacco) (Bolduc et al., 2003; Huckelhoven et al., 2003; Kawai et al., 1999; Kawai-Yamada et al., 2001; Lam et al., 2001; Sanchez et al., 2000). Moreover, the function of plant homologues of BI-1 appears to be at least partly conserved with its human counterpart, given that BI-1 orthologs of rice and *Arabidopsis* also rescue in the yeast-based Bax-lethality assay (Kawai et al., 1999; Sanchez et al., 2000) and BI-1 homologs of oilseed rape and tobacco rescue against Bax-induced apoptosis in human cells (Bolduc et al., 2003). Importantly, *Arabidopsis* BI-1 has been shown to protect transgenic plants against cell death induced by ectopic expression of mammalian Bax (Kawai-Yamada et al., 2001), indicating an in vivo role for BI-1 in cytoprotective pathways in planta and suggesting that the biochemical mechanism regulated by BI-1 is evolutionarily conserved. BI-1 overexpression also regulates resistance to fungal pathogens in barley, probably due to its cell death-suppressive effects (Huckelhoven et al., 2003). Conversely, antisense-mediated downregulation of BI-1 in tobacco BY-2 cells results in accelerated cell death upon carbon starvation (Bolduc and Brisson, 2002). Interestingly, endogenous expression of BI-1 is induced during wound-healing responses and upon exposure to certain pathogens in plants (Huckelhoven et al., 2001; Sanchez et al., 2000), suggesting that BI-1 may play a role in host-defense mechanisms during times of stress. In this regard, endogenous BI-1 expression is downregulated by treatment of cultured rice cells (*O. sativa*) with cytotoxic extracts from rice blast fungus (*Magnaporthe grisea*), while overexpression of *At*-BI-1 sustains survival (Matsumura et al., 2003). Thus, BI-1 represents the first endogenous gene to be identified that regulates cell death in both plant and animal cells.

In this report, we used a combination of functional cloning to identify additional BI-1 homologs from plant and animal eukaryotic species and performed a comparative analysis of the BI-1 homologs of humans (*Homo sapiens*), insects (*Drosophila*), tomato (*Lycopersicon*), rice (*Oryza*), mustard (*Arabidopsis*), and budding yeast (*Saccharomyces cerevisiae*). Our findings reveal conservation of function of these eukaryotic BI-1 protein, implying an evolutionarily preserved role for BI-1 in cytoprotection.

2. Materials and methods

2.1. Plasmids

Human BI-1 and BI-1 homologs from other species were cloned into the yeast-compatible expression plasmids p426-GPD (ATCC) or pESC-URA3 (Stratagene), with C-terminal Myc-tags. To generate p426-GPD-Myc, a ~0.7-kbp fragment of pcDNA3Myc-dBok was first prepared by digestion with *Hin*dIII, blunting of the

*Hin*dIII ends using a Klenow-mediated fill-in reaction, then digestion with XhoI. This fragment was then subcloned into SmaI–XhoI-digested p426-GPD (Zhang and Reed, 2001). *Arabidopsis* BI-1 ("a-BI-1") and rice BI-1 ("r-BI 1") homologs were described previously (Kawai et al., 1999; Yu et al., 2002). Tomato BI 1 ("t BI 1") and *Drosophila* BI-1 ("d-BI-1") homologs were derived through cDNA library screen of tomato and *Drosophila* (ATCC) cDNA libraries. Yeast BI-1 homolog (YNL305c) (hereinafter termed "y-BI-1") was obtained from ResGen. A genomic fragment encoding a bacterial BI-1-like protein (hereinafter termed "e-BI-1") was obtained by PCR using *Escherichia coli* strain (XL-1Blue) DNA as a template. PCR was used to amplify the desired open reading frames of BI-1 homologs, with *Eco*RI and XhoI restriction sites incorporated in the amplification primers for subsequent digestion and cloning. Primers used include: 5′-ggaattcatggacagattcccacttc-3′and 5′-gctcgagctagggtcgactacggcggttgccgaagatcc-3′for eBI-1 (hypothetical protein YhbL [NP_752798.1; gi number 6246758); 5′-ggaattcatggcagatactgcgaattaca-3′and 5′-gctcgagctagggtcgacttttagttttgttctggcggcg-3′for dBI-1 (NM_139948); 5′-cggatccatgtcaggtcctccacctcc-3′and 5′-gctcgagctagggtcgactattgtcgtcgttagagttgg-3′for y-BI-1 (NC_001146); 5′-ggaattcatggaaggtttcacatcgttc-3′and 5′-gctcgagctagggtcgactgtttctcctcttcttcttcttc-3′for t-BI-1 (AF390556); 5′-ggaattcatggatgcgttctcttccttc-3′and 5′-gctcgagctagggtcgactgtttctccttttcttcttc-3′for a-BI-1 (AB025927); 5′-ggaattcatggacgccttctactcgac-3′ and 5′-gctcgagctagggtcgactagacctcttcttcctcttc-3′for r-BI-1 (AB025926); 5′-ggaattcatgaacatatttgatcgaaag-3′and 5′-gctcgagctagggtcgacttttcttctctttcttcttatc-3′ for human BI-1 ("h-BI-1") (XM_035490). The PCR products were digested with *Eco*RI and XhoI, then cloned into the corresponding sites in p426-GPD or p426-GPD-Myc.

Mutants of h-BI-1 were generated by deleting final amino acids distal to the last predicted transmembrane (TM) domain, thus deleting the last nine amino acids of the protein, or by exchanging C-terminal charged residues for alanine (C9A) using PCR-based methods. Primers for C-terminal truncation of h-BI-1 included 5′-ggaattcatgaacatatttgatcgaaag-3′and 5′-ccgctcgaggggtcgactattcatggccaggatcatgag-3′ for h-BI-1, while primers for construction of h-BI-1(C9A) were 5′-ggaattcatgaacatatttgatcgaaag-3′and 5′-ccgctcgagctagggtcgactagctgccg cggccgctgcagctgcagcattcatggccaggatcatc-3′. The C9A mutant of h-BI-1 thus contains nine consecutive alanines instead of EKDKKKEKK at C-terminus. In addition to human BI-1, PCR was used to generate mutants of BI-1 homologs of other species that also lacked the C-terminal charged resides. The primers for mutation used included: 5′-ggaattcatggcagatactgcgaattacatc-3′and 5′-ggcctcgagctattgcgtcagtataatcagcaaacg-3′for dBI-1; 5 and 5′-ggcctcgagctaagatgcattctttaacatgatgat cag-3′for t-BI-1; 5′-cgggatccatgtcaggtcctccacctcc-3′and 5′-ggcctcgagctaggccaaaatccttaaaatagacaaa for yBI-1. PCR conditions employed were 95 °C for 30 s, 55 °C for 1 min, and 72 °C for 30 s for a total of 30 cycles using a High Fidelity PCR system (Roche, Mannheim, Germany).

2.2. cDNA library screening

For library screening, yeast strain QX95001 containing YEp51-Bax was grown in SC medium supplemented with leucine (SC-L) to early log phase ($OD_{600}=0.3-0.5$). Then, 100 μg of either *Drosophila* cDNA library (lambda YES-*Drosophila* third instar cDNA library, ATCC) or tomato cDNA library in pJG45 was transformed into QX95001 using the LiOAc method. Transformants were plated directly onto agar plates containing SC medium supplemented with leucine, uracil, and either glucose (SC-U-L/Glu) or galactose (SC-U-T/Gal), and colonies were allowed to grow at 30 °C for 5–7 days. Emerging colonies were then streaked onto galactose-containing SC-U-L plates again to confirm the growth phenotype. Then, the cDNAs that conferred resistance to Bax-induced death were plasmid-rescued into bacteria, and the resulting plasmid DNA was retransformed into QX95001 yeast containing YEp51-Bax, and the cells were grown on SC-U-L/Gal plates to confirm ability to rescue from Bax-induced lethality (Xu et al., 1999). For plasmids that consistently rescued yeast from Bax, the expression the Bax protein was assayed using lysates from cells grown in galactose-containing medium by immunoblotting, using anti-Bax antibody.

2.3. Yeast viability assays

To determine whether BI-1-encoding plasmids rescue yeast from Bax-induced lethality, yeast containing YEp51-Bax and various p426-myc-BI-1 plasmids were grown in SC-U-L/glucose media overnight. The yeast cultures were then serial 10-fold diluted into SC medium, and 5 μl of each dilution was dropped onto SC-U-L/galactose or SC-U-L/glucose plates. Cells were incubated at 30 °C for ~ 5 days and photographed.

For heat-shock experiments, EGY48 strain yeast containing plasmids encoding various BI-1 homologs were grown in SC-U media overnight. Cultures were diluted to $OD_{600}=0.1$ and grown at 30 °C to early log phase ($OD_{600}=0.3-0.5$). Cultures were then serial 10-fold diluted in ddH_2O and incubated at 50 °C (heat shock) or left at room temperature (mock treatment) for 30 min before plating onto SC-U/glucose medium. After 5–7 days incubation at 30 °C, colonies were counted, and the proportion of surviving colonies was determined by dividing the values for heat-shock-treated from mock-treated samples.

For oxidative stress experiments, EGY48 strains containing BI-1 homologs were grown in SC-U media overnight. Cultures were diluted to $OD_{600}=0.1$ in ddH_2O and treated with or without 3 mM H_2O_2 for 6 h. Cultures were then washed in SC medium, serial 10-fold diluted, and plated on SC-U/glucose. After 5–7 days incubation at 30 °C, colonies

were counted, and the proportion of colonies surviving H_2O_2 exposure was determined by dividing the values for H_2O_2-treated from mock-treated samples.

Similar heat-shock and H_2O_2 treatments were also used to evaluate the relative sensitivity to stress of wild-type and BI-1-deficient (ΔyBI) yeast using *S. cerevisiae* Hansen strain BY4741 (*mat a his3D1 leu2D0 met15D0 ura3D0*), and its deletion derivative YNL305C (ResGen). Cells were grown in YPD media with various concentrations of H_2O_2.

2.4. Immunoblotting

Yeast were grown in SC-U/glucose media overnight. Cultures were then diluted, and the cells were grown to early

A

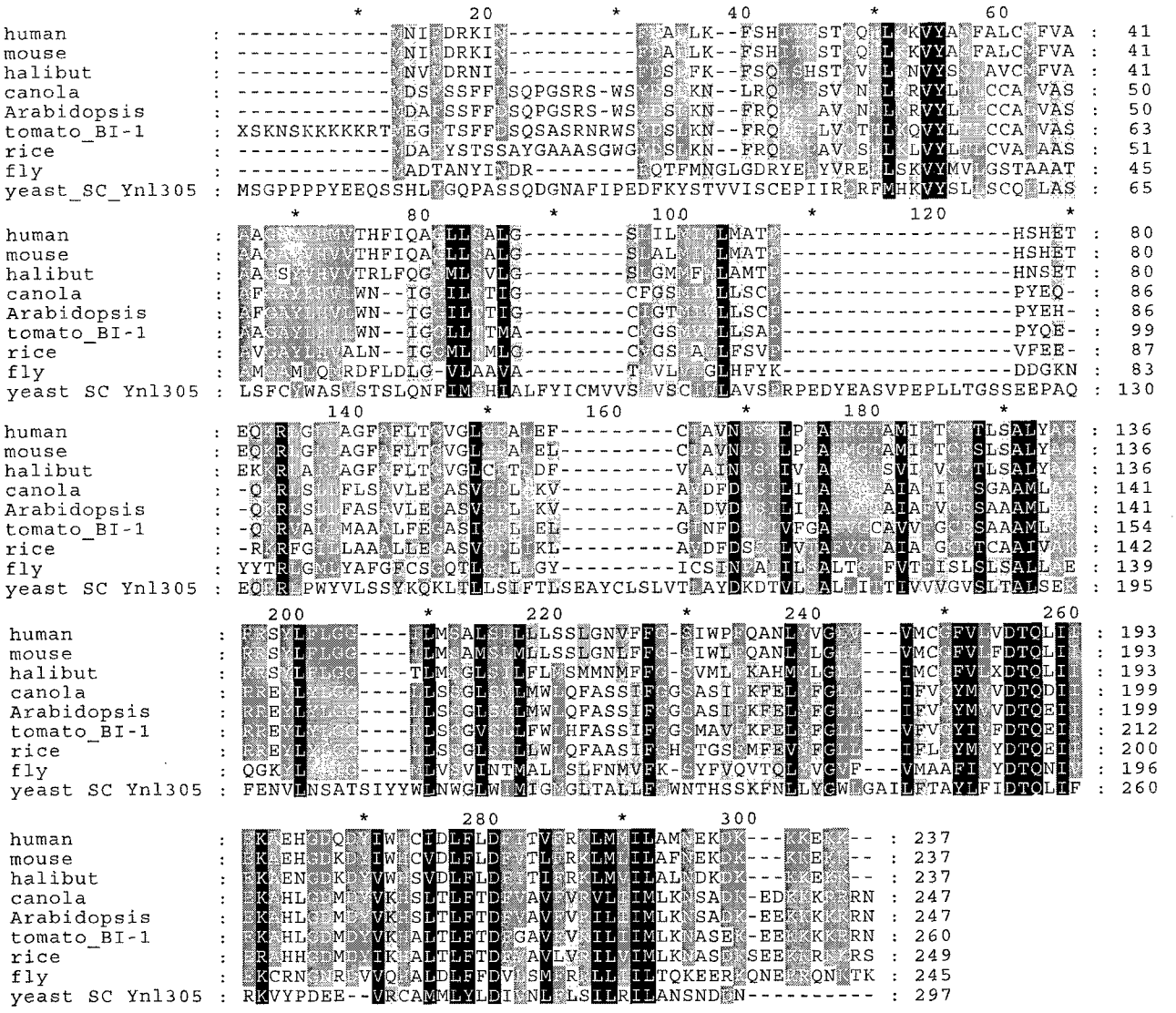

Fig. 1. Bioinformatics analysis of the BI-1 family. (A) A multiple-sequence alignment is presented for the BI-1 orthologs from human, mouse, halibut, fruit fly (*Drosophila*), canola, rice, *Arabidopsis*, and tomato, as well as the BI-1 homolog of budding yeast (*S. cerevisiae*). Several other mammalian BI-1 orthologs (rat, bovine, sheep) were omitted since they are 99% identical to human and mouse sequences. The alignment was prepared using T-coffee (Notredame et al., 2000) by first aligning all highly homologous proteins from higher organism to each other, and then aligning the most divergent protein (yeast) against the profile. Identical amino acids are presented as black blocks, while highly conserved residues are denoted in gray blocks. (B) A phylogeny tree analysis is presented for selected members of the extended BI-1 family, showing the four major branches of the family, plus the yeast BI-1-like protein. Only selected sequences for branches that are not orthologous to BI-1 are presented. A true BI-1 ortholog is not found in *C. elegans*, or lower eukaryotes, but is seen in *Plasmodium falciparum*. Accession numbers are as follows: (human BI-1: gi4507433, NP003208.1; mouse BI-1: gi21311961, NP080945.1; rat BI-1: gi456209, CAA53471.1; halibut BI-1: gi12229683, Q91A79; *Arabidopsis* BI-1: gi21593125, AAM65074.1; canola BI-1: gi14719274, AAK73101.1; rice BI-1: gi12229685, Q9MBD8; *Drosophila* BI-1 alpha: gi21355991, NP648205.1 CG7188-PA; yeast BI-1: gi6324024, NP014094.1).

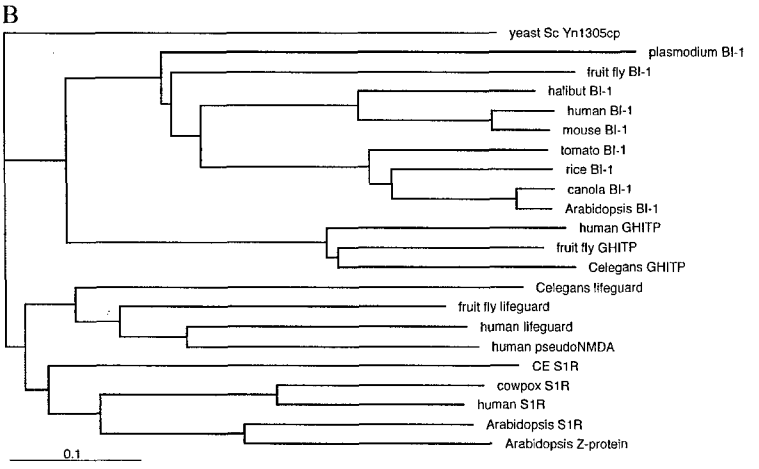

Fig. 1 (*continued*).

log phase (OD_{600} = 0.3–0.5), at which point protein lysates were made and analyzed by immunoblotting using monoclonal Myc antibody (Santa Cruz Biotech) with enhanced chemiluminescence (ECL)-based detection (Amersham).

2.5. Subcellular fractionation

Subcellular fraction of yeast cells was performed essentially as described (Glick and Pon, 1995). Briefly, yeast strains containing either Myc-BI-1 or Myc-BI-1C9A were grown overnight in SC-U/glucose media at 30 °C. The cells were then collected by centrifugation, washed with ddH_2O, and incubated in Tris–DTT solution (0.1 M Tris–SO_4, pH 9.4, 10 mM DTT) for 15 min at 30 °C. Then, cells were pelleted by centrifugation, and resuspended in buffer A (1.2 M sorbitol, 20 mM potassium phosphate, pH 7.4) containing Zymolyase 20T (ICN, 2.5 mg/g of yeast) and incubated for 30 min at 30 °C with gentle shaking to convert cells to spheroplasts. Spheroplasts were sedimented by centrifugation for 5 min at 4000 × *g*, resuspended in buffer B (0.6 M sorbitol, 20 mM K+MES, pH 6.0, 0.5 mM PMSF), and washed twice in buffer B, before undergoing homogenization with a glass Dounce homogenizer. The resulting cell lysate was centrifuged for 5 min at 1500 × *g*, and the pellet was collected as the nuclear fraction. After repeating the centrifugation, the resulting supernatant was transferred to fresh tube and centrifuged at 12,000 × *g* for 10 min to produce a membrane/organelle-enriched fraction (pellet) and cytosolic fraction (supernatant). Nuclear, membrane/organelle, and cytosolic fractions were resuspended in buffer B, normalized for input cell number, and analyzed by SDS-PAGE/immunoblotting using Myc-antibody, using an ECL-based detection method.

2.6. Agrobacterium infiltration protocol

The 744-bp ORF encoding t-BI-1 was cloned into the *ClaI* and *AscI* sites of the binary potato virus-x (PVX)-based expression vector, pSfinx (Takken et al., 2000). This construct was introduced into the *Agrobacterium tumefaciens* strain MOG 101, which was then infiltrated into tobacco leaves. Briefly, a single colony from YEP kanamycin (50 mg/l) containing plates was inoculated into 5 ml YEP liquid culture medium containing kanamycin (50 μg/l) and tetracycline (5 μg/l) and cultured overnight at 28 °C. This inoculum was used to seed a 100-ml culture with the same antibiotics and grown at 28 °C until saturated. Cells were pelleted at 4000 × *g* for 10 min and resuspended in induction medium (10.5 g/l K_2HPO_4, 4.5 g/l KH_2PO_4, 1 g/l $(NH_4)_2SO_4$, 0.5 g/l Na-citrate, 1 ml/l of 1 M $MgSO_4$, 10 ml/l of 20% glucose, 25 ml/l of 20% glycerol, and 10 mM MES). Freshly prepared acetosyringone (50 μg/ml) in dimethyl formamide was added, and cells were incubated at 28 °C for 6–8 h. Cells were pelleted and resuspended in infiltration medium (0.5 × Murashige and Skoog Basal medium salts, 10 mM MES [pH 5.6], 150 μg/ml acetosyringone) and grown to an OD_{600} of 0.8. This culture was used to infiltrate the underside of fully expanded healthy leaves in young tobacco (cv. Glurk) plants using a tuberculin syringe without needle. Other leaves were infiltrated with control vector or with infiltration media (mock inoculation). Plants were watered several hours before use. After infiltration, plants were returned to a growth chamber and maintained at 25 °C for 5 days with a 16:8-h light/dark regimen.

2.7. Plant stress assays

Heat stress was carried out on 1-cm-diameter leaf discs cut from infiltrated leaves. A minimum of 20 discs were incubated at 55 °C for 20 min in a hybridization oven and subsequently returned to room temperature under continuous light. Samples were examined 48 h later. Cold shock was administered at − 15 °C for 8 min. Samples were then returned to room temperature and examined 48 h later. Salt stress was carried out by floating the leaf discs on 200 mM

NaCl solution. Samples were monitored as before. Oxidative stress was imposed by floating the leaf discs on 20 mM H_2O_2 followed by incubation in the dark. Samples were monitored as before.

2.8. DNA fragmentation assays

Samples were frozen in liquid nitrogen at various times after subjecting plants to stress (as above) and ground into powder using a mortar and pestle. DNA was extracted using standard protocols (Balk and Leaver, 2001) and analyzed for ladder formation by electrophoresis in a 2% agarose gels. Gels were impregnated with 1 μg/ml ethidium bromide and photographed under UV illumination.

3. Results

3.1. Functional screening of cDNA libraries for Bax suppressors reveals BI-1 homologs

Ectopic expression of mammalian Bax protein in yeast results in cell death, surpressing colony formation (Xu and Reed, 1998). Previously, we used this assay to screen human cDNA libraries, identifying h-BI-1 as a cytoprotective protein that rescues yeast against Bax, without interfering with Bax protein expression. To explore whether analogous proteins exist in other species, we obtained cDNA libraries derived from an insect (*Drosophila melanogaster*) and a plant (*Lycopersicon esculentum*) and screened them for cDNAs capable of rescuing yeast from Bax-mediated lethality. For these experiments, Bax was expressed under the control for a *GAL10* promoter, providing for inducible expression upon plating cells on galactose-containing media. The cDNA libraries were cloned into yeast expression plasmids that rely on constitutive promoters for driving expression of cDNAs in yeast.

From approximately a half-million yeast transformants expressing the *Drosophila* library, four cDNAs were ultimately identified which rescued yeast from Bax without suppressing Bax protein expression. DNA sequencing revealed that all four of these cDNAs contained the complete open reading frame (ORF) of *Drosophila* BI-1 (d-BI-1). Similarly, screening of approximately one million yeast transformants using a tomato cDNA library resulted in nine cDNAs that displayed an ability to rescue from Bax. Of these, two proved to be tomato BI-1 homologs (t-BI-1).

Fig. 1A compares the amino acid sequences of mammalian BI-1 homologs with d-BI-1 and t-BI-1. In addition, the *Arabidopsis* (a-BI-1), rice BI-1 (r-BI-1), and selected other plant BI-1 proteins are also presented. All of these proteins contain at least five predicted hydrophobic transmembrane α-helices, implying a conserved structure.

3.2. Identification of BI-1-related proteins in yeast and other organisms

Using the sequence of a human BI-1, we initiated a series of automated BLAST and Psi-BLAST searches, using the saturated BLAST algorithm (Li et al., 2000). Over 200 proteins in eukaryotes and bacteria (but not archea) were identified, including potential BI-1 homologs in animals (mouse, *Drosophila*, *Caenorhabditis elegans*), plants (*A. thaliana*, rice and canola), yeast/fungi (*S. cerevisiae* and *Emericella nidulans*), as well as all complete bacterial genomes and several viruses (e.g., pox viruses of cows,

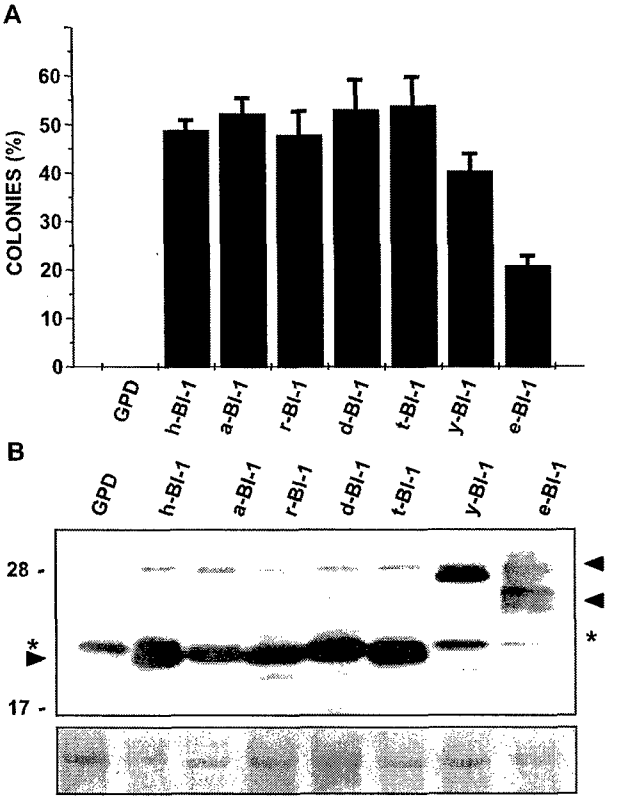

Fig. 2. BI-1 homologs protect against Bax-induced lethality in yeast. (A) Yeast containing YEp51-Bax and p426-GDP-plasmid encoding various myc-tagged BI-1 homologs from human (h), *Arabdopsis* (a), rice (r), *Drosophila* (d), tomato (t), yeast (y) and *E. coli* (e) were grown in SC-U-L/glucose overnight, then diluted into SC-U-L/galactose and spread on galactose-containing plates to induce Bax expression. After 5 days growth at 30 °C, the number of colonies was counted and expressed as a percentage relative to the number of colonies growing on SC-U-L/glu plate. GPD refers to cells transformed with the p426-GDP plasmid lacking a cDNA insert, which served as a negative control. (B) The yeast transformants described above were grown overnight in SC-U-L/glu. Detergent lysates were normalized for total protein content and subject to immunoblot analysis using c-Myc antibody (top). The asterisk denotes a nonspecific band detected by the secondary antibody used for these assays. Note that yeast BI-1 (y-BI-1) is a larger protein and that eBI-1 is ubiquitinated when expressed in yeast (unpublished observations). The lower panel represents a randomly selected protein from the Ponceau-S stained blot, which serves as a control for protein loading.

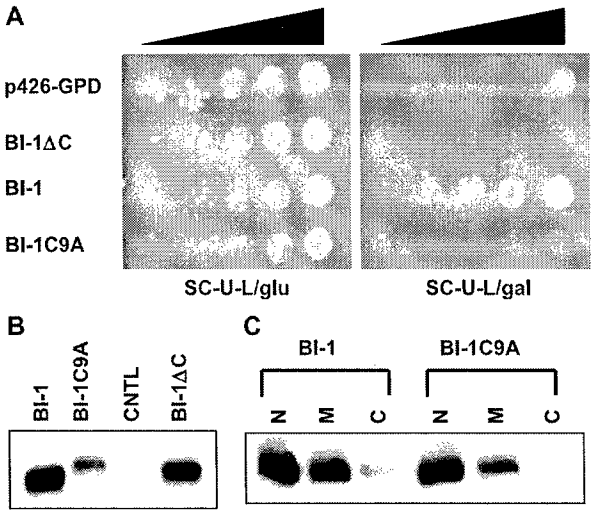

Fig. 3. Cytoprotective function of human BI-1 requires the C-terminal domain. (A) Yeast strains containing YEp51-Bax and p426-GPD plasmids encoding Myc-h-BI-1, Myc-h-BI-1 lacking the C-terminal nine amino acids, or Myc-BI-1 (C9A), in which the last nine amino acids of the protein were converted to alanines were grown in SC-U-L/glucose overnight. Cultures were serial-diluted, and 4 μl was dropped onto glucose or galactose plates. (B) Expression of BI-1 mutants was determined by immunoblotting with c-Myc antibody, using detergent lysates from transformants normalized for total protein content. (C) The cellular locations of the Myc-h-BI-1 and Myc-h-BI-1(C9A) proteins were compared by subcellular fractionation, where cytosolic (C), nuclear (N), and membrane (M) fractions were normalized for cell equivalents and analyzed by immunoblotting using anti-Myc antibody.

camels and monkeys; Cytomegalogviruses of humans and chimpanzees; and human herpes virus). BI-1 homologs can be either nearly identical or display profound sequence divergence, sharing as little as 15% amino acid sequence identify across the full length of the proteins, but all show well-defined sequence conservation in the predicted four C-terminal transmembrane α-helices. In all higher organisms, at least four groups of BI-1 paralogs are evident, though the exact number of homologs in each group is difficult to establish because of multiple splicing variants: (1) the BI-1 family, which also has homologs in plants; (2) the GHITP family of proteins, which are most closely related to GHITP, a growth hormone-inducible transmembrane protein; (3) the LFG (Lifeguard) family of proteins, related to the an anti-apoptotic protein that provides protection selectively from Fas-mediated cell death (Somia et al., 1999), and which also includes a closely related family of proteins that were initially annotated as NMDA-receptors; and (4) uncharacterized proteins from animals and plants closely homologous to the S1R protein of pox viruses (Fig. 1B).

3.3. Functional comparison of BI-1 homologs from different species

To compare the functions of the yeast BI-1-like protein with its counterparts from animals and plants, we overexpressed y-Bi-1 in yeast and tested its ability to rescue against Bax-induced lethality, using a colony formation assay. As expected, essentially no colonies formed when yeast cells were transformed with YEp51-Bax and a control plasmid lacking a cDNA insert (p426), and then plated onto galactose to induce Bax expression (Fig. 2). In contrast, co-transformation of yeast with YEp51-Bax and p426-plasmids encoding human and plant (rice, tomato, mustard) BI-1 proteins under the control a strong constitutive promoter (GDP) restored growth of colonies. Similarly, overexpression of yBI-1 rescued yeast from Bax-mediated lethality

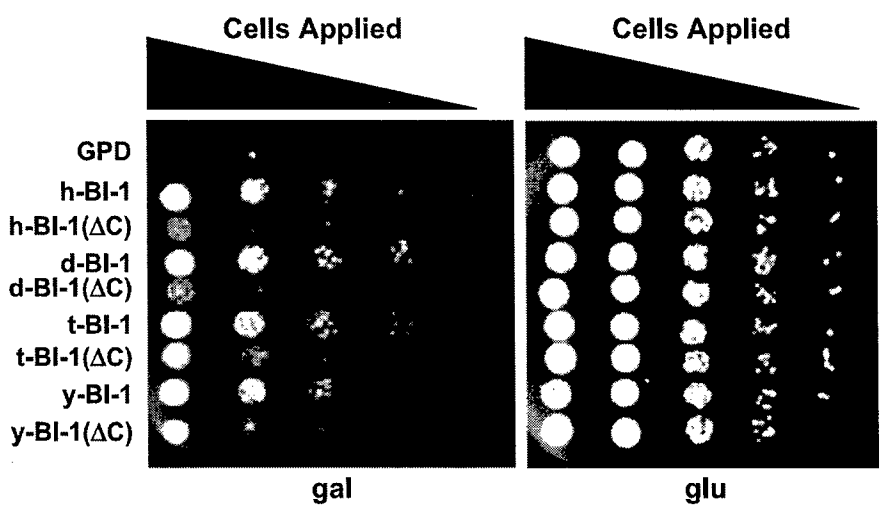

Fig. 4. Deletion of the C-terminal cytosolic domain abrogates cytoprotective function of BI-1 homologs. Yeast containing YEp51-Bax and p426-GDP plasmids encoding various myc-tagged BI-1 homologs or ΔC mutants were grown in SC-U-L/glucose overnight, then resuspended in either SC-U-L/glucose (right) or SC-U-L/galactose (left). Cultures were serial 10-fold diluted (from left to right), and 5 μl aliquots were dropped onto glucose (right)- or galactose (left)-containing plates. Plates were photographed after 5 days growth at 30 °C.

almost as efficiently as the BI-1 homologs from animals and plants (Fig. 2A). The *E. coli* protein sharing similarity to BI-1 was only partially effective at rescuing yeast from Bax, though this protein also was not expressed at levels as high as the eukaryotic BI-1 proteins, as determined by immunoblot experiments relying on the Myc-epitope tags engineered into all these proteins for immunodetection (Fig. 2B). Loading of comparable levels of total proteins from transformed yeast was confirmed by Ponceau-S staining of blots (Fig. 2B, bottom panel). We conclude therefore that the yeast homolog of BI-1 is capable of rescuing yeast from Bax-mediated lethality, akin to its counterparts in animals and plants.

3.4. Structure–function comparisons of BI-1 homologs

All of the identified BI-1 homologs contain a series of predicted transmembrane α-helices, followed by a C-terminal domain that is predicted to reside in the cytosol of cells based on the predicted topology of these proteins in membranes. We therefore explored the role of this cytosolic C-terminal domain with respect to suppression of Bax-induced lethality in yeast. Pilot experiments were first performed with the human BI-1 protein.

Two types of mutations were produced—one in which the last nine amino acids were deleted (BI-1 ΔC), and another in which the last nine amino acids of h-BI-1 were converted to alanines (BI-1 C9A). The cDNAs encoding wild-type and mutant h-BI-1 proteins were subcloned into p426-GPD and transformed into yeast containing YEp51-Bax and grown in glucose-containing medium to repress Bax expression. Then, cells were serially 10-fold diluted and spread onto either glucose or galactose plates.

As shown in Fig. 3A, all transformants grew equally well when plated on glucose, which suppresses Bax expression from the YEp51 plasmid. In contrast, when plated on galactose to induce Bax expression, growth of yeast transformed with p426-GPD control plasmid was markedly suppressed, while wild-type h-BI-1 rescued growth. Growth of yeast transformed with plasmids encoding mutant BI-1 proteins, BI-1 ΔC and BI-1 C9A, was also markedly suppressed, indicating a loss of function (Fig. 3A).

Immunoblotting analysis of lysates from these transformants (grown in glucose-containing medium) demonstrated production of both wild-type and mutant BI-1 proteins, though the levels of the BI-1 C9A protein were somewhat lower than wild-type BI-1 and BI-1 ΔC (Fig. 3B). Subcellular fractionation studies indicated that both wild-type and mutant BI-1 proteins were associated predominantly with the membrane and nuclear fractions, but were largely excluded from the cytosol (Fig. 3C). Based on immunofluorescence microscopy (not shown), the nuclear association of BI-1 protein appears to reflect association of this protein with the ER, which is contiguous with the nuclear envelope. Thus, despite their expression and proper targeting in cells, mutation of the C-terminal domain of BI-1 abolishes its ability to suppress Bax-induced death in yeast.

We then prepared similar C-terminal deletion mutants of the BI-1 homologs of *Drosophila*, tomato, and yeast, testing their function in the yeast-based Bax assay. When co-transformed with YEp51-Bax and plated on glucose, all transformants grew equally well, as determined by drop assays using serial 10-fold dilutions of yeast cultures. In contrast, when plated on galactose to induce Bax expression, the full-length BI-1 proteins from human, *Drosophila*, tomato, and yeast rescued, while the ΔC mutants were

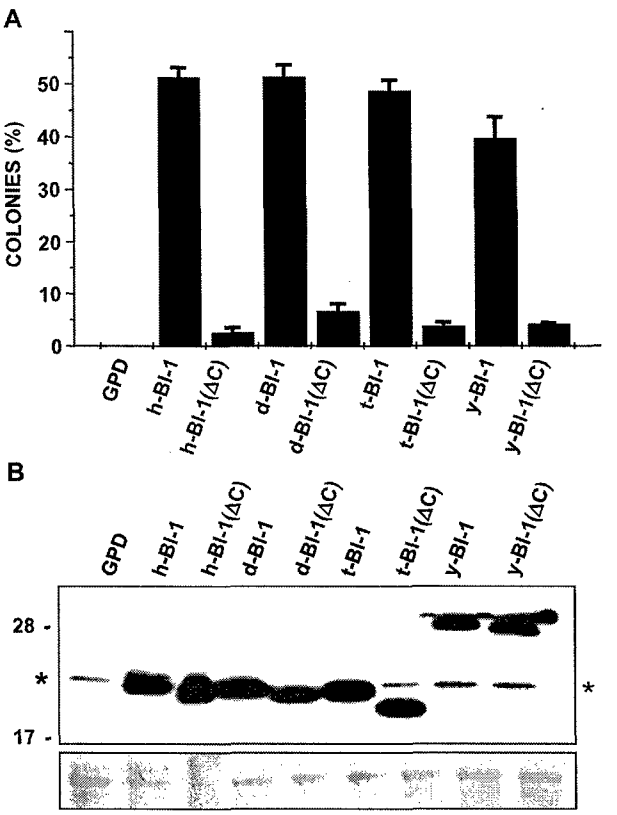

Fig. 5. Expression and functional characterization of BI-1 ΔC mutants. (A) Yeast strains containing YEp51-Bax and various p426-GPD plasmids encoding full-length or ΔC mutant BI-1 homologs were grown in SC-U-L/glucose overnight, then diluted into SC-U-L/galactose and spread on galactose-containing plates to induce Bax expression. After 5 days growth at 30 °C, the number of colonies was counted and expressed as a percentage relative to the number of colonies grown in SC-U-L/glucose plates. GPD refers to cells transformed with the p426-GDP plasmid lacking a cDNA insert, which served as a negative control. (B) The yeast transformants described above were grown overnight in SC-U-L/glu. Detergent lysates were normalized for total protein content and subject to immunoblot analysis using c-Myc antibody (top). The asterisk denotes a nonspecific band detected by the secondary antibody used for these assays. Note that yeast BI-1 (y-BI-1) protein is a larger protein. The lower panel represents a randomly selected protein from the Ponceau-S stained blot, which serves as a control for protein loading.

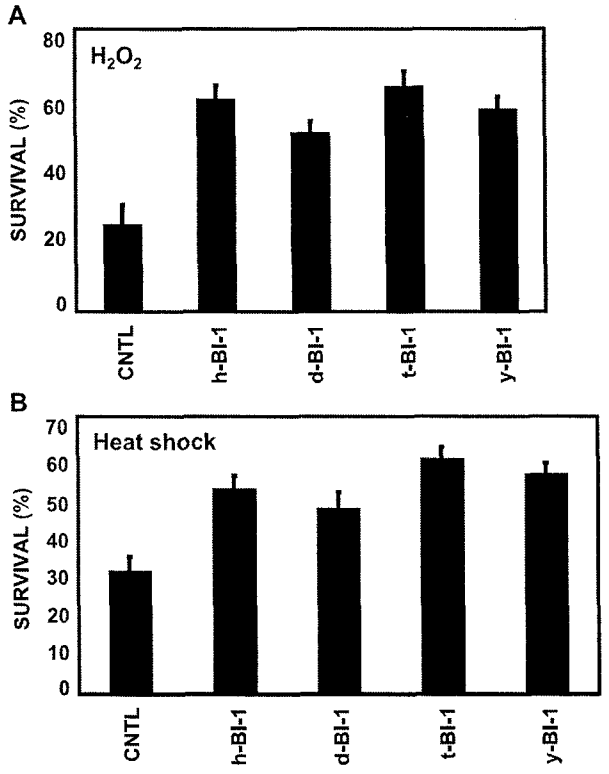

Fig. 6. BI-1 homologs protect yeast against death induced by oxidative stress or heat shock. EGY48 strain yeast containing p426-GPD plasmids encoding various Myc-tagged BI-1 homologs were grown in SC-U media overnight. (A) Cultures were then diluted to $OD_{600}=0.1$ in ddH_2O with or without 3 mM H_2O_2 for 6 h. Cultures were then serial-diluted and plated. After 5 days incubation at 30 °C, the number of surviving colonies was counted. Data are expressed as percentage relative to cells that did not receive H_2O_2 treatment. CNTL refers to yeast transformed with p426-GDP plasmid lacking an insert. (B) Alternatively, cell cultures were diluted to $OD_{600}=0.1$ in SC-U and grown to $OD_{600}=0.4$. Cells were then serial-diluted in ddH_2O and incubated at either room temperature (control) or 50 °C for 30 min before plating and determining the percentage of surviving colony forming units (CFUs) relative to control cells.

markedly impaired in their ability to protect yeast cells from Bax (Fig. 4).

Similar results were obtained by assaying colony formation (Fig. 5A). Again, full-length BI-1 proteins rescued yeast from Bax-induced lethality, while the ΔC mutants were largely inactive. Immunoblot analysis demonstrated production of the full-length and ΔC mutant proteins (Fig. 5B), excluding differences in the levels of these proteins as a trivial explanation for their differential effects on Bax-induced lethality in yeast. Loading of comparable levels of total proteins from transformed yeast was confirmed by Ponceau-S staining of blots (Fig. 5B, bottom panel). We conclude therefore that the homologs of BI-1 from humans, plants, and yeast exhibit conserved structure–function relations.

3.5. BI-1 homologs protect yeast against heat-shock and oxidative stress

To further compare the cytoprotective properties of various BI-1 homologs, we tested their effects on killing of yeast by heat shock and hydrogen peroxide, modeling our experiments after prior studies of yeast apoptosis (reviewed in Jin and Reed, 2002). Exposure of control yeast to 3 mM H_2O_2 for 6 h resulted in ~ 75% reduction in viable colony forming units (CFUs). In contrast, yeast expressing human, *Arabidopsis*, *Drosophila*, or yeast BI-1 proteins were markedly resistant to cell death induced by H_2O_2, with >50% of CFUs surviving the treatment with this oxidant (Fig. 6A) ($p<0.0001$ for all BI-1 homologs tested). Similarly, yeast expressing these BI-1 homologs were about twice as resistant to the effects of heat shock (50 °C for 30 min) as control cells (Fig. 6B). We conclude therefore that animal, plant, and yeast BI-1 proteins share an evolutionarily conserved cytoprotective function that extends beyond suppression of Bax-induced killing of yeast and includes protection of yeast from heat shock and oxidative stress as well.

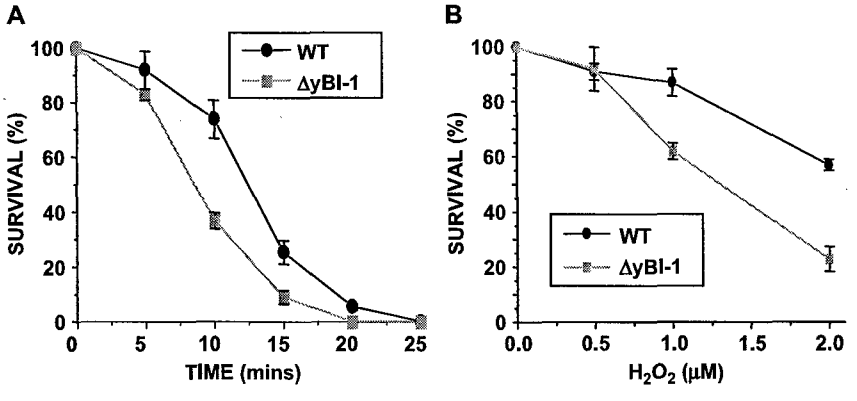

Fig. 7. Endogenous BI-1 protects yeast against stress. (A) Wild-type and ΔyBI-1 deletion strains were grown in YPD media overnight. Cells were then diluted to $OD_{600}=0.1$ in YPD and grown to $OD_{600}=0.4$. Cultures were then serial-diluted and heat-shocked at 50 °C for various times and plated onto YPD plates. (B) Yeast strains were grown in YPD overnight. Cells were then diluted in ddH_2O to $OD_{600}=0.1$ with different concentrations of H_2O_2, and incubated for 6 h. Cells were then resuspended in medium, washed, and spread onto YPD plates. For both (A) and (B), the number of colonies emerging after 5 days culture at 30 °C was counted and expressed as a percentage of surviving cells relative to the number of colonies growing in SC-U-L/glucose plate.

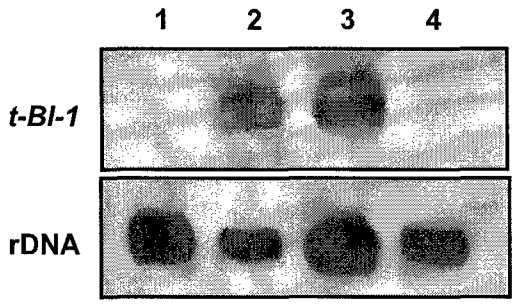

Fig. 8. Analysis of t-BI-1 transgene expression in plant leaves. Selected tobacco leaves (*N. tabacum* cv. Glurk) were infiltrated with t-BI-1 or control bacteria. At 5 days post-inoculation, total RNA was isolated from plants, and 10 μg was analyzed by Northern blotting, using a ^{32}P-labeled t-BI-1 cDNA probe (upper panel). Lane 1: RNA from tobacco leaf infiltrated with vector encoding tomato rubisco small subunit gene; Lanes 2 and 3: RNA from tobacco leaves infiltrated with tomato t-BI-1; Lane 4: tobacco leaf infiltrated with empty vector. The filter was stripped and probed with ribosomal DNA (rDNA) to ensure equivalent RNA loading for each sample (bottom panel).

3.6. BI-1-deficient yeast are more sensitive to stress

Since overexpression of y-BI-1 in yeast protects against stress, we explored the effects of disruption of the endogenous gene encoding this protein in *S. cerevisiae*. For these experiments, isogenic strains of normal and ΔyBI-1 yeast were obtained and subjected to either heat shock or oxidative stress for defined periods of time, then cells were plated and cultured at 30 °C for 5 days to measure viable colony forming units (CFU). Exposure of wild-type yeast to 50 °C resulted in a time-dependent reduction in the cell survival, with 10–15 min exposure resulting in >50% reduction in CFUs (Fig. 7A). In contrast, ΔyBI-1 cells were more sensitive to the lethal effects of heat shock, with exposures of 5–10 min being sufficient to reduce viability by >50%. Similarly, in experiments involving exposure of yeast to various concentrations of H_2O_2, again BI-1-deficient cells exhibited increased sensitivity compared to wild-type cells (Fig. 7B). Conversely, when ΔBI-y strain yeast cells were transformed with yBI-encoding plasmid, resistance to heat shock and H_2O_2 was restored (not shown). We conclude that loss of function of the endogenous yeast BI-1 gene is associated with increased sensitivity of yeast to lethal stress.

3.7. t-BI-1 protects plants from stress

To determine whether plant BI-1 proteins display cytoprotective functions in vivo, we used an *Agrobacterium*-based gene delivery method to test the effects of tomato BI-1 in tobacco plants. For these experiments, t-BI-1 cDNA was engineered into a binary potato virus x (PVX)-based expression vector (pSfinx), which was then introduced into an *A. tumefaciens* strain (MOG 101). These t-BI-1 encoding

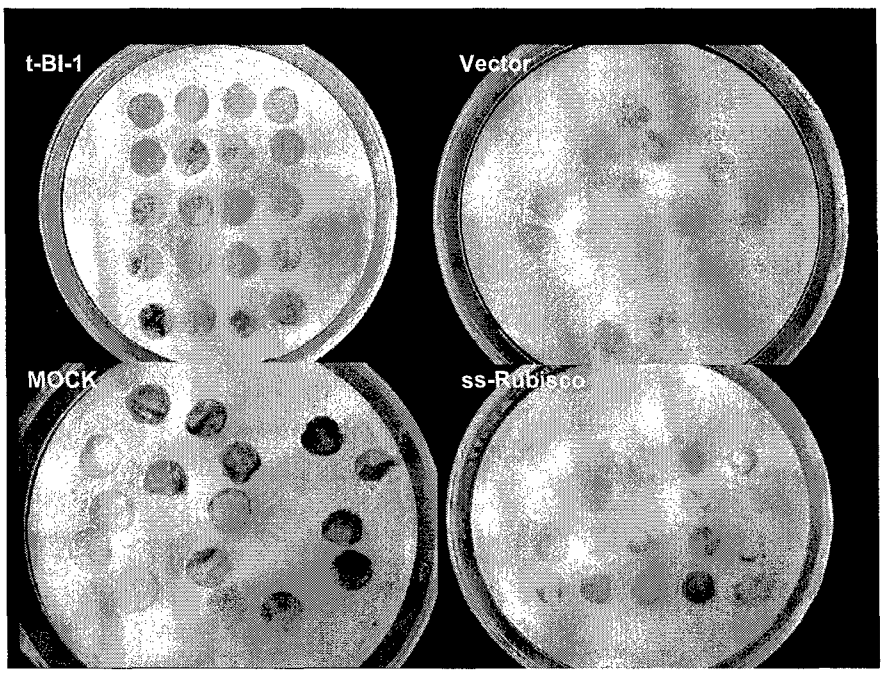

Fig. 9. Tomato BI-1 protects plant leaves from heat shock. Wild-type tobacco leaves (*N. tabacum* cv. Glurk) of similar age were infiltrated via *Agrobacterium* as described in Materials and methods. Plants were infiltrated with t-BI-1, empty vector, mock inoculation or the tomato small subunit of ribulose 1.5 biphosphate arboxylase/oxygenase (ss-Rubisco). Following infiltration, plants were maintained at 25 °C for 5 days, at which point 1-cm discs were cut from the infiltrated leaves with a cork borer. Discs were placed in a moist petri dish and subjected to a heat stress of 55 °C for 20 min. Representative samples evaluated after 48 h are shown.

bacteria where then grown and infiltrated into tobacco leaves.

Previous experiments with control constructs indicated optimal transgene expression occurred between 5 and 7 days after infiltration from the PVX coat protein promoter. We therefore tested for transgene expression in leaves infiltrated with either control or t-BI-1 bacteria at 6 days, by Northern blot analysis using a ^{32}P-labeled t-BI-1 cDNA probe. As shown in Fig. 8, transcripts corresponding to the t-BI-1 transgene were readily detectable in infiltrated leaves, but not in either mock-treated or control vector-treated leaves. Re-probing the blot with a rRNA probe controlled for total RNA loading (Fig. 8).

Next, we compared the relative resistance to abiotic stress of leaf discs infiltrated with t-BI-1 or control vectors, using heat shock, cold shock, and hyper-salinity as stresses. In heat shock studies (55 °C for 20 min), control vector and mock-inoculated discs showed loss of chlorophyll and browning within 48–72 h after heat shock (Fig. 9). In contrast, t-BI-1-infiltrated discs remained green and largely normal in appearance. Expression of an unrelated tomato gene, the RUBISCO small subunit, in leaf discs did not protect against heat shock, providing further evidence of the specificity of these results and emphasizing that protection is not afforded by any transgene. Similar results were obtained with cold shock (−15 °C for 8 min). Cold-shocked leaf discs expressing t-BI-1 showed no loss of chlorophyll, while control discs exhibited bleaching and browning after 48 h (Fig. 10). Salt-stressed leaf discs from all samples exhibited a water-soaked phenotype and did not show any dramatic morphological differences at 48 h. However, analysis of DNA extracted from the t-BI-1 and control samples by agarose gel electrophoresis showed the presence of double-stranded DNA breaks in a "DNA ladder" pattern typical of programmed cell death in the control samples but not in t-BI-1 samples (not shown). These results were confirmed by using another vector pCAMBIA 1303 in which t-BI-1 was expressed from a different promoter (CAMV 35S) (not shown).

4. Discussion

We present evidence here that BI-1 homologs of animals, plants, and yeast exhibit conserved cytoprotective functions. When overexpressed in yeast, these BI-1 family proteins provide increased resistance against the lethal effects of Bax, H_2O_2, and heat shock. Interestingly, deletion of a C-terminal domain from BI-1 family proteins abrogated their cytoprotective activity, demonstrating an important role for this region of these proteins in fulfilling their protective functions. How BI-1 family proteins protect cells against diverse stimuli remains to be determined. These integral membrane proteins possess multiple predicted transmembrane segments, suggesting they may affect membrane stability or transport of ions or other types of molecules across membranes.

Previous studies demonstrated that overexpression of the *Arabidopsis* BI-1 homolog in plants provides protection against ectopically expressed Bax, confirming that BI-1 homologs can display cytoprotective functions in planta (Kawai-Yamada et al., 2001). However, while these experiments with ectopic Bax expression provided proof of concept evidence of in vivo protection by BI-1, they left open the question of whether BI-1 could protect in planta against stressful stimuli that rely on endogenous cell death mechanisms rather than expression of a foreign protein. We therefore undertook studies of the effects of the tomato homolog of BI-1 on cytodestruction induced in tobacco leaves by abiotic stresses such as heat shock, cold shock, hyper-salinity, and oxidants (H_2O_2). Overexpression of t-BI-1 in plant leaves clearly protected against heat and cold stress, preventing or markedly delaying chlorosis. Of note, the ability of BI-1 to protect against cell destruction induced by extremes of temperature could have practical applications in agriculture, if extendable to intact plants in the field.

Besides abiotic stresses, cell suicide plays an important role in interactions of plants with a variety of infectious pathogens, including bacteria, fungi, and viruses. The best studied of these plant responses to pathogens is the so-called

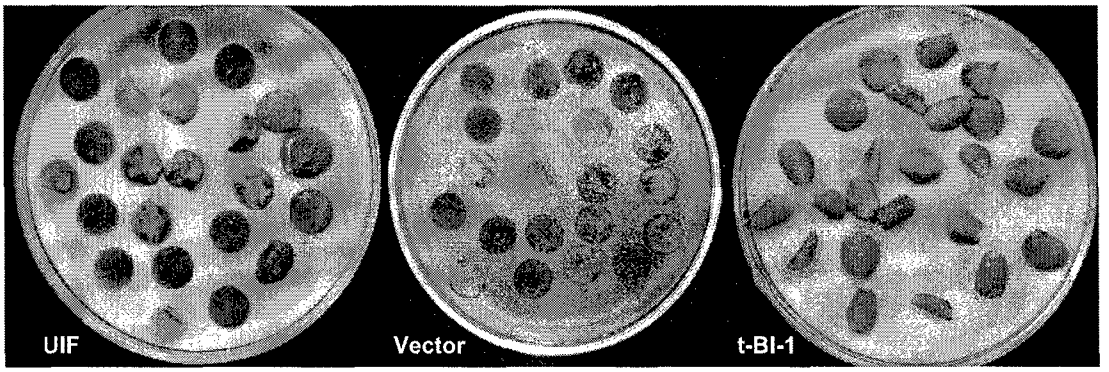

Fig. 10. Tomato BI-1 protects plant leaves from cold exposure. Wild-type tobacco leaves were treated as described in Section 2. Five days after infiltration, leaf discs were subjected to −15 °C for 8 min. Samples evaluated after 48 h are shown.

Hypersensitive Response (HR). Upon exposure to certain pathogens, plant cells in the immediate affected area undergo a cell suicide response that is theoretically intended to kill cells near the site of infection, thereby limiting spread of pathogens (Greenberg et al., 1994). The HR involves the expression of a variety of plant defense genes, accumulation of O_2^- and H_2O_2, and induction of programmed cell death. Parallels with the animal cell death machinery have been suggested by reports that (a) the HR induced by tobacco mosaic virus (TMV) in tobacco plants is associated with generation of caspase-like protease activity (Del Pozo and Lam, 1998); and (b) caspase-inhibitory peptides can block bacteria-induced PCD in *Arabidopsis* without significantly affecting the induction of HR-associated defense genes (Del Pozo and Lam, 1998). Moreover, many plant resistance genes ("R" genes) belong to a family of ATP-binding proteins with sequence similarity to CED-4/Apaf-1 family proteins implicated in apoptosis regulation in animal cells (van der Biezen and Jones, 1998).

Though the cell suicide response may be effective in limiting the spread of viruses which rely entirely on the host cell for replication of its genome, it is counterproductive for limiting many bacterial and fungal pathogens. This may be especially true for necrotizing pathogens that utilize the decaying cell corps as a food base. For example, economically significant fungal pathogens secrete phytotoxins that trigger cell suicide responses, including *Fusarium moniliforme*, which causes stalk and ear rot of maize (secretes fumonisins) and *Alternaria alternata*, which produces stem canker disease in tomato plants (secretes AAL toxins) (Jones and Dangl, 1996; Wang et al., 1996). By killing cells of the plants, they gain access to the nutrients they need to grow from cell corps. Thus, it will be interesting to explore whether BI-1 genes can confer protection against such necrotizing plant pathogens. In this regard, transgenic tobacco expressing negative regulators of apoptosis (Bcl-2; Bcl-xl; CED-9; Op-IAP) displayed resistance when challenged by several necrotrophic fungi. Importantly, DNA laddering and TUNEL-positive cells were observed when wild-type, susceptible tobacco was inoculated with the necrotrophic fungus, *Sclerotinia sclerotiorum*, while transgenic plants did not display these apoptotic features (Dickman et al., 2001; Dickman, unpublished). Cytoprotection mediated by BI-1 or other proteins, nevertheless, could be counterproductive for some host–pathogen interactions, as suggested by recent analysis of barley infected with powdery mildew virus—a pathogen that establishes compatible interactions with host plants by penetrating living cells (Huckelhoven et al., 2003).

In summary, we have identified additional BI-1 homologs from plants (tomato), insects (*Drosophila*), and yeast and have demonstrated that these and other members of the BI-1 family display evolutionarily conserved functions as cytoprotective proteins. Future studies will address the molecular mechanisms of cytoprotection by BI-1 and will explore practical applications of utilizing BI-1 homologs to engineer resistant strains of commercially important crops.

Acknowledgements

We thank J. Valois for manuscript preparation, and the NIH for generous support (AG15393).

References

Balk, J., Leaver, C.J., 2001. The PET1-CMS mitochondrial mutation in sunflower is associated with premature programmed cell death and cytochrome *c* release. Plant Cell 13, 1803–1818.

Bolduc, N., Brisson, L.F., 2002. Antisense down regulation of NtBI-1 in tobacco BY-2 cells induces accelerated cell death upon carbon starvation. FEBS Lett. 532, 111–114.

Bolduc, N., Ouellet, M., Pitre, F., Brisson, L.F., 2003. Molecular characterization of two plant BI-1 homologues which suppress Bax-induced apoptosis in human 293 cells. Planta 216, 377–386.

Burns, T.F., El-Deiry, W.S., 2001. Identification of inhibitors of TRAIL-induced death (ITIDs) in the TRAIL sensitive colon carcinoma cell line, SW480, using a genetic approach. J. Biol. Chem. 276, 37879–37886.

Danon, A., Delorme, V., Mailhac, N., Gallois, P., 2000. Plant programmed cell death: a common way to die. Plant Physiol. Biochem. 38, 647–655.

Del Pozo, O., Lam, E., 1998. Caspases and programmed cell death in the hypersensitive response of plants to pathogens. Curr. Biol. 8, 1129–1132.

Dickman, M.B., Park, Y.K., Oltersdorf, T., Li, W., Clemente, T., French, R., 2001. Abrogation of disease development in plants expressing animal anti-apoptotic genes. Proc. Natl. Acad. Sci. U. S. A. 98, 6957–6962.

Glick, B.S., Pon, L.A., 1995. Isolation of highly purified mitochondria from *Saccharomyces cerevisiae*. Methods Enzymol. 260, 213–223.

Greenberg, J.T., Guo, A., Klessig, D.F., Ausubel, F.M., 1994. Programmed cell death in plants: a pathogen-triggered response activated coordinately with multiple defense functions. Cell 77, 551–563.

Huckelhoven, R., Dechert, C., Trujillo, M., Kogel, K.H., 2001. Differential expression of putative cell death regulator genes in near-isogenic, resistant and susceptible barley lines during interaction with the powdery mildew fungus. Plant Mol. Biol. 47, 739–748.

Huckelhoven, R., Dechert, C., Kogel, K.-H., 2003. Overexpression of barley BAX inhibitor 1 induces breakdown of *mlo*-mediated penetration resistance to *Blumeria graminis*. Proc. Natl. Acad. Sci. U. S. A. 100, 5555–5560.

Jin, C., Reed, J.C., 2002. Yeast and apoptosis. Nat. Rev. Mol. Cell. Biol. 3, 453–459.

Jones, A.M., Dangl, J.L., 1996. Logjam at the Styx: programmed cell death in plants. Trends Plant Sci. 1, 114–119.

Kawai, M., Pan, L., Reed, J.C., Uchimiya, H., 1999. Evolutionally conserved plant homologue of the bax inhibitor-1 (BI-1) gene capable of suppressing bax-induced cell death in yeast. FEBS Lett. 464, 143–147.

Kawai-Yamada, M., Jin, L., Yoshinaga, K., Hirata, A., Uchimiya, H., 2001. Mammalian Bax-induced plant cell death can be down-regulated by overexpression of *Arabidopsis* Bax Inhibitor-1 (*AtBI-1*). Proc. Natl. Acad. Sci. U. S. A. 98, 12295–12300.

Lacomme, C., Cruz, S.S., 1999. Bax-induced cell death in tobacco is similar to the hypersensititve response. Proc. Natl. Acad. Sci. U. S. A. 96, 7956–7961.

Lam, E., Kato, N., Lawton, M., 2001. Programmed cell death, mitochondria and the plant hypersensitive response. Nature 411, 848–853.

Li, W.Z., Pio, F., Pawlowski, K., Godzik, A., 2000. Saturated BLAST: an

automated multiple intermediate sequence search used to detect distant homology. Bioinformatics 16, 1105–1110.

Matsumura, H., Nirasawa, S., Kiba, A., Urasaki, N., Saitoh, H., Ito, M., Kawai-Yamada, M., Uchimiya, H., Terauchi, R., 2003. Overexpression of Bax inhibitor suppresses the fungal elicitor-induced cell death in rice (*Oryza sativa* L.) cells. Plant J. 33.

Metzstein, M., Stanfield, G., Horvitz, H., 1998. Genetics of programmed cell death in *C. elegans*: past, present and future. Trends Genet. 14, 410–416.

Mitsuhara, I., Malik, K., Miura, M., Ohashi, Y., 1999. Animal cell-death suppressors bcl-xL and ced-9 inhibit cell death in tobacco plants. Curr. Biol. 9, 775–778.

Notredame, C., Higgins, D., Heringa, J., 2000. T-Coffee: a novel method for multiple sequence alignments. J. Mol. Biol. 302, 205–217.

Pennell, R.I., Lamb, C., 1997. Programmed cell death in plants. Plant Cell 9, 12.

Perfettini, J.-L., Reed, J.C., Israël, N., Martinou, J.-C., Dautry-Varsat, A., Ojcius, D.M., 2002. Role of Bcl-2 family members in caspase-independent apoptosis during *Chlamydia* infection. Infect. Immunol. 70, 55–61.

Richael, C., Lincoln, J.E., Bostock, R.M., Gilchrist, D.G., 2001. Caspase inhibitors reduce symptom development and limit bacterial proliferation in susceptible plant tissues. Physiol. Mol. Plant Pathol. 59, 213–221.

Sanchez, P., de Torres, M., Grant, M., 2000. AtBI-1, a plant homologue of Bax inhibitor-1, suppresses Bax-induced cell death in yeast and is rapidly upregulated during wounding and pathogen challenge. Plant J. 21, 393–399.

Solomon, M., Belenshi, B., Delledonne, M., Levine, A., 1999. The involvement of cysteine proteases and protease inhibitor genes in the regulation of programmed cell death in plants. Plant Cell 11, 431–444.

Somia, N.V., Schmitt, M.J., Vetter, D.E., Van Antwerp, D., Heinemann, S.F., Verma, I.M., 1999. LFG: an anti-apoptotic gene that provides protection from Fas-mediated cell death. Proc. Natl. Acad. Sci. U. S. A. 96, 12667–12672.

Takken, F.L., Luderer, R., Gabriels, S.H., Westerink, N., Lu, R., de Wit, P.J., Joosten, M.H., 2000. A functional cloning strategy, based on a binary PVX-expression vector, to isolate HR-inducing cDNAs of plant pathogens. Plant J. 24, 275–283.

van der Biezen, E., Jones, J., 1998. The NB-ARC domain: a novel signalling motif shared by plant resistance gene products and regulators of cell death in animals. Curr. Biol. 8, R226–R227.

Wang, M., Oppedijk, B.J., Lu, B.V., Schilperoot, R.A., 1996. Apoptosis: a functional paradigm for programmed plant cell death induced by a host-selective phytotoxin and invoked during development. Plant Cell 8, 375–391.

Xu, Q., Reed, J.C., 1998. BAX inhibitor-1, a mammalian apoptosis suppressor identified by functional screening in yeast. Mol. Cell 1, 337–346.

Xu, Q., Jurgensmeier, J., Reed, J.C., 1999. Methods of assaying Bcl-2 and Bax family proteins in yeast. Methods 17, 292–304.

Yu, L.-H., Kawai-Yamada, M., Naito, M., Watanabe, K., Reed, J.C., Uchimiya, H., 2002. Induction of mammalian cell death by a plant Bax inhibitor. FEBS Lett. 512, 308–312.

Zhang, H., Reed, J.C., 2001. Studies of apoptosis proteins in yeast. In: Schwartz, L., Ashwell, J., Wilson, L., Matsudaira, P. (Eds.), Methods in Cell Biology, vol. 66. Academic Press, pp. 453–468.

Bcl-2-mediated alterations in endoplasmic reticulum Ca^{2+} analyzed with an improved genetically encoded fluorescent sensor

Amy E. Palmer*, Can Jin†, John C. Reed†, and Roger Y. Tsien*‡

*Department of Pharmacology and Howard Hughes Medical Institute, University of California at San Diego, 9500 Gilman Drive, La Jolla, CA 92093-0647; and †The Burnham Institute, La Jolla, CA 92037

Contributed by Roger Y. Tsien, November 1, 2004

The endoplasmic reticulum (ER) serves as a cellular storehouse for Ca^{2+}, and Ca^{2+} released from the ER plays a role in a host of critical signaling reactions, including exocytosis, contraction, metabolism, regulation of transcription, fertilization, and apoptosis. Given the central role played by the ER, our understanding of these signaling processes could be greatly enhanced by the ability to image $[Ca^{2+}]_{ER}$ directly in individual cells. We created a genetically encoded Ca^{2+} indicator by redesigning the binding interface of calmodulin and a calmodulin-binding peptide. The sensor has improved reaction kinetics and a K_d ideal for imaging Ca^{2+} in the ER and is no longer perturbed by large excesses of native calmodulin. Importantly, it provides a significant improvement over all previous methods for monitoring $[Ca^{2+}]_{ER}$ and has been used to directly show that, in MCF-7 breast cancer cells, the antiapoptotic protein B cell lymphoma 2 (Bcl-2) (*i*) lowers $[Ca^{2+}]_{ER}$ by increasing Ca^{2+} leakage under resting conditions and (*ii*) alters Ca^{2+} oscillations induced by ATP, and that acute inhibition of Bcl-2 by the green tea compound epigallocatechin gallate results in an increase in $[Ca^{2+}]_{ER}$ due to inhibition of Bcl-2-mediated Ca^{2+} leakage.

calcium | cameleon

To date, researchers have attempted to use a number of strategies to deduce the role of $[Ca^{2+}]_{ER}$ in signaling processes, but all possess shortcomings (1, 2). Conventional methods use cytosolic small-molecule Ca^{2+} indicators to infer that an observed signal likely originated from the endoplasmic reticulum (ER). However, as more studies identify the complex interplay among levels of Ca^{2+} in the ER and Ca^{2+} influx (3), as well as a close interaction network between the ER and mitochondria (4, 5), it seems increasingly important for our understanding of signaling processes that organelle Ca^{2+} be observed directly to differentiate Ca^{2+} signals from different organelles. Ca^{2+} indicator dyes can be loaded at 37°C rather than 25°C, thus favoring the loading of internal compartments. However, this method loads all internal compartments (not just the ER), and the remaining cytosolic dye must be effectively removed, or quenched. ER-targeted aequorin probes (6) can be genetically targeted to the ER to measure $[Ca^{2+}]_{ER}$ directly, but the aequorin probes are luminescent and therefore not bright enough for single-cell imaging without specialized equipment. Perhaps more problematic is that for aequorin to be active it must be reconstituted with the coelenterazine cofactor, and to do so the ER must initially be completely depleted of Ca^{2+}. Finally, the low-affinity FRET-based cameleon (7) YC4.3ER can also be genetically targeted and enables single-cell imaging, but its K_d for Ca^{2+} is not well suited to monitor changes in $[Ca^{2+}]_{ER}$, and therefore it has a low sensitivity.

Given the critical role of apoptosis in human diseases as well as normal physiology and the increasing evidence that the balance of B cell lymphoma 2 (Bcl-2) family proteins plays a role in the tumorigenesis of a number of cancers (8), a fundamental need exists to better understand how these proteins interact and the multiple mechanisms by which they influence apoptotic cascades. An important aspect of this is identifying inhibitors of different Bcl-2 family members that could serve as tools to perturb and thereby better our understanding of the signaling cascades, as well as to act as potential therapeutic agents. We set out to generate an indicator for $[Ca^{2+}]_{ER}$ so that we could examine the role of $[Ca^{2+}]_{ER}$ in the regulation of Bcl-2 family-mediated apoptosis. Although most studies have focused on the role of the mitochondria in apoptosis, recently it has been shown that Bcl-2 family members can localize to the ER and alter $[Ca^{2+}]_{ER}$, thus adding another dimension to the role of Bcl-2 family members in apoptosis (9–13). Importantly, it has been shown that changes in $[Ca^{2+}]_{ER}$ can directly influence the propensity of a given stimulus to lead to apoptosis (12, 14), although there have been a number of conflicting reports (15) as to exactly how the antiapoptotic protein Bcl-2 influences $[Ca^{2+}]_{ER}$. Of particular interest is a recent report that Bcl-2 functionally interacts with inositol 1,4,5-trisphosphate (IP_3) receptors (IP_3Rs) in WEHI7.2 T cells, suggesting that this interaction might be the mechanism by which Bcl-2 alters ER Ca^{2+} homeostasis (16). The creation of a robust and reliable sensor to directly monitor $[Ca^{2+}]_{ER}$ could help alleviate some of the uncertainties associated with indirect Ca^{2+} measurements and would provide a significant advantage in probing questions related to Ca^{2+} homeostasis in the ER.

Materials and Methods

Peptide synthesis and Biacore (Neuchâtel, Switzerland) experiments were performed as described in *Supporting Text*, which is published as supporting information on the PNAS web site. The mutant peptide and calmodulins (CaMs) were cloned between a truncated enhanced cyan fluorescent protein (CFP) and citrine fluorescent protein (17), as described (7). The constructs were cloned between the *Bam*HI/*Eco*RI sites in pRSETB or pBAD for protein purification and pcDNA3 for expression in mammalian cells. To generate an ER-targeted cameleon, the calreticulin signal sequence MLLPVLLLGLLGAAAD was added 5′ to CFP, and an ER retention sequence, KDEL, was added to the 3′ end of citrine.

For protein purification, cameleons were expressed in either JM109 (Stratagene) or LMG194 (Invitrogen) and grown overnight at 25°C. Constructs in pBAD/LMG194 were induced with 0.2% arabinose. Protein was extracted with Bacterial Protein Extraction Reagent (Pierce), purified via an N-terminal 6×His-

Freely available online through the PNAS open access option.

Abbreviations: ER, endoplasmic reticulum; SERCA, sarcoendoplasmic reticulum Ca^{2+} ATPase; CaM, calmodulin; skMLCK, skeletal muscle myosin light chain kinase; Bcl-2, B cell lymphoma 2; IP_3, inositol 1,4,5-trisphosphate; IP_3R, IP_3 receptor; EGCG, epigallocatechin gallate; EC, epicatechin; CFP, cyan fluorescent protein; HBSS, Hanks' balanced salt solution; D1, Design 1.

Data deposition: The sequence reported in this paper has been deposited in the GenBank database (accession no. AY796115).

‡To whom correspondence should be addressed. E-mail: rtsien@ucsd.edu.

www.pnas.org/cgi/doi/10.1073/pnas.0408030101

tag by using Ni-NTA agarose, and buffer-exchanged into 10 mM 4-morpholinepropanesulfonic acid/100 mM NaCl, pH 7.4, by using Amicon Centricon-30 columns (Millipore). Absorbance measurements were conducted on a Cary 3E UV-Visible spectrometer (Varian). Fluorescence measurements were conducted on a Spex (Spex Industries, Metuchen, NJ) Fluorolog-3 Fluorimeter (Horiba group) at a cameleon concentration of 0.4 μM. Ca^{2+}/EGTA, and Ca^{2+}/*N*-(2-hydroxyethyl)ethylene dinitrilo-*N*,*N*′,*N*′-triacetic acid (HEEDTA) buffers were prepared as described (18, 19) and were used in Ca^{2+} titrations to achieve concentrations of <50 μM. All solutions of >50 μM were unbuffered.

Stopped-flow experiments were performed on an Applied Photophysics (Surrey, U.K.) Stopped Flow. Equal volumes of cameleon (final concentration of 0.8 μM) and Ca^{2+} (various concentrations) were rapidly mixed, and the fluorescence was monitored by using an excitation wavelength of 420 nm and an emission cutoff filter of 500 nm. The observed first-order rate constant (k_{obs}) was calculated from each averaged ($n > 4$) data set by nonlinear regression analysis.

Cell-culturing details are provided in *Supporting Text*. For imaging, cells were rinsed twice and then maintained in Hanks' balanced salt solution (HBSS) with 20 mM Hepes and 2 g/liter D-glucose at pH 7.4. Ca^{2+}-free solutions were generated by adding 0.5 mM EGTA, 1 mM Mg^{2+}, 1 g/liter glucose, and 20 mM Hepes to Ca^{2+} and Mg^{2+}-free HBSS (GIBCO). For experiments in which both the ER and cytosolic Ca^{2+} levels were monitored, cells were treated with 4 μM fura-2-AM (Molecular Probes) with 0.04% Pleuronic F-127 in HBSS for 30 min at room temperature. Cells were then washed with HBSS and allowed to incubate at room temperature for 15 min to ensure cleavage of the acetoxymethyl ester. (−)Epigallocatechin gallate (EGCG) and (−)epicatechin (EC) were purchased from Sigma, dissolved in 100% DMSO, and stored at −80°C until use.

To calibrate the cameleon probe in the ER, R_{min} was obtained by treating the cells with 3 mM EGTA and 2 μM ionomycin, and R_{max} was determined by treating cells with 25 μM digitonin, followed by 5–10 mM Ca^{2+}, 1 mM ATP, and 1 mM Mg^{2+}. The R_{min} and R_{max} values were used to convert cell data to % FRET (of maximum). Finally, the apparent K_{d1} (0.58), K_{d2} (56.46), R_{max1} (0.28), R_{max2} (0.72), n_1 (1.18), and n_2 (1.67) values obtained from fitting the *in vitro* data with $R = \{R_{max1}[Ca^{2+}]^{n1}/(K_{d1}^{n1}+[Ca^{2+}]^{n1})\} + \{R_{max2}[Ca^{2+}]^{n2}/(K_{d2}^{n2}+[Ca^{2+}]^{n2})\}$ were used in the calibration. To calibrate fura-2, cells were treated with 8 μM ionomycin and 10 mM EGTA in Ca^{2+}-free HBSS to obtain R_{min}, followed by 2 μM ionomycin and 20 mM Ca^{2+} in HBSS to obtain R_{max}. The *in situ* R_{min} and R_{max} values were adjusted (multiplied by 0.85) to account for the minimum viscosity effect (20). The standard equation: $K_d[(R-R_{min})/(R_{max}-R)]\cdot S_f/S_b$ was used to convert the Fura-2 350:380 ratio to $[Ca^{2+}]_{cyt}$, where S_f and S_b are the emission intensity at 380 nm for Ca^{2+}-free and Ca^{2+}-bound fura-2, respectively.

Cells were imaged on a Zeiss Axiovert 200M microscope with a cooled charge-coupled device camera (Roper Scientific, Trenton, NJ), controlled by METAFLUOR 6.1 software (Universal Imaging, Downington, PA). Emission ratio imaging of the cameleon was accomplished by using a 436DF20 excitation filter, 450-nm dichroic mirror, and two emission filters (475/40 for enhanced CFP and 535/25 for citrine) controlled by a Lambda 10-2 filter changer (Sutter Instruments, Novato, CA). Excitation ratio imaging for fura-2 was accomplished by using 350/10 and 380/10 excitation filters, a 450-nm dichroic mirror, and a 535/45 emission filter. Fluorescence images were background corrected. Exposure times were typically 100–1,000 ms, and images were collected every 8–20 s.

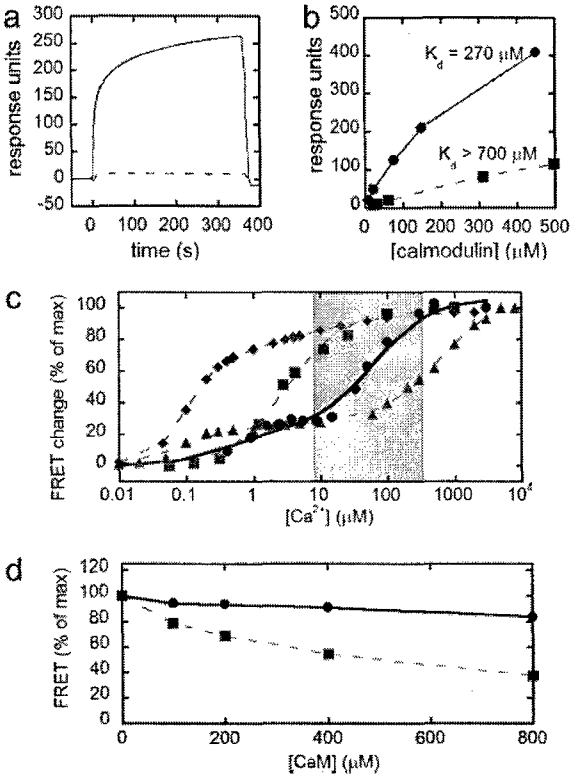

Fig. 1. *In vitro* characterization of the mutant CaM and peptide and the resulting redesigned cameleon. (*a*) Biacore sensorgram of WT CaM binding to skMLCK (solid line) and four-charge reversal skMLCK (dashed line). CaM was injected over the surface in the presence of saturating Ca^{2+} starting at time t = 0 for 360 s. (*b*) Binding of WT (squares, dashed line) and mutant (circles, solid line) CaM to mutant skMLCK with four-charge reversals. The binding of CaM reached a steady state during the association phase, and therefore a Scatchard analysis was used to determine the dissociation constants (Fig. 8). (*c*) *In vitro* calcium titration curves of YC2.1 (diamonds, dashed line), YC3.3 (squares, dashed line), YC4.3 (triangles, dashed line), and D1 (circles, solid line), along with corresponding fits of the data. The gray box represents the typical range of $[Ca^{2+}]$ in the ER, from resting to the depleted state. (*d*) Percent of the maximum FRET response of YC3.3 (squares) and D1 (circles) with increasing concentrations of WT CaM.

Results

To create a sensor that would be appropriate for monitoring $[Ca^{2+}]_{ER}$ in single living cells, we started with the original cameleon construct, comprised of two fluorescent proteins (CFP and citrine) and two sensing proteins [CaM and a CaM-binding peptide derived from skeletal muscle myosin light chain kinase (skMLCK)] that undergo a conformational change upon binding (7). Our goal was to redesign the binding interface between CaM and the peptide to generate highly specific protein/peptide pairs that would display a range of Ca^{2+} affinities and that would not be perturbed by endogenous proteins, such as WT CaM. This was particularly important, given that previous cameleons have suffered from perturbation by endogenous proteins (21, 22). Toward this end, we initially generated peptides that would not bind to WT CaM and then sought to reengineer CaM to reconstitute binding to the mutant peptides.

As a starting point for redesign, we targeted the six possible salt-bridge interactions identified in the NMR solution structure between CaM and the skMLCK peptide (23). A series of biotinylated peptides was synthesized in which a basic residue (either K or R) at the N and C termini of the peptide was replaced with an acidic E residue. Charge reversals were made sequentially, generating peptides with two, four, and six charge

CELL BIOLOGY

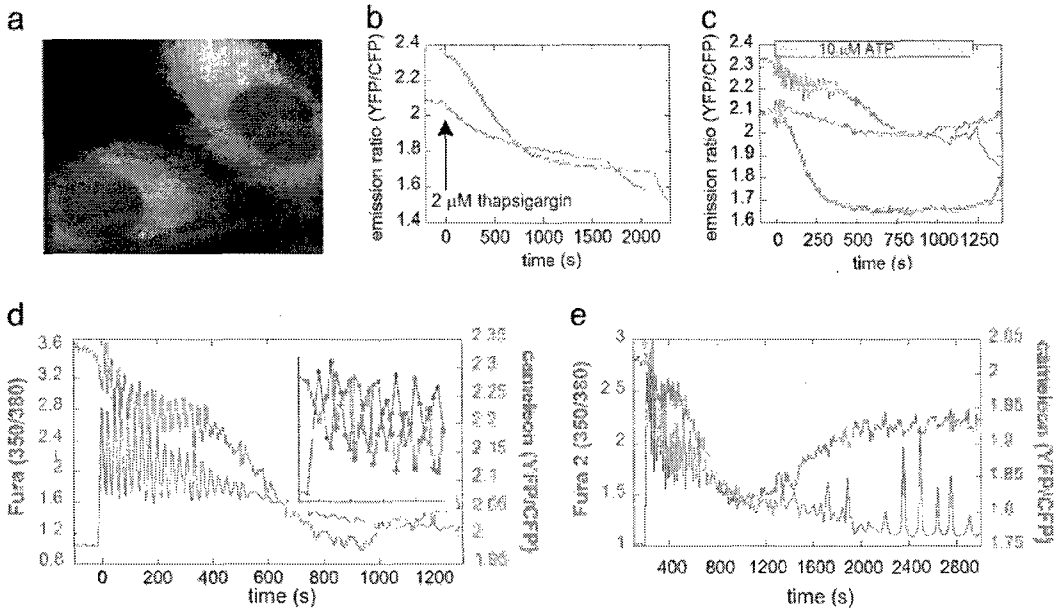

Fig. 2. Comparison of the response of ER-targeted YC4.3 and D1 in HeLa cells. (*a*) Fluorescence image of D1ER in HeLa cells showing effective ER localization. (*b*) Emission ratio of D1 (red) and YC4.3 (blue) in the ER upon treatment with thapsigargin. (*c*) Emission ratio of D1 (red lines, representing two different cells) and YC4.3 (blue) in the ER upon treatment with ATP. (*d*) Simultaneous imaging of Ca^{2+} in the cytosol (using fura-2, green) and ER (D1, red). The left axis represents the excitation ratio of fura-2 (350/380 nm), and the right axis represents the emission ratio of the cameleon (citrine/CFP). (*e*) Same experimental conditions as in *d* but for an extended amount of time. In the continued presence of 10 μM ATP, the ER begins to refill with Ca^{2+} after ≈1,000 s.

reversals until all of the salt-bridge interactions were destroyed. Binding of CaM to the peptides was assayed by using surface plasmon resonance (Biacore 3000), in which binding events are optically detected as a change in the refractive index at the surface. To accomplish this, biotinylated peptides were coupled to a streptavidin-coated chip, and CaM was injected over the surface in the presence of Ca^{2+} (Fig. 6, which is published as supporting information on the PNAS web site). Initially, we verified that binding of CaM to the WT skMLCK was ≈10 nM, comparable to previously reported values obtained in solution (Fig. 7, which is published as supporting information on the PNAS web site). The mutant peptide with four charge reversals displayed a dramatically lower affinity for CaM than the WT skMLCK peptide (Fig. 1*a*). Injection of increasing concentrations of CaM enabled determination of the $K_d > 700$ μM (Fig. 8, which is published as supporting information on the PNAS web site). Thus, four charge reversals were sufficient to decrease the affinity for WT CaM by $>10^4$.

A small library of CaM mutants in which the four complementary positions in CaM (E11, E84, E87, and E127) were changed to E, K, or R was then assayed for binding to both WT skMLCK and the mutant peptide. The best hit had a K_d of 270 μM, and therefore a higher affinity than WT CaM for the mutant peptide (Fig. 1*b*). Upon sequencing, this mutant was identified as E11K, E84R, E87K, or E127E. Mutation of E127 to R did not increase the affinity of CaM for the peptide (data not shown).

The mutant CaM/peptide pair, designated as Design 1 (D1), was cloned between CFP and citrine to yield a reengineered cameleon. Under saturating conditions of Ca^{2+}, the cameleon showed a decrease in CFP emission and an increase in citrine emission, indicative of increased FRET. The magnitude of the FRET change was comparable to that observed for the original cameleons. Fig. 1*c* shows the Ca^{2+} titration curves of the design along with previous cameleons (YC2, YC3, and YC4). D1 has a biphasic Ca^{2+} response, and a two-site saturation fit yielded K_d values of 0.81 and 60 μM. The two dissociation constants likely result from the different affinities of the N- and C-terminal domains of CaM for Ca^{2+}, as observed for YC2.1 and YC4.3 (7). Fig. 1*c* shows that the cameleon fills a gap in Ca^{2+} sensitivity, falling directly between YC3.3 and YC4.3. Because the ER is expected to range from hundreds of micromolar (resting state) to low micromolar (depleted state), this sensor is ideally suited for imaging Ca^{2+} in the ER.

An important part of our design strategy was to develop a sensor that would not be perturbed by endogenous cellular proteins, such as WT CaM, because this has posed a problem for previous cameleons (21). Fig. 1*d* shows the FRET response of YC3.3 and the D1 in the presence of excess CaM. For YC3.3, the FRET response under saturating Ca^{2+} conditions decreases with the addition of increasing concentrations of CaM, because excess CaM in solution binds to the skMLCK portion of the cameleon, forming an intermolecular complex and preventing the sensor from registering a FRET increase. Importantly, in the charge reversal redesign (D1), addition of increasing CaM has almost no effect on the FRET response, indicating that this cameleon is not perturbed by large excesses of CaM.

Stopped-flow fluorescence measurements were undertaken to determine the binding kinetics of the cameleon. Rapid mixing of the cameleon protein with various concentrations of Ca^{2+} resulted in a rapid increase in FRET. The initial responses were fitted with a single exponential to obtain the observed rate (k_{obs}). A fit to the data (Fig. 9, which is published as supporting information on the PNAS web site) yields k_{on} of 3.6×10^6 $M^{-1}\cdot s^{-1}$, k_{off} of 256 s^{-1}, and K_d of 69 μM for D1, where the observed K_d corresponds well to the results from the Ca^{2+} titration curve. Therefore, although this cameleon has a k_{on} similar to previous cameleons, it has a much faster k_{off} (250 s^{-1} instead of 10 s^{-1}), making it more appropriate to monitor rapidly changing Ca^{2+} dynamics.

Addition of the calreticulin signal sequence and a KDEL ER-retention tag led to effective and specific localization of the cameleon to the ER in mammalian cells (Fig. 2*a*). Fig. 2 *b* and *c* show the dramatic improvement in $[Ca^{2+}]_{ER}$ sensitivity of

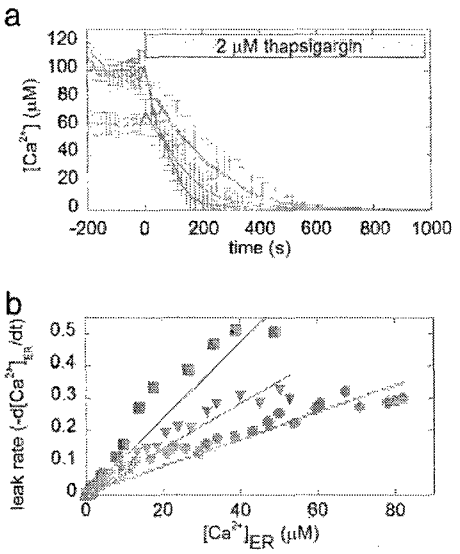

Fig. 3. The effect of Bcl-2 overexpression on the $[Ca^{2+}]_{ER}$ of MCF-7 cells. (*a*) Comparison of $[Ca^{2+}]_{ER}$ in neo (red), Bcl-2 (blue), and Bcl-2 also overexpressing SERCA2b (green) cells. Each trace represents the average of more than five cells. Emission ratios were converted into $[Ca^{2+}]$, as described in *Materials and Methods*. Thapsigargin was added at time $t = 0$ in the absence of external Ca^{2+} to prevent Ca^{2+} influx due to capacitative Ca^{2+} entry. (*b*) Leakage rate of Ca^{2+} from the ER as a function of $[Ca^{2+}]_{ER}$ for Bcl-2 (blue), neo (red), and Bcl-2 overexpressing SERCA2b (green) cells.

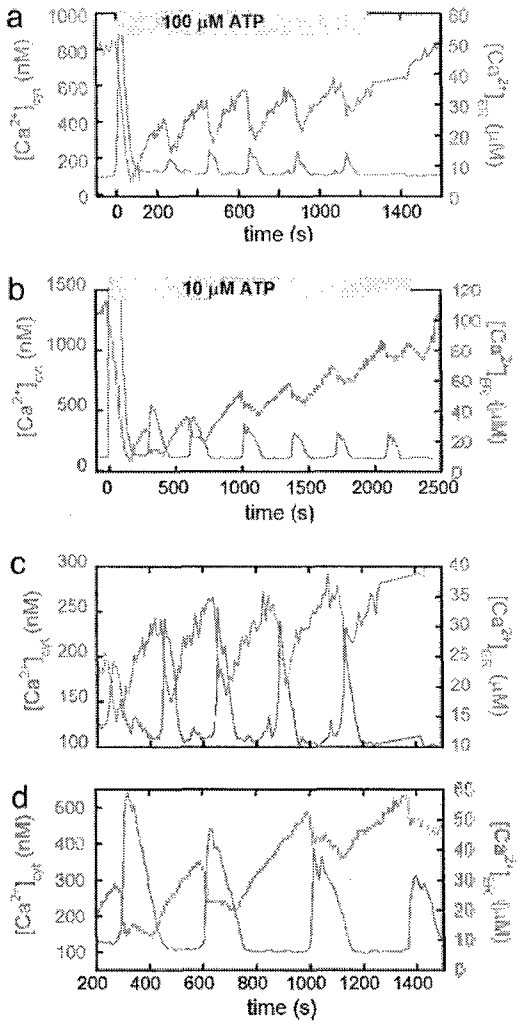

Fig. 4. Comparison between ATP-induced Ca^{2+} oscillations in the cytosol and the ER for Bcl-2 and neo MCF-7 cells. The differences between Bcl-2 (*a* and *c*) and neo (*b* and *d*) cells are highlighted in *c* and *d*, which are on the same timescale and focus on the oscillations induced by ATP. The $[Ca^{2+}]_{cyt}$ signal is in green, and the $[Ca^{2+}]_{ER}$ signal is in blue for Bcl-2 and red for neo cells. The fura-2 excitation ratio (350/380 nm) and cameleon emission ratio (citrine/CFP) were converted to $[Ca^{2+}]$, as outlined in *Materials and Methods*.

D1ER over YC4.3ER, which was previously the best indicator for directly monitoring $[Ca^{2+}]_{ER}$ at the single-cell level. Treatment of HeLa cells with pharmacological blockers such as thapsigargin, the irreversible sarcoendoplasmic reticulum Ca^{2+} ATPase (SERCA) inhibitor (Fig. 2*b*), or with agonists such as ATP, which results in IP_3 production and activation of IP_3R (Fig. 2*c*), causes a depletion in $[Ca^{2+}]_{ER}$ that is robust and readily visible by using D1ER. Additionally, upon ATP treatment, oscillations in $[Ca^{2+}]_{ER}$ were directly observed with D1ER, whereas YC4.3ER was not sensitive enough to detect oscillations. The D1ER cameleon is not saturated under resting conditions, because treatment with 25 μM digitonin and 5 mM Ca^{2+} led to a ratio increase (data not shown); thus, D1ER is poised to detect both increases and decreases in $[Ca^{2+}]_{ER}$.

Because CFP and citrine are spectrally distinct from the excitation and emission of fura-2, D1ER can be used in conjunction with this high-affinity Ca^{2+} indicator in the cytosol to simultaneously monitor both $[Ca^{2+}]_{ER}$ and $[Ca^{2+}]_{cyt}$ (Fig. 2 *d* and *e*). As can be seen from Fig. 2*d*, in HeLa cells upon stimulation with 10 μM ATP, there is a rise in $[Ca^{2+}]_{cyt}$ followed by rapid oscillations. These oscillations are also observed in the ER, and, as evidenced by the data in Fig. 2*d Inset*, the $[Ca^{2+}]_{ER}$ oscillations are directly anticorrelated with those in the cytosol. Dampening out of the oscillations coincides with a large decrease in $[Ca^{2+}]_{ER}$. At longer time points (Fig. 2*e*), once the $[Ca^{2+}]_{cyt}$ has returned to essentially basal levels, lower-frequency sustained oscillations are observed in the cytosol, as described (24). We can now observe that these oscillations occur only when the ER starts to refill, presumably due to capacitative Ca^{2+} entry.

Given the dramatic improvement in our ability to directly measure $[Ca^{2+}]_{ER}$ at the single-cell level with D1ER and the potential to monitor Ca^{2+} simultaneously in the ER and the cytosol, we turned our focus to the effect of the antiapoptotic Bcl-2 protein on $[Ca^{2+}]_{ER}$ in MCF-7 breast cancer epithelial cell lines stably expressing either a control plasmid (neo) or Bcl-2 (25). As reported (25), overexpression of Bcl-2 in MCF-7 cells protected against apoptosis induced by thapsigargin, staurosporine, and H_2O_2. Fig. 3*a* shows that in MCF-7 Bcl-2 cells, $[Ca^{2+}]_{ER}$ is decreased by ≈40% [from an average of 103 ± 12 μM in neo cells (n = 45 cells) to 66 ± 7 μM in Bcl-2 cells (n = 79 cells)]. Overexpression of SERCA2b in the Bcl-2 cells restores $[Ca^{2+}]_{ER}$ to control levels. Blocking SERCA pumps with thapsigargin causes depletion of $[Ca^{2+}]_{ER}$ due to leak of Ca^{2+} across the ER membrane (Fig. 3*a*). Taking the derivative of the change in $[Ca^{2+}]_{ER}$ upon thapsigargin treatment enables a comparison of the leakage rate for neo and Bcl-2 cells, and Bcl-2 cells overexpressing SERCA2b. As is evident from Fig. 3*b*, the leakage rate for Bcl-2 cells is greater than that for neo cells, indicating that under resting conditions, there is less $[Ca^{2+}]_{ER}$ in Bcl-2 cells, because Bcl-2 increases the leak of Ca^{2+} out of the ER, as has been found in some other cell types (10, 11, 26). In cells overexpressing both Bcl-2 and SERCA2b, the leakage rate is still much greater than in control cells, indicating that the increase in resting $[Ca^{2+}]_{ER}$ levels is due to increased pumping of Ca^{2+} into the ER rather than a decreased leak.

The molecular mechanism by which Bcl-2 alters Ca^{2+} homeostasis is still unclear. Bcl-2 may facilitate Ca^{2+} leakage from

CELL BIOLOGY

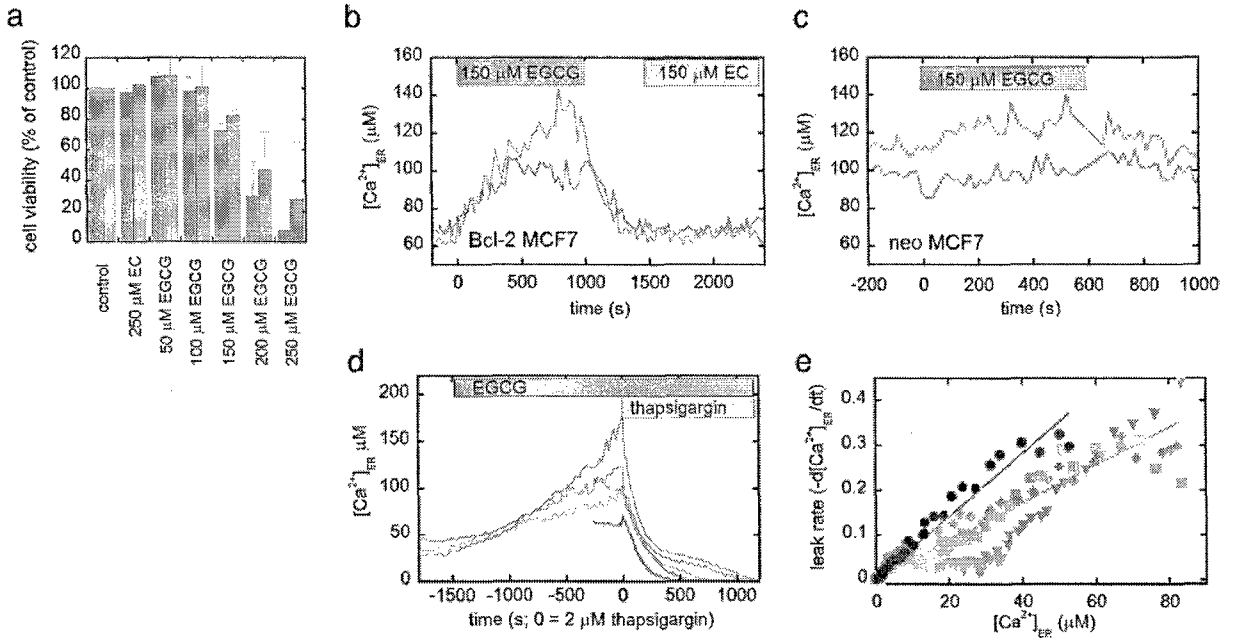

Fig. 5. The effect of the green tea compound EGCG and a control compound EC on apoptosis and $[Ca^{2+}]_{ER}$ of MCF-7 cells. (*a*) Cell viability (percent of the control), as determined by FACS analysis of propidium iodide and annexin V-stained neo (red) and Bcl-2 (blue) cells after 48-h treatment with nothing (control), EC, and increasing concentrations of EGCG. (*b*) Treatment of MCF-7 cells overexpressing Bcl-2 with EGCG and EC, as denoted by the green and blue boxes. The traces represent two different cells. (*c*) Treatment of MCF-7 neo cells with EGCG, as denoted by the green box. The traces represent two different cells. It should be noted that EC did not cause an increase in $[Ca^{2+}]_{ER}$ in neo cells. (*d*) Bcl-2 cells treated with EGCG (green traces, each representing an individual cell) compared with neo (red) and Bcl-2 (blue) cells. At time $t = 0$, cells were treated with 2 μM thapsigargin in the absence of external Ca^{2+} to determine the ER Ca^{2-} leakage rate. (*e*) Comparison of the leakage rates of Ca^{2+} from the ER for Bcl-2 (blue circles), neo (red diamonds), and Bcl-2 cells pretreated with EGCG (green, upside-down triangles and squares), showing the decreased leakage rate upon EGCG treatment.

the ER by forming a channel, either by homooligomerizing or by interacting with another member of the Bcl-2 family, because it has been reported that in planar lipid bilayers, Bcl-2 can form a cation selective channel at physiological pH (27). Alternatively, Bcl-2 could interact with and alter the function of an endogenous release channel or pore-forming protein in the ER. Indeed, in a recent study, Bcl-2 was found to interact with the IP_3R in WEHI7.2 T cells by coimmunoprecipitation, and this interaction appeared to influence the amount of Ca^{2+} released from the ER and the open probability of the IP_3R in lipid bilayers (16). If Bcl-2 interacts with the IP_3R in MCF-7 cells, it would potentially alter Ca^{2+} oscillations triggered by ATP. Any differences between Bcl-2 and neo cells could be detected by simultaneously monitoring the ER and the cytosol.

Treatment of MCF-7 cells with ATP results in a large release of Ca^{2+} from the ER into the cytosol, followed by Ca^{2+} oscillations in both the ER and the cytosol upon refilling of the ER (Fig. 4). Bcl-2 cells required a larger dose of ATP than neo cells for oscillations to be induced (100 vs. 10 μM), suggesting that they are less sensitive to ATP. Fig. 4 *a* and *b* show responses of representative single Bcl-2 and neo cells. It is evident that less Ca^{2+} is released into the cytosol in Bcl-2 cells, both in the initial dump and in subsequent oscillations. The average initial decrease in $[Ca^{2+}]_{ER}$ is 51 $\pm$ 4 μM for Bcl-2 cells and 85 $\pm$ 9 μM for neo cells, resulting in average cytosolic increases of 890 $\pm$ 370 nM for Bcl-2 and 1580 $\pm$ 650 nM for neo ($n = 12$ for Bcl-2 cells and $n = 11$ for neo cells). Importantly, in both Bcl-2 and neo cells, $[Ca^{2+}]_{ER}$ decreases to $\approx$ 5 μM after the initial release; therefore, the smaller Ca^{2+} release in Bcl-2 cells results from the lower Ca^{2+} level in the ER under resting conditions.

Aside from the intensity of the Ca^{2+} oscillations, the most significant difference between the Bcl-2 and neo cells is that the oscillations are typically more rapid and the duration of ER Ca^{2+} release is shorter in Bcl-2 overexpressing cells (Fig. 4 *c* and *d*). As a consequence, Bcl-2 cells tend to oscillate at a higher frequency. Oscillation data from more individual cells are presented in Fig. 10, which is published as supporting information on the PNAS web site, demonstrating that, although there is some variability in the oscillations, the trends in oscillation frequency and duration are maintained.

Identifying novel inhibitors of Bcl-2 should provide insight into the role of Bcl-2 in endogenous signaling cascades leading to apoptosis, as well as lead to the potential development of therapeutic agents. Previously, Leone *et al.* (28) found that (−)EGCG, the most abundant component of green tea, could bind to the hydrophobic pocket of Bcl-2 *in vitro* and inhibit its interaction (K_i = 335 nM) with a peptide derived from the proapoptotic BH3-only protein Bad, whereas a compound lacking the gallate moiety, (−)EC, had no effect (see Fig. 11, which is published as supporting information on the PNAS web site, for structures). We treated both neo and Bcl-2 cells with EGCG and found that the compound could induce apoptosis in a dose-dependent manner, as determined by FACS analysis of propidium iodide- and annexin V-stained cells (Fig. 5*a*; details of assay given in *Supporting Text*). Importantly, EGCG was much more effective than other proapoptotic stimuli such as thapsigargin and H_2O_2 in inducing apoptosis in Bcl-2 cells, indicating that it was capable of overcoming protection by Bcl-2. Given that green tea polyphenols have been shown to inhibit tumor formation and growth in certain models (29), this raises the possibility that this antitumor activity could be partially related to overcoming Bcl-2 protection of cancer cells.

To gain more insight into how EGCG overcomes Bcl-2 protection, we examined the effect of EGCG on $[Ca^{2+}]_{ER}$. As can be shown from Fig. 5*b*, treatment of Bcl-2 cells with 150 μM EGCG results in an immediate increase in $[Ca^{2+}]_{ER}$, from an average of $\approx$60 to $\approx$125 μM. This effect can be reversed upon washing out the inhibitor. On the contrary, the control com-

pound, EC, has no effect on $[Ca^{2+}]_{ER}$. Fig. 5*c* shows that in neo cells there is either no increase or a very modest increase in $[Ca^{2+}]_{ER}$, consistent with inhibition of the small amount of endogenous Bcl-2 in these cells. To determine the cause of the Ca^{2+} increase, we pretreated Bcl-2 cells with EGCG and then added thapsigargin (Fig. 5*d*) to monitor the leak rate. As can be seen from Fig. 5*e*, EGCG causes a dramatic decrease in the Ca^{2+} leak rate of Bcl-2 cells, such that the leak is the same or slower than that in neo cells. This suggests that the binding of EGCG to Bcl-2 prevents Bcl-2 from increasing the Ca^{2+} leak rate.

Discussion

The improved ER-targeted cameleon poses a number of significant advantages over all previous methods for monitoring $[Ca^{2+}]_{ER}$. Compared with the ER-targeted aequorin probes, the cameleon signal is ratiometric, permits single-cell resolution, and is compatible with fura-2 in the same cell. Importantly, these characteristics enable the monitoring of Ca^{2+} oscillations within the ER. Additionally, the cameleon is not consumed by Ca^{2+} as aequorin is, and therefore the instantaneous signal depends only on Ca^{2+} and not the entire past history of Ca^{2+} in the cell (1). Because the cameleons and aequorins have different Ca^{2+} response curves, they should yield different mean $[Ca^{2+}]$ whenever there is spatial heterogeneity in $[Ca^{2+}]$. The cameleons would tend to give slightly lower mean $[Ca^{2+}]$ values than aequorins.

The improved ER-targeted cameleon enabled us to show that Bcl-2 plays an important role in governing $[Ca^{2+}]_{ER}$ in breast cancer cells by altering the resting level of $[Ca^{2+}]_{ER}$ as well as the amplitude, duration, and frequency of IP_3-mediated Ca^{2+} oscillations. Our study does not directly address whether Bcl-2 interacts with the IP_3R in MCF-7 cells, because Ca^{2+} oscillations are controlled by a host of factors, including the level of Ca^{2+} in the ER and capacitative calcium entry, both of which are altered in Bcl-2-overexpressing cells (9, 11, 26). However, our data show that, in addition to altering the resting level and leak rate of $[Ca^{2+}]_{ER}$, Bcl-2 overexpression can also modify fundamental Ca^{2+} signaling processes such as the nature of IP_3-induced Ca^{2+} oscillations. This raises the intriguing possibility that Bcl-2 may have an effect on signaling pathways that are downstream of Ca^{2+} oscillations and therefore has the potential to influence processes such as exocytosis, mitochondrial redox state, and differential gene transcription (30–32). This disruption of Ca^{2+} homeostasis by Bcl-2 may be essential in determining the susceptibility of breast cancer cells to different apoptotic stimuli, because Scorrano *et al.* (12) have found that certain apoptotic stimuli (lipid second messengers and oxidative stress, staurosporine, etoposide, and brefeldin-A) depend either critically or partially on ER Ca^{2+}.

We have also identified a small-molecule inhibitor (EGCG) of Bcl-2 that can overcome Bcl-2 protection and induce apoptosis in breast cancer cells. Interestingly, this inhibitor also reverses the effect of Bcl-2 on $[Ca^{2+}]_{ER}$. Because EGCG is known to bind in the hydrophobic groove and prevent the interaction of Bcl-2 with BH3-only peptides, this suggests that binding in this hydrophobic pocket inhibits the channel function of Bcl-2, either by preventing its interaction with other proteins or by causing a conformational change in Bcl-2 itself. Recently, Bassik *et al.* (33) found that phosphorylation within the unstructured loop region between the BH3 and BH4 domains of Bcl-2 inhibited the interaction between Bcl-2 and proapoptotic family members and caused an increase in Ca^{2+} leak rate (33). They also showed that the ability to bind BH3-only proteins, but not Bax or Bak, was critical for Bcl-2 to lower $[Ca^{2+}]_{ER}$. The combination of that study with the present one strongly suggests that Bcl-2 must interact with other proteins (either itself or other family members) through the hydrophobic groove to facilitate leakage of Ca^{2+} from the ER. It also implies that the interaction of other family members with Bcl-2 localized to the ER can have a dramatic effect on $[Ca^{2+}]_{ER}$ and potentially apoptosis. We are currently examining whether a direct connection exists between blockage of the channel function, increase in $[Ca^{2+}]_{ER}$, and the increased apoptosis observed in the Bcl-2-overexpressing cells.

We thank L. Xu, S. R. Adams, L. Gross, P. Steinbach, and Q. Xiong for assistance and advice and Professor J. Adams for the use of his Applied Photophysics stopped-flow instrument. This work was supported by Ruth L. Kirschstein National Research Service Award Postdoctoral Fellowship F32-GM067488-01 (to A.E.P.), Department of Defense Postdoctoral Fellowship DAMD17-99-1-9096 (to C.J.), Department of Energy Grant DE-FG-01-ER63276 (to R.Y.T.), and National Institutes of Health Grants NS27177 (to R.Y.T.) and GM60554 (to J.C.R.).

1. Alvarez, J. & Montero, M. (2002) *Cell Calcium* **32,** 251–260.
2. Solovyova, N. & Verkhratsky, A. (2002) *J. Neurosci. Methods* **122,** 1–12.
3. Sneyd, J., Tsaneva-Atanasova, K., Yule, D. I., Thompson, J. L. & Shuttleworth, T. J. (2004) *Proc. Natl. Acad. Sci. USA* **101,** 1392–1396.
4. Arnaudeau, S., Kelley, W. L., Walsh, J. V., Jr., & Demaurex, N. (2001) *J. Biol. Chem.* **276,** 29430–29439.
5. Filippin, L., Magalhaes, P. J., Benedetto, G. D., Colella, M. & Pozzan, T. (2003) *J. Biol. Chem.* **278,** 39224–39234.
6. Brini, M., Pinton, P., Pozzan, T. & Rizzuto, R. (1999) *Microsc. Res. Tech.* **46,** 380–389.
7. Miyawaki, A., Llopis, J., Heim, R., McCaffery, J. M., Adams, J. A., Ikura, M. & Tsien, R. Y. (1997) *Nature* **388,** 882–887.
8. Cory, S. & Adams, J. M. (2002) *Nat. Rev. Cancer* **2,** 647–656.
9. Lam, M., Dubyak, G., Chen, L., Nunez, G., Miesfeld, R. & Distelhorst, C. W. (1994) *Proc. Natl. Acad. Sci. USA* **91,** 6569–6573.
10. Foyouzi-Youssefi, R., Arnaudeau, S., Borner, C., Kelly, W. L., Tschopp, J., Lew, D. P., Demaurex, N. & Krause, K.-H. (2000) *Proc. Natl. Acad. Sci. USA* **97,** 5723–5728.
11. Pinton, P., Ferrari, D., Magalhaes, P., Schulze-Osthoff, K., Virgilio, F. D., Pozzan, T. & Rizzuto, R. (2000) *J. Cell Biol.* **148,** 857–862.
12. Scorrano, L., Oakes, S. A., Opferman, J. T., Chang, E. H., Sorcinelli, M. D., Pozzan, T. & Korsmeyer, S. J. (2003) *Science* **300,** 135–139.
13. Baffy, G., Miyashita, T., Williamson, J. R. & Reed, J. C. (1993) *J. Biol. Chem.* **268,** 6511–6519.
14. Pinton, P., Ferrari, D., Rapizzi, E., Virgilio, F. D., Pozzan, T. & Rizzuto, R. (2001) *EMBO J.* **20,** 2690–2701.
15. Distelhorst, C. W. & Shore, G. C. (2004) *Oncogene* **23,** 2875–2880.
16. Chen, R., Valencia, I., Zhong, F., McColl, K. S., Roderick, H. L., Bootman, M. D., Berridge, M. J., Conway, S. J., Holmes, A. B., Mignery, G. A., *et al.* (2004) *J. Cell Biol.* **166,** 193–203.
17. Griesbeck, O., Baird, G. S., Campbell, R. E., Zacharias, D. A. & Tsien, R. Y. (2001) *J. Biol. Chem.* **276,** 29188–29194.
18. Tsien, R. Y. & Pozzan, T. (1989) *Methods Enzymol.* **172,** 230–263.
19. Tsien, R. Y. & Rink, T. J. (1983) in *Current Methods in Cellular Neurobiology,* ed. Barber, J. L. (Wiley, New York), Vol. 3, pp. 249–312.
20. Poenie, M. (1990) *Cell Calcium* **11,** 85–91.
21. Hasan, M. T., Friedrich, R. W., Larkum, M. E., Euler, T., Both, M., Duebel, J., Waters, J., Giese, G., Bujard, H., Griesbeck, O., *et al.* (2004) *Pub. Lib. Sci.* **2,** 763–775.
22. Heim, N. & Griesbeck, O. (2004) *J. Biol. Chem.* **279,** 14280–14286.
23. Ikura, M., Clore, G. M., Gronenborn, A. M., Zhu, G., Klee, C. B. & Bax, A. (1992) *Science* **256,** 632–638.
24. Bootman, M. D., Cheek, T. R., Moreton, R. M., Bennett, D. L. & Berridge, M. J. (1994) *J. Biol. Chem.* **269,** 24783–24791.
25. Froesch, B. A., Aime-Sempe, C., Leber, B., Andrews, D. & Reed, J. C. (1999) *J. Biol. Chem.* **274,** 6469–6475.
26. Abeele, F. V., Skryma, R., Shuba, Y., Coppenolle, F. V., Slomianny, C., Roudbaraki, M., Mauroy, B., Wuytack, F. & Prevarskaya, N. (2002) *Cancer Cell* **1,** 169–179.
27. Schendel, S. L., Xie, Z., Montall, M. O., Matsuyama, S., Montal, M. & Reed, J. C. (1997) *Proc. Natl. Acad. Sci. USA* **94,** 5113–5118.
28. Leone, M., Zhai, D., Sareth, S., Kitada, S., Reed, J. C. & Pellecchia, M. (2003) *Cancer Res.* **63,** 8118–8121.
29. Yang, C. S. & Wang, Z. Y. (1993) *J. Natl. Cancer Inst.* **85,** 1038–1049.
30. Berridge, M. J., Bootman, M. D. & Roderick, H. L. (2003) *Nat. Mol. Cell Biol.* **4,** 517–529.
31. Berridge, M. J., Lipp, P. & Bootman, M. D. (2000) *Nat. Mol. Cell Biol.* **1,** 11–21.
32. Blaustein, M. P. & Golovina, V. A. (2001) *Trends Neurosci.* **24,** 602–608.
33. Bassik, M. C., Scorrano, L., Oakes, S. A., Pozzan, T. & Korsmeyer, S. J. (2004) *EMBO J.* **23,** 1207–1216.